UNIVERSITY OF VAASA

FACULTY OF TECHNOLOGY

ENERGY TECHNOLOGY

Markus Uuppo

DEACTIVATION EFFECTS OF BIOFUELS ON SCR CATALYSTS

Meta-analysis about the chemical and other deactivation effects when using biofuels

Master's thesis for the degree of Master of Science in Technology, submitted for inspection in Vaasa on September 27, 2012

Supervisor	Seppo Niemi (D.Sc.)
Instructor	Katriina Sirviö (M.Sc.)

TABLE OF CONTENTS

BIBLIOGRAPHY 142

SYMBOLS AND ABBREVIATIONS

Al_2O_3	Aluminium oxide
ASTM	American Society for Testing and Materials
BET surface area	Brunauer - Emmett - Teller -surface area
$Ca(NO_3)_2$	Calcium nitrate
$CaSO_4$	Calcium sulfate
$CO(NH_2)_2$	Urea
cpsi	cells per square inch
CMAD	Count Mean Average Diameter
CO	Carbon Monoxide
$DeNO_X$	Conversion from NO_X to nitrogen and water
DRIFT spectra	Diffuse Reflectance Infrared Fourier Transform spectra
FCEP	Future Combustion Engine Power plant
FSN	Filter Smoke Number
FTIR	Fourier Transform Infrared Spectroscopy
GHSV	Gas Hourly Space Velocity
HDDT	Heavy Duty Diesel Transient
H_3PO_4	Phosphoric acid
ICP	Inductively Coupled Plasma
K_2CO_3	Potassium carbonate
K_2SO_4	Potassium sulfate
K_3PO_4	Potassium phosphate
KCl	Potassium chloride
$KHSO_4$	Potassium bisulfate
KNO_3	Potassium nitrate
$Mg(NO_3)_2$	Magnesium nitrate
N_2O	Nitrous oxide
$NaNO_3$	Sodium nitrate
NH_3	Ammonia
NO_X	Nitrogen oxides, basically NO and NO_2 combined
REM / EDX	Scanning Electron Microscopy (with) Energy-dispersive X-ray Spectroscopy
RME	Rapeseed Methyl Ester
RSO	Rapeseed Oil

RT	Room Temperature
SCR	Selective Catalytic Reduction (of nitrogen oxides)
SO_2	Sulfur dioxide
SO_3	Sulfur trioxide
SVO	Straight Vegetable Oil
TEM	Transmission Electron Microscopy
THC	Total Hydrocarbons
TiO_2	Titanium dioxide
TPD	Temperature-Programmed Desorption
ULSD	Ultra Low Sulfur Diesel
V_2O_5	Vanadium pentoxide
WO_3	Tungsten trioxide
XPS	X-Ray Photoelectron Spectroscopy
XRD	X-Ray Diffraction
$ZnCl_2$	Zinc chloride

LIST OF FIGURES

LIST OF TABLES

VAASAN YLIOPISTO
Teknillinen tiedekunta
Tekijä: Markus Uuppo
Diplomityön nimi: Deactivation effects of biofuels on SCR catalysts
Valvojan nimi: Professori (mts) Seppo Niemi
Ohjaajan nimi: Fil. maist. Katriina Sirviö
Tutkinto: Diplomi-insinööri
Oppiaine: Energiatekniikka
Opintojen aloitusvuosi: 2011
Diplomityön valmistumisvuosi: 2012 **Sivumäärä:** 144

TIIVISTELMÄ

Selective Catalytic Reduction - eli SCR-teknologiaa on yleisesti käytetty typenoksidien vähentämiseen pakokaasuista. Typenoksidit ovat haitallisia ihmisille ja ympäristölle. SCR-katalysaattorit muuntavat typenoksidit typeksi ja vedeksi, käyttäen kiinteää tai nestemäistä ammoniakkia apuna reaktiossa. Teknologiaa käytetään yleisesti niin ajoneuvodieselmoottoreissa kuin voimalaitoksissakin. Tyypillisesti katalyyttimateriaalina toimii vanadiinipentoksidipinnoite.

SCR-katalysaattorin tehokkuus voi laskea ajan myötä. Huonontuminen voi johtua liiasta lämmöstä, tukkiutumisesta tai kemiallisesta myrkyttymisestä. Monet biopolttoaineet voivat sisältää hivenaineita ja tuhkaa, jotka saattavat nopeuttaa huonontumista. Biopolttoaineilla tarkoitetaan kiinteitä tai nestemäisiä uusiutuvia biologisia polttoaineita. Tässä opinnäytetyössä on kerättynä tietoa huonontumisprosessista voimalaitoksista, moottoreista sekä laboratoriotesteistä.

Kalium on kaikkein voimakkain myrkky yksin tai muiden hivenaineiden kanssa. Natrium, kalsium, magnesium ja fosfori ovat myös haitallisia, mutta niiden vaikutukset ovat kovasti riippuvaisia millaisissa, yhdisteissä ne esiintyvät ja mitä muita myrkkyjä on läsnä. Pääasiassa kaikki alkali- ja maa-alkalimetallit ovat haitallisia. Eniten heikkenemistä aiheuttaa aerosolimyrkytys, joka vähentää ammoniakin imeytymistä katalysaattorin pinnalle. Mitä vähemmän ammoniakkia imeytyy, sitä huonompi konversiotehokkuus katalysaattorilla on. Huokosten ja suuaukon tukkiutuminen on toissijainen, mutta kuitenkin tehoa huonontava ilmiö.

AVAINSANAT: SCR-katalysaattori, huonontuminen, dieselmoottori, typenoksidi, päästöjen vähentäminen, voimalaitos

UNIVERSITY OF VAASA
Faculty of technology
Author: Markus Uuppo
Topic of the Thesis: Deactivation effects of biofuels on SCR catalysts
Supervisor: Professor (fixed term) Seppo Niemi
Instructor: M. Sc. Katriina Sirviö
Degree: Master of Science in Technology
Major of Subject: Energy Engineering
Year of Entering the University: 2011
Year of Completing the Thesis: 2012 **Pages:** 144

ABSTRACT

Selective Catalytic Reduction (SCR) technology is widely used for reducing nitrogen oxides (NO_X) from exhaust gases. Nitrogen oxides are harmful for humans and the environment. The SCR catalysts convert nitrogen oxides to nitrogen and water with solid or liquid ammonia. The technology is widely being used with diesel engines in vehicles as well as power plant scale applications. Typically the catalyst is coated with vanadium pentoxide.

The SCR catalysts can lose their activity over time. This deactivation may be due to too much heat, pore blocking or chemical poisoning. Many biofuels can contain trace elements and ash that may accelerate the deactivation. Biofuels are solid or liquid fuels that are made from renewable biological sources. In this thesis some information from power plant and engine testing, as well as laboratory scale testing is gathered in order to understand the deactivation process.

Potassium has the strongest deactivation effect by itself and with other components. Sodium, calcium, magnesium and phosphorus are also found to be harmful, but their effects are more dependent on the compound and the presence of other poisons. Basically all alkaline and earth alkaline metals are harmful. The main reason for deactivation is the aerosol poisoning that chemically decreases the ammonia absorption on the catalyst surface. The less ammonia is absorbed the less conversion will happen inside the catalyst. Pore blocking and blocking the inlet of the catalyst by ash are much less harmful deactivation methods.

KEYWORDS: SCR catalyst, deactivation, diesel engine, nitrogen oxide, emissions reduction, power plant

1. INTRODUCTION

This thesis is a part of the Future Combustion Engine Power plant (FCEP) program, funded by Cleen Ltd. The aim of the program was to determine emission reduction and energy efficiency possibilities concerning engine power plants, and investigate the use of different biofuels. This thesis is an investigation concerning the reduction of nitrogen oxides and the equipment durability when using biofuels.

The Selective Catalytic Reduction (SCR) catalysts are used to convert nitrogen oxides (NO_X) to nitrogen and water. This technology is being used from the 1970's in power plants and later in diesel combustion engines. Vanadium oxide is the most typical active material used in the SCR technology. Ammonia NH_3 in some form is needed in order to convert the compounds back to harmless ones. Ammonia or liquid urea is injected to exhaust gas stream before the catalyst where the chemical reactions make the conversion of the NO_X.

Biofuels are made from renewable sources and used in the same way as the fossil fuels. The name is the same for solid and liquid fuels. In this thesis the aim was to investigate what possible side effects biofuel use might have on SCR equipment. It is well known that biofuels contain trace elements that could be harmful on the chemistry inside the catalyst.

This thesis is a meta-analysis gathering the current knowledge about SCR catalyst deactivation with different biofuels. Unfortunately very few investigations involved combustion engines and liquid biofuels, so direct information was hard to collect. However, solid biofuels have been in use in coal power plants, and lubrication oils can contain same trace elements than biofuels. These have been studied and the results are introduced in this thesis, trying to give information what might happen in continuous liquid biofuel use in an engine with SCR equipment.

The structure of this thesis is little different from the usual. Different investigations are introduced one by one and linked together when necessary. The original article is mentioned

at the beginning of every Chapter and the conclusions are written at the end of them. There were no practical measurements about SCR catalysts during writing this thesis. Due to this the thesis is little longer than usual, and the effects are described as accurate as possible.

2. GENERAL INFORMATION ABOUT BIOFUELS AND SCR CATALYSTS

2.1. A brief to biofuel emissions and their health related aspects

Some studies were gathered together by G.A.M. Janssen from FACT Foundation.

Study 1.

The basic findings of the emissions of engines running on original diesel fuel oil compared to engines running on Straight Vegetable Oil (SVO) are presented in this investigation, without going into details. This is just to show the general and accepted conclusions of emissions on diesel engines running on SVO. The researches and results are explained shortly.

A study of the emissions from tractors for agricultural work was published in 2006. The emissions were measured with unspecified standard diesel oil and pure rapeseed oil. The research department was German “Lehr-, Versuchs- und Fachzentrum Kringell”. Regulated and some unregulated emission components were measured. Two different engines were studied, first being a 6 cylinder, 162 horsepower Diesel engine, type BF6N1013EC and the other being 4 cylinder, 125 horsepower Diesel engine, type BF4M2013C, both engines built by Deutz. The 4 cylinder engine was mounted in a Fendt farmer Vario 412. Both engines were modified to use of SVO as fuel. The 2000/25/EG test procedure was used for all tests, with a few small exceptions.

At high rpm the CO emissions were at the same level with rapeseed oil and diesel. At low rpm the rapeseed oil emitted higher CO emissions than diesel. Hydrocarbon emissions were found to be 2 to 3 times lower with rapeseed oil, at both low and high rpm. NO_X emissions were approximately 10 % higher with rapeseed oil. PM emissions were lower for rapeseed oil at medium to high engine loads, but similar at low loads. The results were alike for both engines. As a general conclusion, at medium to high loads the emissions of regulated com-

pounds were lower with rapeseed oil than with diesel oil. NO_X levels were an exception, being 10-15 % higher with rapeseed oil at medium and high engine loads.

Study 2.

Some health aspects of diesel engine emissions were described and published in a report by Bünger et al. at 2007. In measurements was a diesel engine running on rapeseed oil, rapeseed methyl ester (RME) and standard diesel fuel (meeting the EN 590 standard). The standard European Cycle was used as a testing method. The test engine used was a standard, unmodified Mercedes Benz engine OM 906 LA with turbocharger and intercooler. The engine met the Euro 3 exhaust limits.

It was found that the particle extracts were significantly more mutagenic (5 to 60 times more) compared to the standard diesel fuel's when the engine was running on rapeseed oil. Also the condensates showed a higher mutagenicity up to 13.5 times more than the diesel fuel. With RME the extracts and condensates showed a reasonable but still significant increase in mutagenic response when compared to diesel fuel. The regulated compounds were well below the Euro 3 limit with all fuels, with the exception of NO_X, which was 15-25 % over the limit with biofuels. It was suggested that the higher viscosity of the biofuels and the different combustion behavior in the engine could partly explain the results.

Study 3.

The German environmental institute BIFA described the results of a detailed analysis of the mutagenic properties of rapeseed oil emissions from a diesel engine, published at 2007. The test engine was DAF XF 105 (Euro5) diesel engine, and the test cycle was the 13-step European Stationary Cycle. The engine was modified for rapeseed oil, as specified in DIN 51605 norm, and the reference diesel fuel was standard EN 590.

The findings were contrary to Bünger's findings at Study 2. It was found that the number of revertants found in the extracts from the rapeseed oil were 2 to 3 times lower than when the

diesel fuel was used. A revertant is a measure for the mutagenic properties of a substance, meaning the more revertants equals to more mutagenicity. The total amount of PM was also roughly 2 times lower with the rapeseed oil. The overall conclusion was that the amount of mutagenic substances emitted by the pure rapeseed oil, at properly adjusted engine, was 4 or more times lower than with standard diesel.

Study 4.

A study about gaseous and particle emissions of diesel engines driven with different non-esterified plant oils was published in 2008. The study was published by University of Offenburg, Germany. The engine used for tests was a 4 cylinder, 1.7 litre, Euro 4, 16 valves engine with EGR and VTC turbo charger. A heat exchanger was installed in order to heat the plant oil to 80-90 °C before the injection. A special fuel pump was used to produce the pressure needed for the proper injection. An old non modified heavy duty engine from 1969 was analyzed using the same procedure. Three load conditions were used and four different oils were investigated and compared with conventional unspecified petro-diesel. The oils were rapeseed, sunflower, soy bean and peanut oils.

No large differences were found in emitted particles with different oils with the newer engine. All primary particles emitted were approximately 15 nm, and their TEM pictures (Transmission Electron Microscopy) were very much the same. No ash traces were found, as the composition of particles was carbon. The engine load strongly influenced the amount of the emitted particles, but the amounts were about the same for all the fuels. CO and THC (total hydrocarbons) emissions were below the detection limit, but NO_X values were about 15 % higher for plant oils, except at very high loading where the values were similar for plant oils and diesel fuel.

Experiments with the old non modified heavy duty engine were performed using 6 fuels, petro-diesel, low sulfur diesel, esterified rapeseed oil, pure rapeseed oil, soy oil and waste cooking oil. A remarkable difference was observed between the size and number of particles emitted by the modern and the old engine. The difference was especially big when using rapeseed and waste cooking oils in the old engine. Particles emitted by the plant oils in

the old engine were wax-like, and long chain hydrocarbons were also found. The size of the particles emitted by the old engine with plant oils was very depending on the engine load. Large particles were emitted on low and medium load conditions. Particle sizes were comparable to the particles emitted by the modern engine only at high and very high engine loads with the plant oils. Petro-diesel and low sulfur (S) diesel oil produced similar particle amounts and sizes with both engines.

Some conclusions can be drawn:

- Compared to petro-diesel, the regulated emissions tend to be lower with biodiesel and biofuels, except the amount of NO_X which is usually slightly higher.
- The amount of compounds emitted depends strongly on the type of diesel engine, the configuration and the loading, and the use of an optional catalyser.
- In a properly modified and adapted diesel engine, using biodiesel or SVO results in reduced emissions of non-regulated compounds such as carcinogenic and mutagenic substances.
- The use of SVO in a properly modified diesel engine leads to a further reduction of non-regulated compounds compared to biodiesel.

2.2. Selective catalytic reduction (SCR)

This Chapter along with its Figures and Tables is summarized from the book “Diesel Emissions and Their Control”, written by W. Addy Majewski and Magdi K. Khair, 2006.

Selective catalytic reduction of NO_X by nitrogen compounds, such as urea or ammonia, has been developed for industrial stationary applications. It was introduced in the 1970’s, and

since it has been used in such applications as plant and refinery heaters and boilers in the chemical processing industry, gas turbines and coal-fired cogeneration plants. It has been used with many different fuels, such as pulverized coal, natural gases, industrial gases, crude oil, light or heavy oil, and biomass and liquid biofuels.

2.2.1. Ammonia

Two forms of ammonia can be used in SCR systems: pure anhydrous ammonia or liquid ammonia. Anhydrous ammonia is very toxic, hazardous, and requires a thick-shell, pressurized storage tanks and piping due to its high vapor pressure. Liquid ammonia solution $NH_3 \bullet H_2O$ is less hazardous and thus easier to handle. Typical industrial-grade liquid ammonia contains about 27 % ammonia and 73 % water by weight. It has nearly atmospheric vapor pressure at normal temperatures and can be safely transported on the highways.

Several chemical reactions that occur in the ammonia SCR system are shown below. All of these reactions are desirable and reduce NO_X to elemental nitrogen. Equation (2) is the dominant reaction mechanism. Reactions (3), (4) and (5) involve a nitrogen dioxide reactant. NO_2 concentrations in most flue gases are low, including diesel exhaust under normal conditions. The importance of these reaction paths increases with feed gases containing increased levels of NO_2.

$$6NO + 4NH_3 \rightarrow 5N_2 + 6H_2O \quad (1)$$

$$4NO + 4NH_3 + O_2 \rightarrow 4N_2 + 6H_2O \quad (2)$$

$$6NO_2 + 8NH_3 \rightarrow 7N_2 + 12H_2O \quad (3)$$

$$2NO_2 + 4NH_3 + O_2 \rightarrow 3N_2 + 6H_2O \quad (4)$$

$$NO + NO_2 + 2NH_3 \rightarrow 2N_2 + 3H_2O \quad (5)$$

Some undesirable processes may also occur in the SCR system, meaning basically competitive and non-selective reactions with oxygen. These reactions produce secondary emissions,

or unproductively consume ammonia, at best. Partial oxidation of ammonia, shown in equations (6) and (7), may either produce nitrous oxide N_2O or elemental nitrogen. Complete oxidation of ammonia, given by equation (8), generates nitric oxide NO.

$2NH_3 + 2O_2 \rightarrow N_2O + 3H_2O$ (6)

$4NH_3 + 3O_2 \rightarrow 2N_2 + 6H_2O$ (7)

$4NH_3 + 5O_2 \rightarrow 4NO + 6H_2O$ (8)

At low temperatures, like below 100 °C to 200 °C, ammonia can also react with NO_2 to produce explosive ammonium nitrate NH_4NO_3 through equation (9). This reaction can be avoided by making sure that the temperature is over 200 °C all the time when the system is operating. The tendency of NH_4NO_3 may also be minimized by supplying less than the precise amount of NH_3 necessary for the stoichiometric reaction with NOx, if the conversion levels are low enough this way.

$2NH_3 + 2NO_2 + H_2O \rightarrow NH_4NO_3 + NH_4NO_2$ (9)

When the fuel and the flue gas contain S, SO_2 can be oxidized to SO_3 with the following formation of H_2SO_4 in reaction with H_2O, equations (10) and (11). NH_3 also can also unite with SO_3 to form $(NH_4)_2SO_4$ (12) and NH_4HSO_4 (13), that deposit on and foul the catalyst as well as other equipment. Fouling by ammonium sulfate may lead to deactivation at temperatures below 250 °C.

$2SO_2 + O_2 \rightarrow 2SO_3$ (10)

$SO_3 + H_2O \rightarrow H_2SO_4$ (11)

$NH_3 + SO_3 + H_2O \rightarrow NH_4HSO_4$ (12)

$2NH_3 + SO_3 + H_2O \rightarrow (NH_4)_2SO_4$ (13)

The injection rate of ammonia needs to be very precise, as insufficient injection may result in too low NO_X conversions, and too high injection rate results in release of ammonia to the

atmosphere. Ammonia emissions are called ammonia slip. The ammonia slip increases with higher NH_3/NO_X ratios. According to the dominant SCR reaction (2) the stoichiometric ratio in the system is about 1. Ratios over 1 immediately increase ammonia slip. In practice the used ratios are between 0.9 and 1, when the ammonia slip is minimized but the NO_X conversion is still satisfactory. The maximum ammonia slip is always specified in stationary applications, being usually from 5 to 10 ppm NH_3. These concentrations of ammonia are still usually undetectable by human nose. The ammonia slip can also be controlled by an oxidation catalyst, which could be installed downstream of the SCR catalyst. This is a good way for controlling, but increases the costs.

Figure 1 shows an example relationship between the NH_3/NO_X ratio, NO_X conversion, temperature, and ammonia slip. As seen in the Figure, the ammonia slip decreases with increasing temperature, while the NO_X conversion in SCR catalyst may either increase or decrease with temperature, depending on the temperature range and catalyst system. Aqueous ammonia injection system is presented in Figure 2.

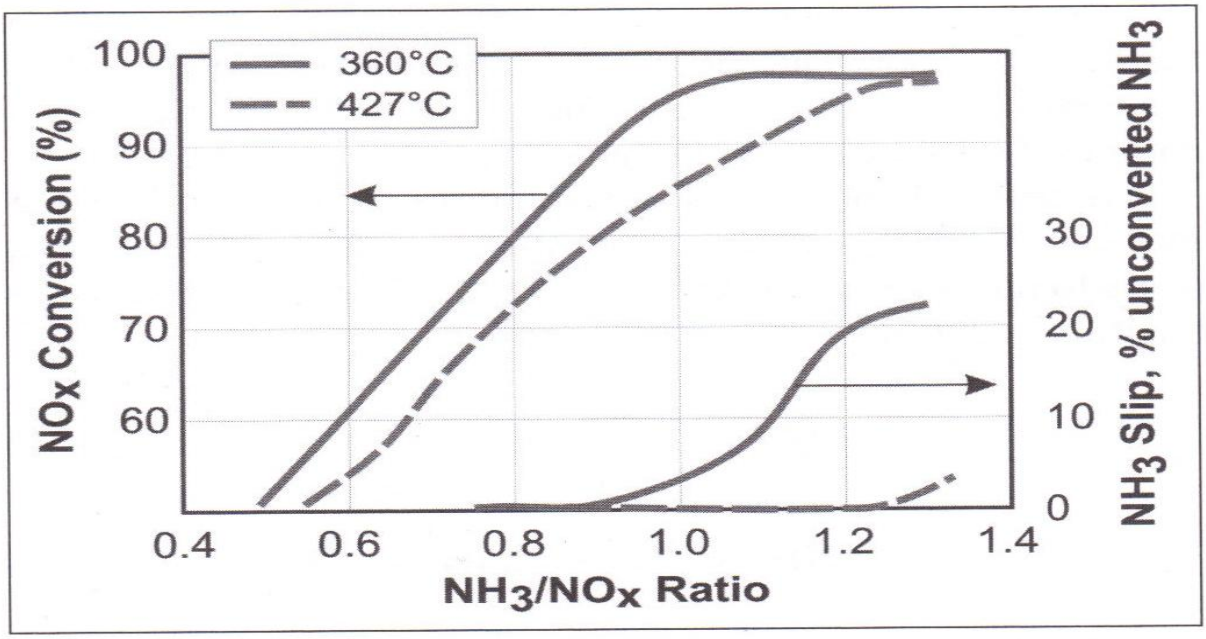

Figure 1. NO_X conversion and ammonia slip for different NH_3/NO_X ratios. V_2O_5/TiO_2 SCR catalyst, 200 cpsi (cells per square inch). (Majewski & Khair, 2006)

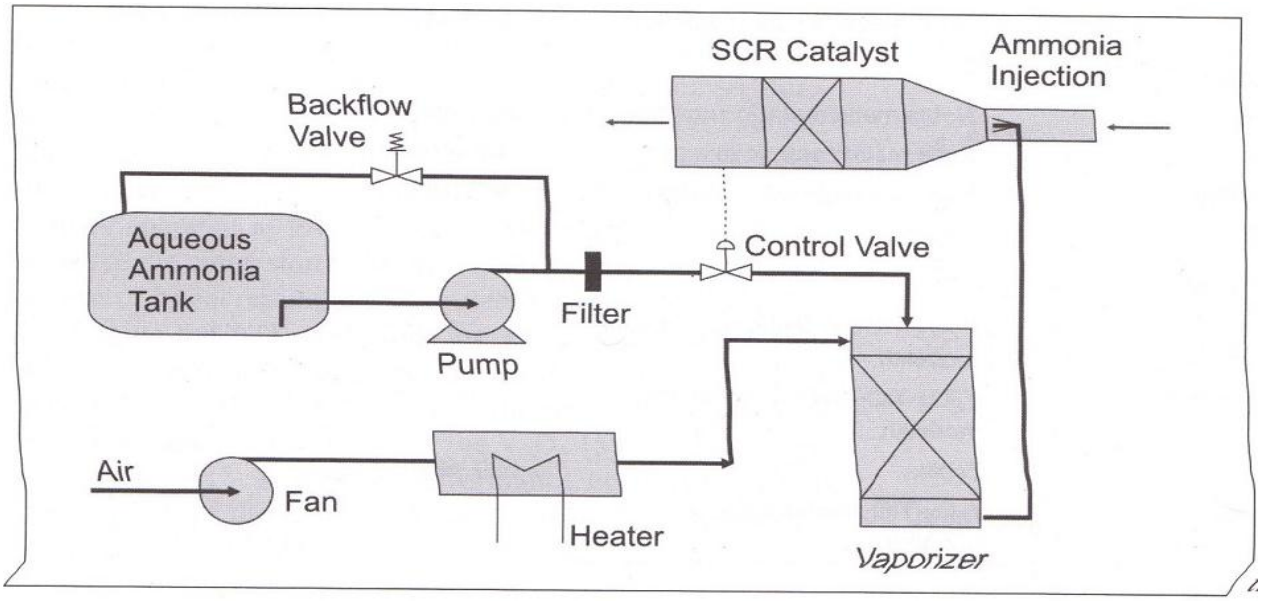

Figure 2. Aqueous ammonia injection system. (Majewski & Khair, 2006)

2.2.2. Urea

Due to toxicity and handling problems of ammonia, other SCR reductants have also been in search. Technically the alternative reductant has to easily and completely decompose to ammonia and not to produce harmful by-products under the conditions of the SCR reactor. Non-toxicity, easy to transport and handle, inexpensiveness and common availability are also very desirable features. Urea, $CO(NH_2)_2$, is the most widely accepted reductant at the moment. Other alternates that have been considered include carbamate salts, e.g. ammonium carbamate NH_2COONH_4.

Urea meets the criteria of nontoxicity and safety in handling and transportation, and it is also commonly available. Therefore it is practically the only reductant that can be considered in mobile applications at the moment. Water solutions of the urea seem to be more acceptable than solid urea.

Aqueous urea solutions used in SCR systems typically have a concentration of 32.5 wt. %. At this concentration urea forms an eutectic solution characterized by the lowest crystallization point of -11 °C. The known marketing name for this urea solution is “AdBlue”.

Adblue or other liquid urea solutions are injected directly to exhaust gas stream. At temperatures over 160 °C urea begins to decompose and hydrolyze according to the following reactions:

$CO(NH_2)_2 + \text{heat} \rightarrow 2NH_2 + CO$ (14)

$CO(NH_2)_2 + H_2O \rightarrow 2NH_3 + CO_2$ (15)

The thermal decomposition (14) is confirmed by proofed formation of CO during SCR processes with urea. The NH_2 radical can then react with NO:

$NH_2 + NO \rightarrow N_2 + H_2O$ (16)

If the urea is fed into the system at temperatures lower than 160 °C, it may foul and deactivate the catalyst. This happens probably due to the production of polymeric species that mask the surface of catalyst. This may cause serious harm in low temperature applications.

Ammonia created in equation (15) reacts with NO_X according to the equations (1) through (5). From equation (15) can be calculated that 1 kg of urea is equivalent to 0.566 kg of ammonia reagent. For 32.5 % urea solution, 1 kg of the solution is equivalent to 0.184 kg of ammonia. The principle of urea injection system is presented in Figure 3.

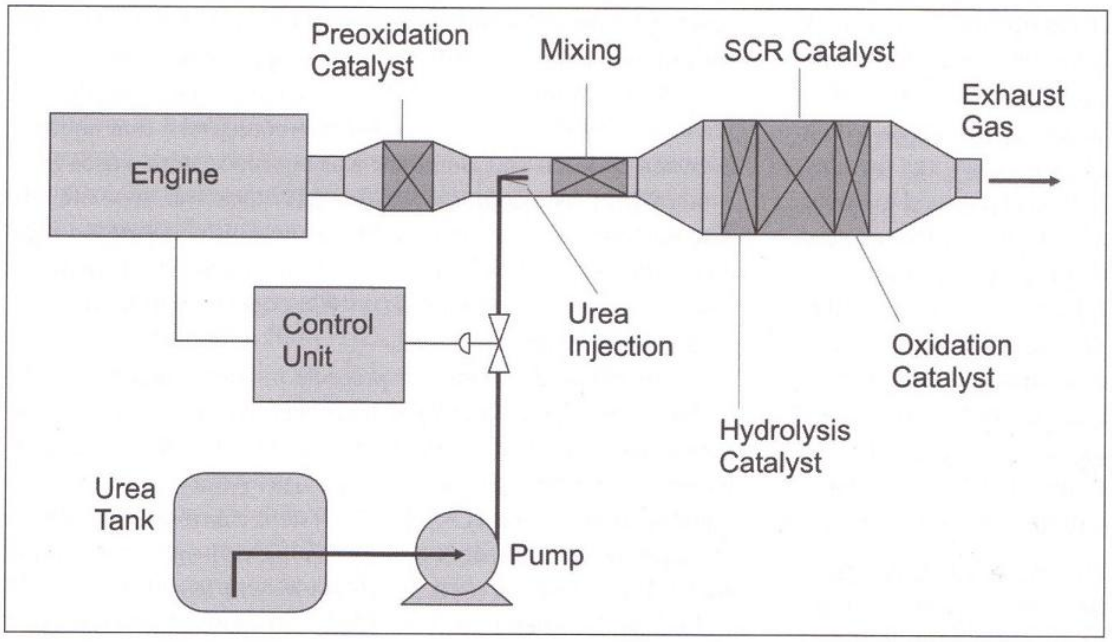

Figure 3.The principle of urea injection system. (Majewski & Khair, 2006)

Types of catalysts

Several types of catalysts can be used in SCR systems. The NO_X reduction was first discovered over a Platinum catalyst. It can be used only at temperatures under 250 °C due to its poor selectivity of NO_X at higher temperatures. A comparison of different catalyst materials and their working temperature ranges is shown in Figure 4.

Platinum catalysts lose their NO_X reduction activity above approximately 250 °C. The first catalyst used for higher temperatures was a V_2O_5/Al_2O_3 catalyst. However, its use is limited to S-free fuels because the aluminum reacted with SO_3 to form $Al_2(SO_4)_3$, which causes catalyst deactivation. To solve this problem, a nonsulfating TiO_2 carrier was used for the V_2O_5, which then came very popular. These catalysts had wider operating temperature windows and functioned better at higher temperatures than Pt. Other base metals oxides like tungsten trioxide WO_3 and molybdenum trioxide MoO_3, are often added to V_2O_5 as promoters to further decrease SO_3 formation and to result in longer catalyst life. Zeolite-based catalysts have been developed to function at even higher temperatures, as seen in Figure 4.

The active catalyst components and their operating temperature ranges are shown in Table 1. The temperatures are approximate only.

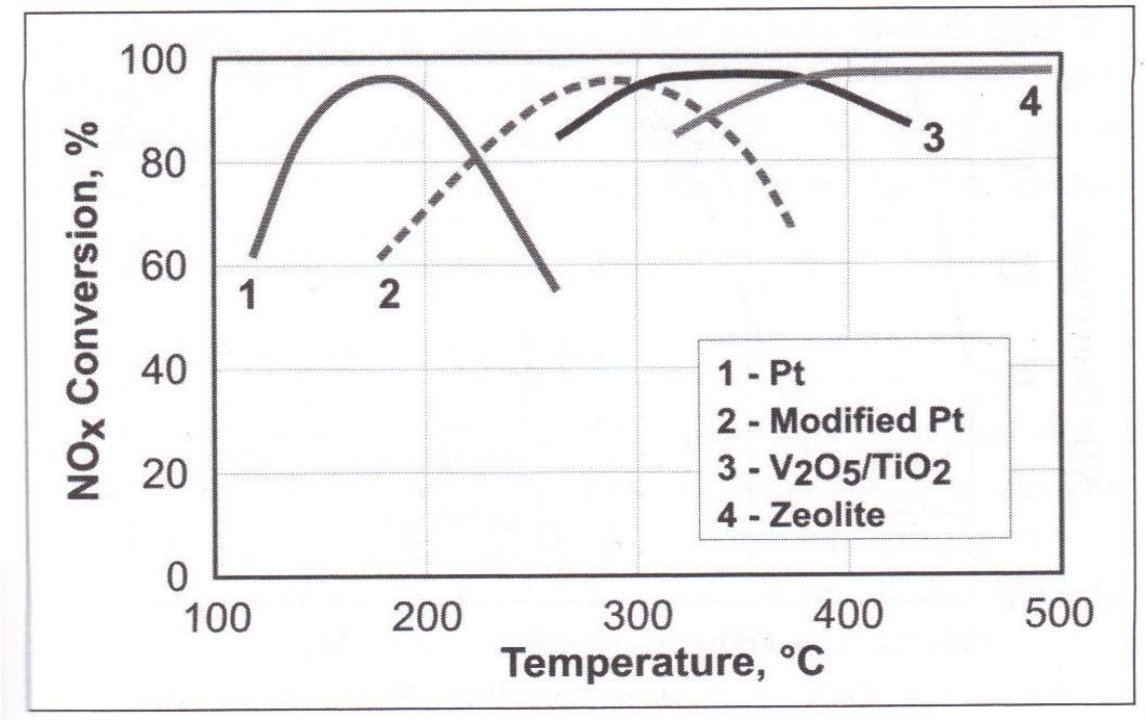

Figure 4. Operating temperature windows for different SCR catalysts. (Majewski & Khair, 2006)

Table 1. Temperature ranges of SCR catalyst materials. (Majewski & Khair, 2006)

Temperature ranges of SCR catalyst materials	
Catalyst material	Temperature range, °C
Platinum (Pt)	175-250
Vanadium (V_2O_5)	300-450
Zeolite	350-600

2.2.3. Platinum catalysts

SCR reactions from (1) to (5) take place in the platinum catalyst at low temperatures, and NO_X conversion increases with increasing temperature, peaking at slightly below 200 °C, as was seen in the Figure 4. At about 225 to 250 °C the oxidation of NH_3 to NO and H_2O becomes dominant, reaction (8). Then the conversion rate begins to fall dramatically. To use the platinum catalyst one must control the exhaust gas temperature and ensure that it stays above approximately 200 °C to avoid NH_4NO_3 formation, reaction (9), but does not exceed 225 °C, at which point the catalyst loses its selectivity toward the NO_X reduction reaction. This narrow window for temperature control adds complexity and costs on the overall process design, and the Platinum is already very expensive material. Therefore this technology is not commonly used today.

2.2.4. Vanadium / Titanium catalyst

V_2O_5-based catalysts operate best in the temperature range between 260 and 450 °C, and are considered as medium temperature catalysts. The effective temperature range is much wider than with Pt, but the range is not steady. NO_X conversion begins at approximately

225 °C rising to a plateau at about 400 °C, following to decrease in conversion due to ammonia oxidation which becomes dominant. According to Figure 4, the selectivity is lost above about 425 °C. However, newer formulations extend up to about 500 °C.

If the temperature in the V_2O_5 / TiO_2 catalyst system exceeds a certain level, high-surface-area anatase phase of TiO_2 irreversibly converts to rutile with a surface area of less than 10 m^2/g. This conversion normally takes place at about 500 to 550 °C, but catalysts can include stabilizers to increase their thermal durability. Most frequently used stabilizer for vanadia/titania formulations is tungsten trioxide WO_3. V_2O_5-WO_3/TiO_2 systems have become very common SCR catalysts for both stationary and mobile applications. Stabilized V_2O_5-TiO_2 catalysts are reported to be thermally stable up to 700 °C. Figure 5 illustrates an example of such catalyst, showing a dramatic loss of activity after aging at 750 °C for 100 hours.

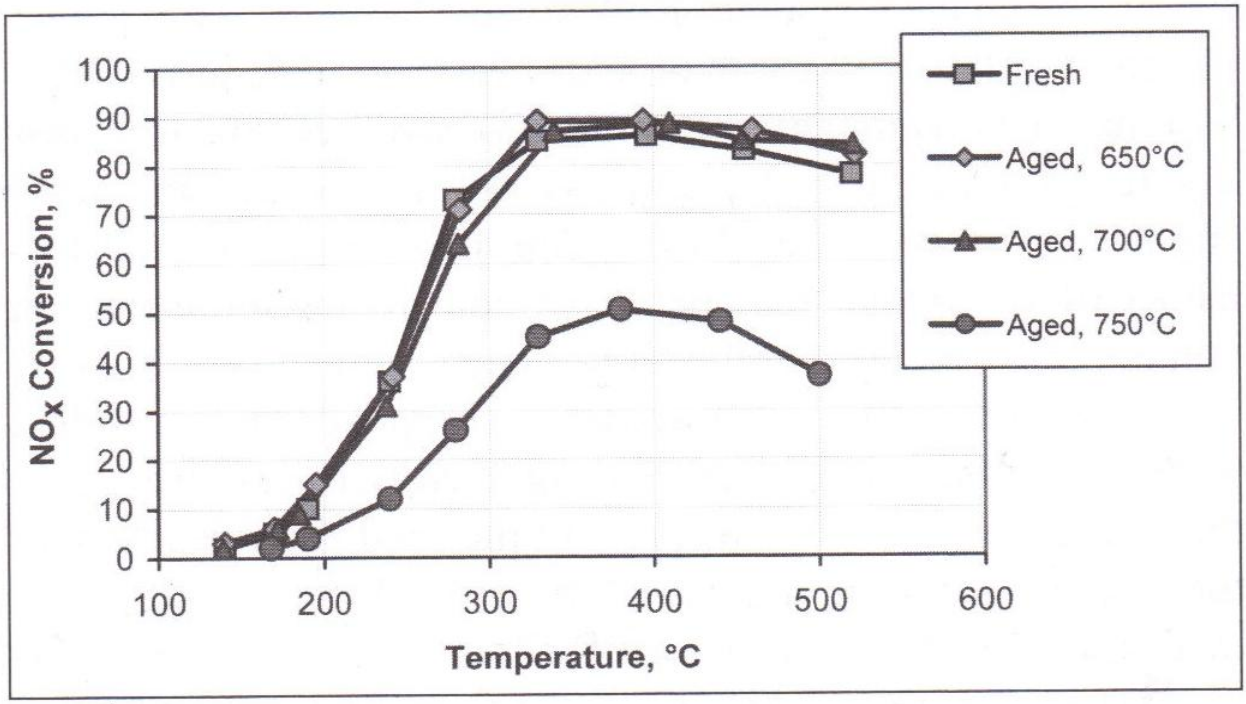

Figure 5. Thermal ageing of V_2O_5-WO_3/TiO_2 catalyst for 100 hours of furnace, ageing in 10 % H_2O and 20 ppm SO_2. (Majewski & Khair, 2006)

2.2.5. Zeolite catalysts

Zeolites are microporous, aluminosilicate minerals. The first active SCR catalyst zeolite was a mordenite. The common mordenites have crystalline structures with a SiO_2 : Al_2O_3 ratio of about 10. The catalyst manufacturers do not usually reveal the precise chemical composition of the zeolites. Zeolite SCR catalysts are commonly available for stationary engines that operate at temperatures up to 600 °C. When NO_X is present, the catalyst does not oxidize ammonia to NO according to reaction (8). Unlike Pt or V_2O_5 catalysts, its desirable selectivity towards NO_X conversion continually increases when temperature increases, as shown in Figure 4. The possible problem is to reach high enough temperatures in the first place.

Besides its good features it is also very vulnerable when water vapor is included in the system. At exposure temperatures over 600 °C with a high water content in process stream, zeolites tend to deactivate by dealumination, where the Al^{+3} ion in the $SiO_2 – Al_2O_3$ framework drifts out of the structure. This leads to permanent deactivation, which can result in collapse of the crystalline structure in extreme cases.

2.2.6. Supplementary catalysts

As mentioned earlier, the SCR system may also include an oxidation catalyst after the SCR catalyst to control the ammonia slip. Typically it is a Pt/Al_2O_3 oxidation catalyst, quite the same size as preoxidation catalyst, but less loaded with metal. Some are reported to be 10 g/ft^3 (~0.35 g/dm^3). A hydrolysis catalyst can also be placed before the SCR catalyst. It is usually a base metal oxide formulation.

3. DEACTIVATION OF V_2O_5/WO_3-TiO_2 SCR CATALYSTS

3.1. CHEMICAL DEACTIVATION

Chapter 3.1. with its Figures and Tables is fully based on an article written by Oliver Kröcher and Martin Elsener, 2008.

3.1.1. Introduction

In this investigation some catalyst samples were exposed to different lubrication oil additives and to potassium (K) which simulates of being from raps methyl ester added to Diesel fuel. The additives were Ca, Mg, Zn, P, B and Mo. Standard V_2O_5/WO_3-TiO_2 catalyst samples were first impregnated with water soluble compounds of these elements and then calcined at 400 and 550 °C. The mission was to investigate the chemical deactivation potential of the single elements and their combinations. Ca, Zn, P and K are all ordinary trace elements of liquid biofuels. The catalyst samples used here were similar to a heavy duty Diesel truck SCR catalyst. Investigation's interest was on pure chemical deactivation, excluding other mechanisms such as pore blocking.

Standard metal substrates with a cell density of 400 cpsi, length of 21 mm and diameter of 21 mm, volume of 7.2 cm^3 were coated by Wacker Chemie with 1.3 g of a V_2O_5/WO_3-TiO_2 catalyst which was developed for SCR onboard of heavy-duty Diesel vehicles. The catalysts were warmed for 50 hours at 550 °C before the tests. The tests were began with 0.4 mol% of doping element based on the sum of titanium, tungsten and vanadium, which was equal to 20 mol% based on vanadium. The catalyst module was dipped in aqueous solution for 2 s, and after that the module was shortly blown out to remove excess impregnation solution without change in the solution uptake. The chemicals used for aqueous impregnations are shown in Table 2. Prior the first measurement, all the catalyst samples were sul-

fated with 100 ppm SO_2 at 400 °C for 5 h. After weighing the catalyst module it was dried at 90 °C and then calcined at 400 °C for 5 h. Then the catalyst performance was measured, and after the measurements all the catalysts were calcined again, this time at 550 °C for 5 h, and then tested again. The exhaust gas used for tests consisted of 10 % O_2, 5 % H_2O, 1000 ppm NO, 0 to about 2000 ppm NH_3 and balance N_2.

Table 2. Doping elements. (Kröcher & Elsener, 2008)

Element	Precursor	Formula	Quality	Supplier
Potassium (K)	Potassium carbonate	K_2CO_3	Puriss.	Fluka
	Potassium sulfate	K_2SO_4	Pro analysi	Merck
	Potassium hydrogensulfate	$KHSO_4$	Pro analysi	Merck
Molybdenum (Mo)	Ammonium molybdate	$(NH_4)_6Mo_7O_{24}{\cdot}4H_2O$	Ultra (>99%)	Fluka
Phosphorus (P)	Orthophosphoric acid (85%)	H_3PO_4	Pro analysi	Merck
Sulphur (S)	Sulphur dioxide	SO_2	1% in N_2 (>99.9%)	Carbagas
Zinc (Zn)	Zinc acetate	$Zn(CH_3COO)_2{\cdot}2H_2O$	Puriss.	Fluka
Boron (B)	Orthoboric acid	H_3BO_3	Puriss.	Fluka
Calcium (Ca)	Calcium acetate	$Ca(CH_3COO)_2{\cdot}xH_2O$	96%	Merck
Magnesium (Mg)	Magnesium acetate	$Mg(CH_3COO)_2{\cdot}4H_2O$	Purum	Fluka

3.1.2. Doping with single elements

After calcination at 400 °C for 5h

Figure 6 shows the NO_X reduction at 10 ppm ammonia slip for a new undoped catalyst and the single doped catalysts after calcinations of 400 and 550 °C for 5 h. For boron as ortho-boric acid no deactivation of any kind was found, and for molybdenum only slight decrease at 200 and 250 °C. The addition of molybdenum increased N_2O formation up to three times more to 40 ppm at 450 °C, not seen on the Figure. Doping with phosphorus (P) resulted in moderate decrease of activity, as at below 300 °C it was 20-25 % less than original activity but at 450 °C the decrease was only 3-4 %. The k_{mass} was also lowered to 80-85 % of its original value. The relative k_{mass} value represents the intrinsic activity loss of the catalyst at

low temperatures, under 300 °C. Zn addition caused about 50 % loss of the catalyst activity k_{mass}. The reduction at high temperatures was 80-90 % of the original value, but at lower temperatures the loss of activity was much more significant. The Ca addition caused an activity drop to 40 % of the original value. This was seen on the entire temperature range. Also Mg caused clear activity loss at all temperatures, but it was less hazardous than Ca. The addition of K caused very severe deactivation. The catalyst activity was less than 10 % of its original value. This indicates that K is a very strong poison for vanadium-based catalyst, and 0.4 mol% is heavily too much for the catalyst.

After calcination at 550 °C for 5h

After the first measurement the catalysts were calcined again but at temperature of 550 °C, to intensify the solid-state reactions of the catalysts with the dopants. The boron doped catalyst showed the same activity again. The activities of the others were increased by 10-20 %, meaning that the deactivation was partly restored by the second calcination. No increase in N_2O formation was observed for any other doped catalysts except for the molybdenum contained sample. The N_2O formation was affected in parallel to the deactivation, but these results were not shown more detailed in the study.

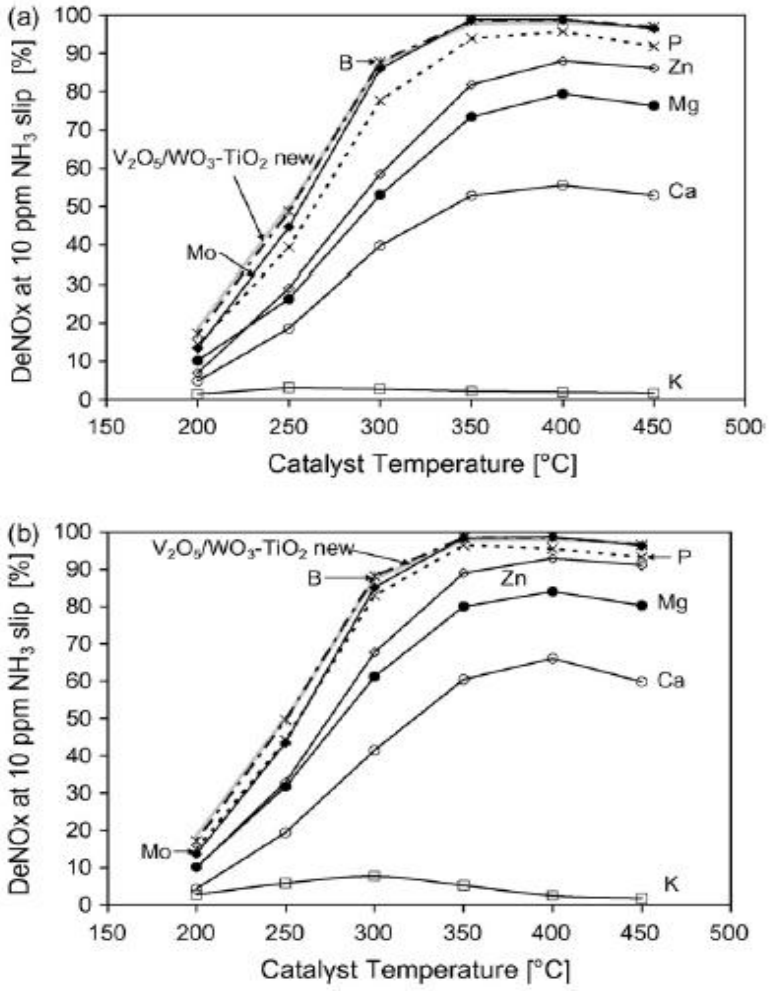

Figure 6. Catalysts doped with single elements after calcinations of (a) 400 °C for 5 h and (b) 550 °C for 5 h. (Kröcher & Elsener, 2008)

Doping with different amounts of K

Doping with 0.4 mol% K resulted in a very strong deactivation. Clearly higher $DeNO_X$ values were observed at low temperatures when the doping was lowered to 0.2 mol%, as seen in Figure 7. Still at 450 °C only 15 % of the original value was measured. With addition of only 0.11 mol% K the deactivation was found to be moderate. These $DeNO_X$ values were between 0.4 mol% of Zn and Ca, indicating that K is about four times stronger poison. Af-

ter the second calcinations the changes in results were similar to other catalysts. Zn, Ca and K are also compared in Figure 18 in Chapter 3.3.

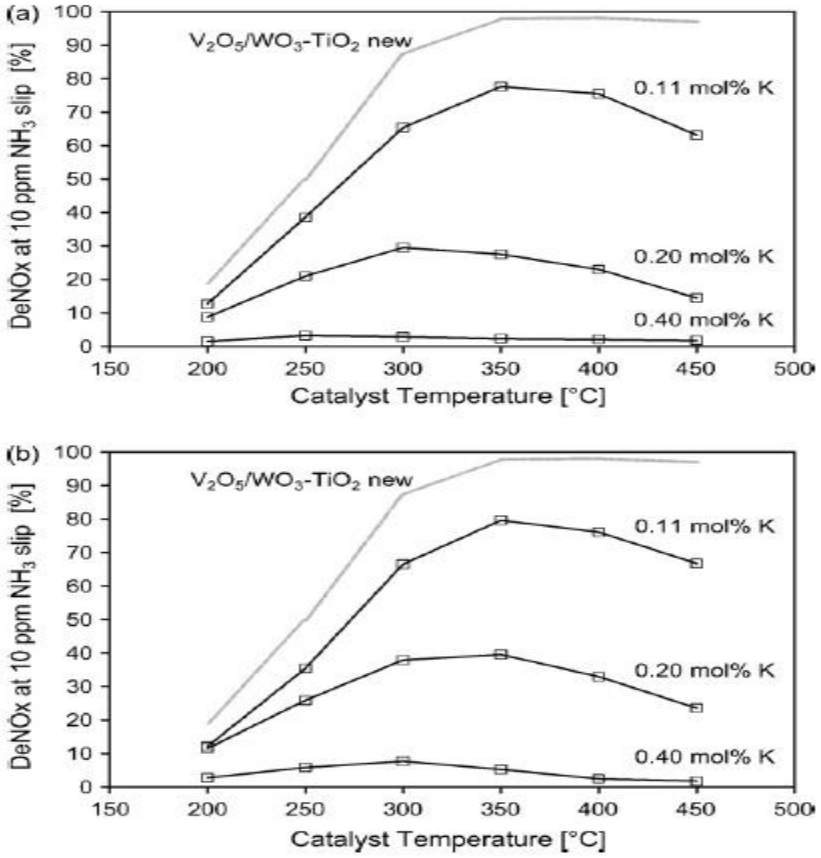

Figure 7. Catalysts deactivated by different amounts of K, after calcinations of (a) 400 °C and (b) 550 °C for 5 h. (Kröcher & Elsener, 2008)

3.1.3. Effect of counter-ions

The influence of counter-ions from inorganic acids was tested by doping catalysts with the same concentration of K in three different forms of K salts. Potash K_2CO_3 was the basic, K_2SO_4 was the neutral and $KHSO_4$ was the acidic salt. Ca was tested as sulfate, phosphate and borate, Mg as sulfate and phosphate, and Zn was as phosphate and borate. The concentration of each element was 0.4 mol%, except for the sulfates of Ca and Mg, which were prepared as sulfates in the catalyst, explained in the study. A simple 1:1 ratio was chosen for the cations and anions, since the real concentration ratios in exhaust gases is still un-

known. There is also a lack of information about how they meet on the surface and what the exact reaction products are.

The results are shown in Figure 8. The deactivation potential of K is so strong that hardly any effect was found for the additional components. $DeNO_X$ decreased below 10 % of the original value for K sulfate, and did not exceed 20 % for K hydrogensulfate. Also the $DeNO_X$ results of K with boron or P were extremely low.

The deactivating effect of Ca strongly depends on the acidity of the compound. $CaSO_4$ showed no deactivating effect at high temperatures. The addition of orthoboric acid slightly improved the Ca doped catalyst, as seen when comparing the Figures 6 and 8.

The suplphated and phosphated Mg doped samples showed a clearly higher activity than the sample without counter-ions. The activity of the catalyst with sulfated Mg was reduced in the second calcination, but with phosphated Mg it stayed about the same.

The combination of Zn with P resulted in a lower deactivation than the Zn alone at lower temperatures, but at 400 and 450 °C the results were about equal. The result with Zn and boron was close to Zn's alone, only little smaller $DeNO_X$ values were observed and after second calcinations the results were practically the same. The activity of the catalysts Zn/B and Zn were improved by the second calcination, but the Zn/P containing catalyst remained roughly at the same level. After all they were at quite the same level.

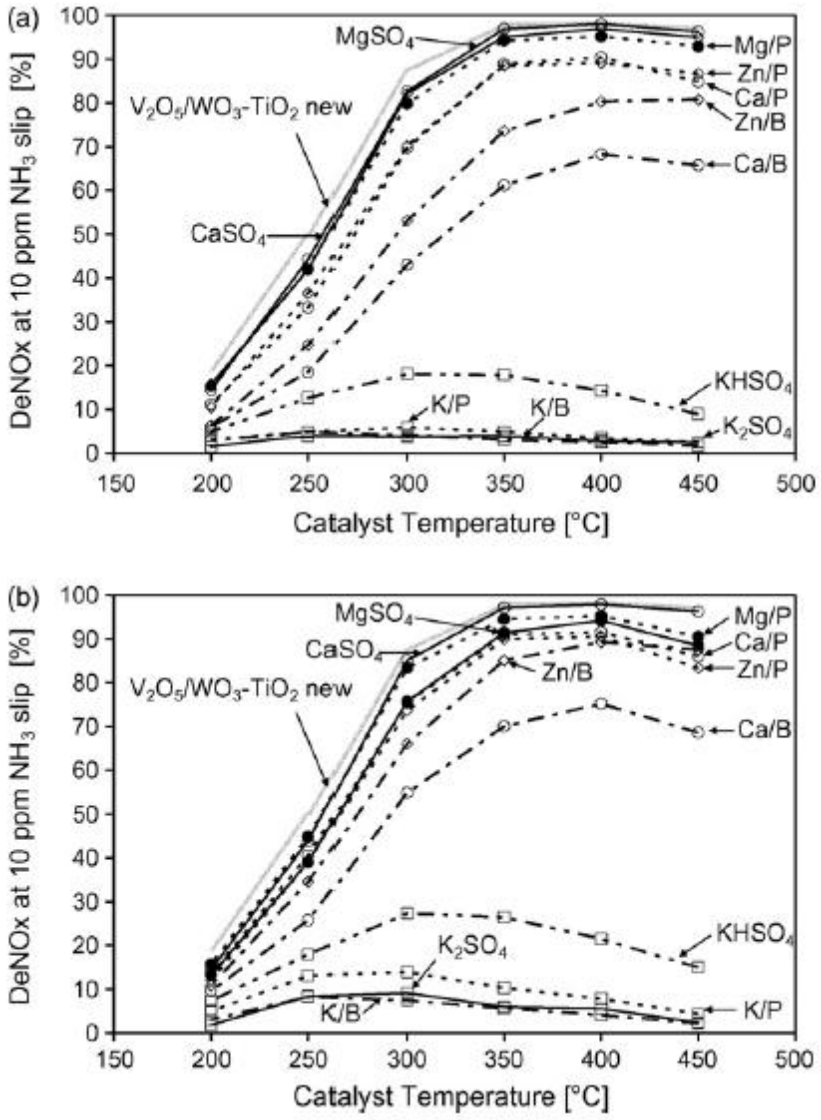

Figure 8. Effect of counter-ions on the deactivation potential, after calcinations of (a) 400 °C and (b) 550 °C for 5 h. (Kröcher & Elsener, 2008)

3.1.4. Doping with combinations of cations and anions

A catalyst with 0.4 mol% boron and P demonstrated just a slight deactivation after the first calcination, being at near the same level as only boron doped catalyst, Figure 9. The original values were reached elsewhere than at 450 °C where a small decrease was found after

the second calcination. The difference between the Zn and the Ca doped catalysts compared to their sulfates doped was notable. The catalysts were strongly deactivated by the Zn and the Ca after the first calcination, whereas the catalyst with their sulfate was comparable to Zn/P sample at Figure 8. After the second calcination the deactivation was slightly increased compared to Zn/P. The catalyst with $CaSO_4$/Zn remained about the same level after the second calcination. The catalysts with P/B, Ca/Zn/P/SO_4 and Ca/P/SO_4 had very similar results between themselves. The K doped catalysts showed strong deactivation results as expected. Also Ca/Zn showed quite severe deactivation, as its best $DeNO_X$ values were around 30 % after the first and around 40 % after the second calcination.

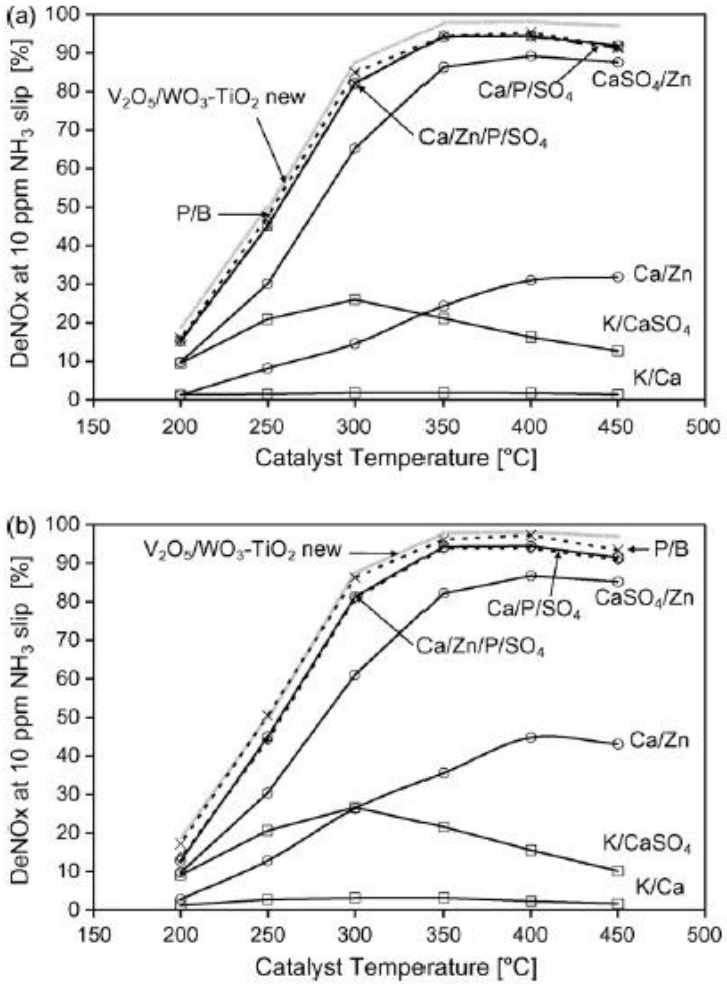

Figure 9. Effect of combinations of elements, after calcinations of (a) 400 °C and (b) 550 °C for 5 h. (Kröcher & Elsener, 2008)

3.1.5. Ammonia adsorption

One very important aspect of SCR performance is its ability to adsorb ammonia. This will be discussed more in this thesis later on. The results of this investigation are shown here very shortly and superficially. The ammonia adsorption ability of the catalyst influenced by K was greatly reduced.

The K containing catalyst exhibited large amounts of ammonia already for small NO_X reductions. With increasing the ammonia dosage the ammonia slip increased as well as the $DeNO_X$ values. The maximum $DeNO_X$ was reached for an ammonia slip of 10,000 ppm, which is obviously too large emission itself and also too expensive in real-life situation. The ammonia slip is shown in Figure 10. As seen in the Figure, the maximum $DeNO_X$ values were only 80-90 % at 400 and 450 °C, meaning that the catalyst could not achieve its original potential, no matter how large the ammonia injection was. Some of the catalyst material was poisoned for good.

The final results of this investigation are shown in Table 3. The mean relative $DeNO_X$ at 10 ppm NH_3 slip after calcinations 1 and 2 are shown, and the elements have been put in order by the deactivation effects. K was easily the strongest poison, but also Ca, Zn and Mg showed medium strong or strong deactivation, which are not acceptable in real-life solutions.

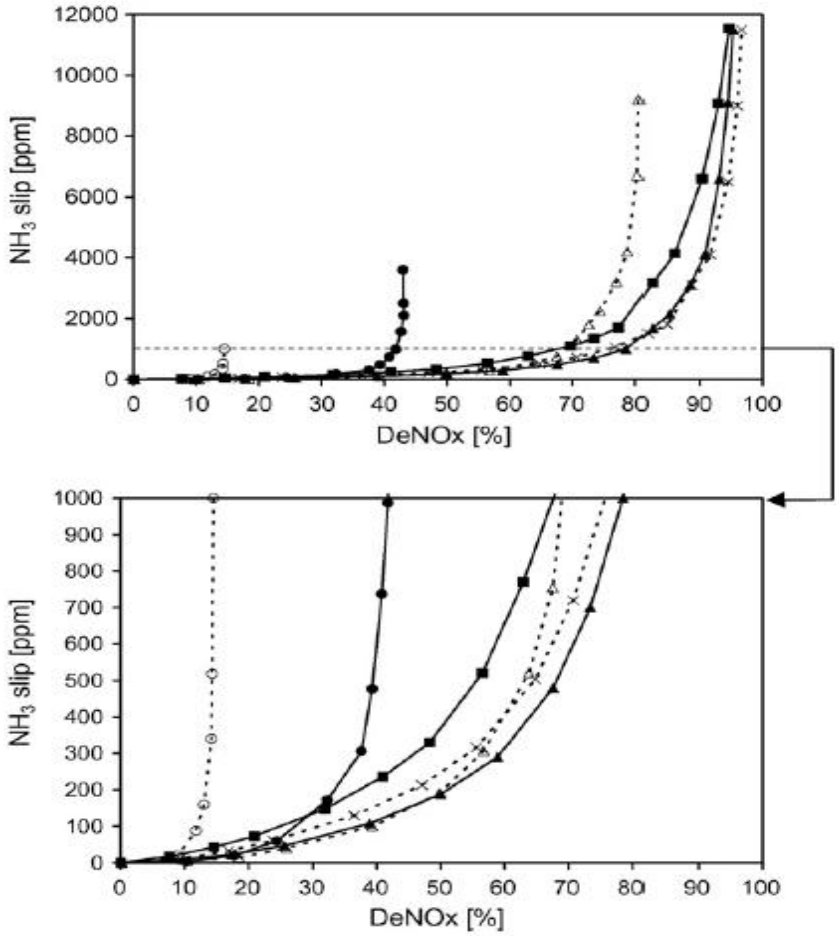

Fig. 6. Ammonia slip as function of $DeNO_x$ for the catalyst sample deactivated by 0.4 mol% K/P. *y*-Axis extended to 1000 and 12,000 ppm NH_3, respectively. (○) 200 °C, (●) 250 °C, (△) 300 °C, (▲) 350 °C, (×) 400 °C, (■) 450 °C.

Figure 10. The ammonia slip for the K/P deactivated catalyst. (Kröcher & Elsener, 2008)

Table 3. Deactivation potential of doping elements. (Kröcher & Elsener, 2008)

Deactivation potential of doping elements on $V_2O_5/WO_3–TiO_2$ SCR catalysts

Mean rel. $DeNO_x$ at 10 ppm NH_3 slip					
Calcination at 400 °C for 5 h	Second calcination at 550 °C for 5 h				
Slight deactivation					
0.98	0.99	B			
0.94	0.97	P/B			
0.93	0.93			$CaSO_4$	
0.93	0.93	Mo			
0.91	0.92			Mg/P	
0.89	0.92	P			
Moderate deactivation					
0.92	0.86			$MgSO_4$	
0.79	0.86			Ca/P	
0.80	0.83		Zn/P		
0.71	0.79		Zn		
0.64	0.78		Zn/B		
0.78	0.76		$Zn/CaSO_4$		
0.73	0.73				0.1 mol% K
0.67	0.73			Mg	
Medium strong deactivation					
0.53	0.64			Ca/B	
0.46	0.50			Ca	
0.32	0.43				0.2 mol% K
Strong deactivation					
0.22	0.33			Ca/Zn	
0.29	0.28				$K/CaSO_4$
0.19	0.28				$KHSO_4$
Very strong deactivation					
0.05	0.12				K/Zn
0.06	0.09				K/B
0.05	0.08				K_2SO_4
0.07	0.15				K/P
0.04	0.07				0.4 mol% K
0.03	0.04				K/Ca

3.1.6. Conclusions

- Potassium (K) showed a very strong deactivation effect alone and with any component included.
- Zn and Ca also showed so high deactivations that 0.4 mol% of poison is too much in real-life situation, except for $CaSO_4$.
- After second calcinations the $DeNO_X$ results were usually little better.

3.2. EFFECTS OF ADDITIVES AND IMPURITIES

Chapter 3.2. with its Figures and Tables is fully based on an article written by D. Nicosia, I. Czekaj and O. Kröcher, 2008.

This investigation follows the previous and tells us more about Ca and K as deactivating agents, and especially extends the DRIFT characterization study.

3.2.1. DRIFT characterization of adsorbed NH_3 species

The differential spectras of the adsorbed ammonia species on the fresh catalyst are shown in Figure 11, and on the Ca- and K-containing catalysts in Figure 12. They were recorded after flushing with N_2 at room temperature (RT) for 30 minutes. Ca- and K-containing samples showed much lower IR-signals of the adsorbed NH_3 species than the fresh sample. This supports the results of the lower NH_3 adsorption in the NH_3-TPD measurements, Figure 19 in next Chapter. A large downhill between 3500 and 2250 cm^{-1} is characteristic for the stretching vibration of weakly adsorbed ammonia. The regions between 1300 and 1700 cm^{-1} and 2200 and 1900 $cm^{-}1$ are the most important to analyze. The former region is known to be where ammonia adsorbs on Brønsted and Lewis acid sites. This region is represented well in Figure 20 in the next Chapter. The bands at 1425 and 1670 cm^{-1} indicate ammonia protonation at Brønsted acid sites. Further on, the band at 1605 cm^{-1} is connected with the ammonia species coordinated to the Lewis acid sites. The region between 2200 and 1900 cm^{-1} is typical for V^{5+} = O sites, magnified in Figures 13 and 14. These signals have been identified as the fundamental $2\nu(V^{5+} = O)$ first overtone vibration. The form of inverse peak points out that V^{5+} = O groups on the catalyst surface were consumed upon reduction with ammonia. The presence of the poisoning elements on the SCR catalyst surface did not stop the ammonia adsorption on the Lewis and the Brønsted acid sites. This is shown in the signals at 1425, 1670 and 1605 cm^{-1} in Figure 12. From Figures 11 and 12 three observations can be pointed out:

- The signal intensity of NH_3 coordinated to Lewis acid sites 1605 cm^{-1} did not change almost at all despite of poisoning
- The poisoning had strong negative effect on the signal intensity at 1425 and 1670 cm^{-1} indicating the adsorption of NH_3 on Brønsted acid sites
- The negative signals between 2200 and 1900 cm^{-1} were much smaller with poisoned samples than fresh sample

These results suggest that the poisoning elements affect only the Brønsted acid sites and the reactivity of the V^{5+} = O sites.

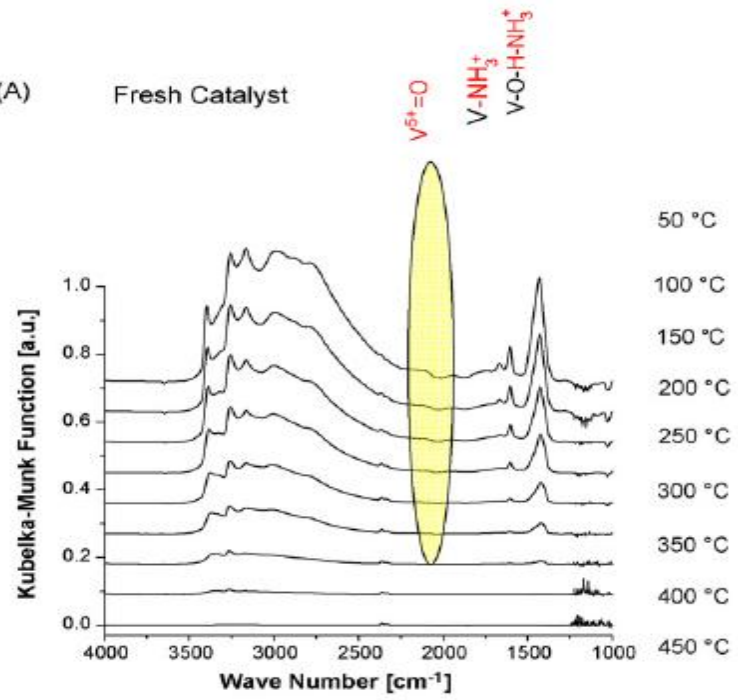

Figure 11. DRIFT spectra of adsorbed NH_3 species on the fresh catalyst from room temperature to 450 °C. (Nicosia *et al.*, 2008)

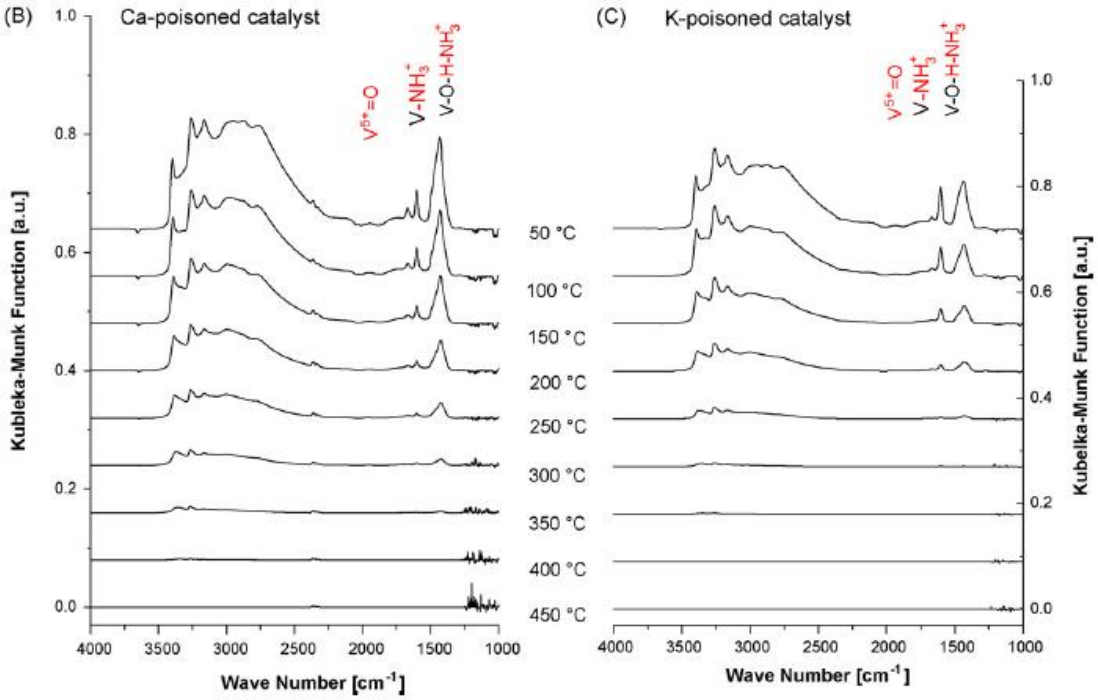

Figure 12. DRIFT spectra of adsorbed NH_3 species on the Ca-containing (B) catalyst and the K-containing catalyst (C) from room temperature to 450 °C. (Nicosia *et al*., 2008)

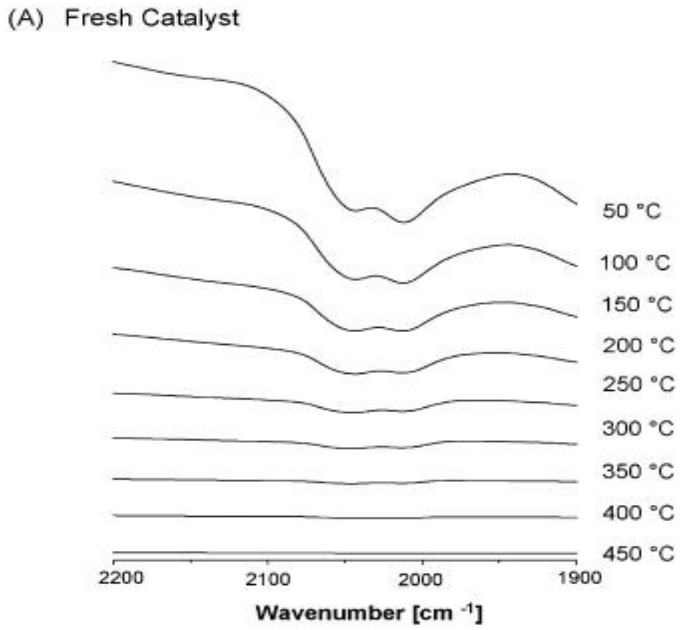

Figure 13. DRIFT spectra of the fundamental $2\nu(V^{5+} = O)$ first overtone, collected from RT to 450 °C after adsorption of NH_3, fresh catalyst. (Nicosia *et al.*, 2008)

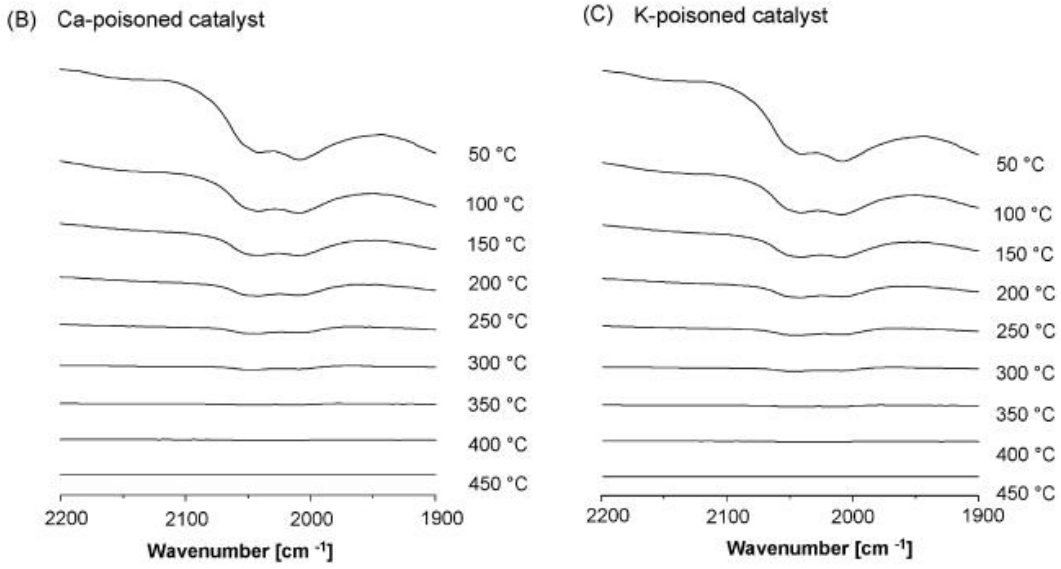

Figure 14. DRIFT spectra of the fundamental $2\nu(V^{5+} = O)$ first overtone, collected from RT to 450 °C after adsorption of NH_3, Ca-poisoned catalyst and K-poisoned catalyst. (Nicosia *et al.*, 2008)

The stability of the NH_3 adsorbed species on the different samples can be compared by following the regeneration of the Brønsted and Lewis sites. Figure 15 shows that the integral intensity of the signal of NH_3 adsorbed on the Lewis acid sites decreased with temperature, independent from the poisoning. As seen in the Figure, the intensity of the signal of NH_3 adsorbed on the Brønsted acid sites followed a trend that strongly depended on the type of poisoning element. The fresh catalyst showed not only the largest NH_3 adsorption on the Brønsted acid sites but also a relatively fast regeneration of the sites. This is evidenced by the strict slope of the curve. The Ca-containing sample did worse than fresh but better than K-containing. The K-containing sample showed the lowest adsorption of the ammonia on the Brønsted acid sites as well as slowest surface regeneration.

Integration of the $2\nu(V^{5+} = O)$ overtone bands also gave results seen in Figure 16. In the Figure a more negative value corresponds to a higher number of $V^{5+} = O$ groups reacted. The results show almost complete regeneration of $V^{5+} = O$ sites after N_2-flushing and heating. This occurred independently of the type of poisoning element. The strong negative values found for the fresh sample already at low temperature suggests that the number of active $V^{5+} = O$ sites was much higher for the fresh sample compared to the poisoned ones, meaning that the poisoning elements prevent these sites from reacting with NH_3.

It has been found by Chen *et al*. (1990) that there is a clear correlation between the poisoning strength and dopant basicity. They concluded that the Brønsted acid sites are responsible for the SCR activity, and thus they are vulnerable for poisons. The authors of this investigation did an examination, trying to find an alternative explanation for the strong deactivating potential of alkali metals. They tried to found spectroscopic evidence for KVO_3 formation, and found it to be quite weak. Only very localized deactivation effect is expected, when KVO_3 is formed at the surface with a single vanadium center. This is opposite to the alkali metals that deactivate already on very low concentrations. This means that there must be a mechanism where more than one vanadium center is affected.

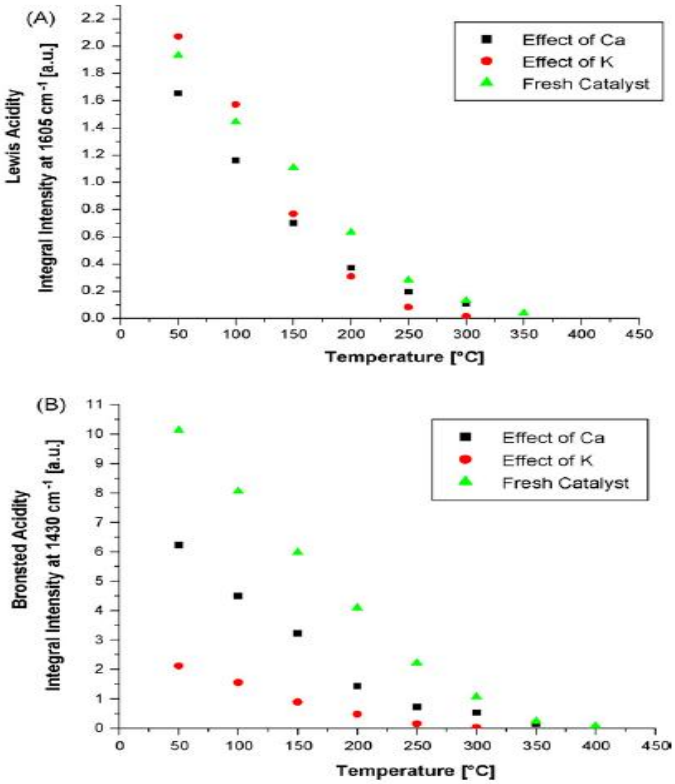

Figure 15. The Effect of temperature on the integral intensity of the NH_3 signal on Lewis acid sites and Brønsted acid sites. (Nicosia *et al.*, 2008)

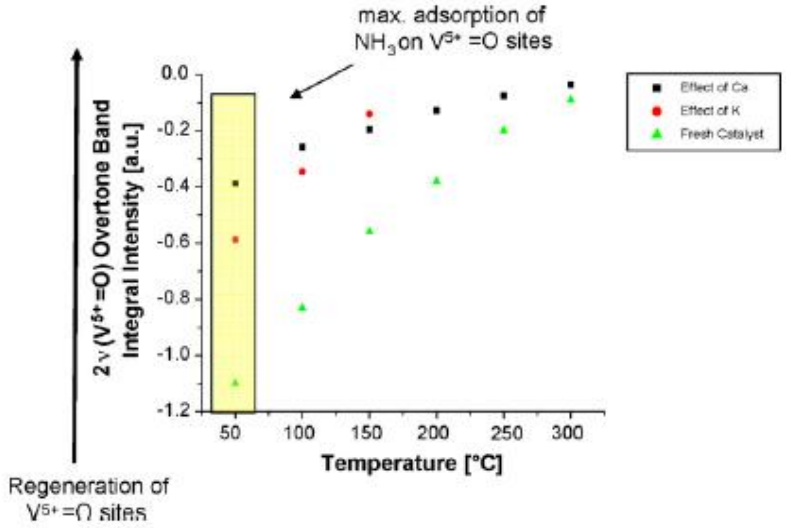

Figure 16. Effect of temperature of the integral intensity of the fundamental $2\nu(V^{5+} = O)$ first overtone vibration. (Nicosia *et al.*, 2008)

3.2.2. X-ray photoelectron spectroscopy and DFT calculations

Without going into details in this survey, some observations were done by the authors. Ca and PO_4 containing catalyst showed a remarkably weak deactivation. The poisoning elements K or Ca interact mainly with the oxygen in the vanadia phase and not with the titanium or tungsten support.

3.2.3. Conclusions

- The poisoning elements affect only the Brønsted acid sites and the reactivity of the $V^{5+} = O$ sites.
- The number of the active $V^{5+} = O$ sites was much higher for the fresh sample compared to the poisoned ones, thus indicating that the poisoning elements prevent these sites from reacting with NH_3.
- The basicity of dopants affects strongly to Brønsted acidity, thus effecting to SCR activity as Brønsted acid sites are responsible of it.

3.3. DEACTIVATION BY BASIC ELEMENTS

Chapter 3.3 with its Figures and Tables is fully based on an article written by D. Nicosia, M. Elsener, O Kröcher and P. Jansohn, 2007.

V_2O_5/WO_3-TiO_2 coated metal substrates from Wacker-Chemie GmbH were impregnated with water soluble compounds of the elements Ca, P, Zn, B, S, Mo and K and their combinations. The total loading of the elements was 0.4 mol%. The coated catalyst modules were tested in a reactor trying to copy the typical conditions of a heavy-duty SCR catalyst system. Model gases were 10 % O_2, 5 % H_2O, 1000 ppm NO and 0-2000 ppm NH_3 at a GHSV of 52,000 h^{-1}.

3.3.1. $DeNO_X$ activity

Figure 17 shows the $DeNO_X$ activity at 10 ppm NH_3 slip for poisoned V_2O_5/WO_3-TiO_2 catalyst samples. The highest NO_X conversion was with fresh catalyst between 200 and 450 °C as expected. Conversion with fresh catalyst reached a plateau at 350 °C, where the activity was about 100 %. The presence of phosphate showed a slight deactivation effect at lower temperatures. Between 350 and 400 °C the activity was still very high, but it started decreasing at 400 °C. Ca caused a strong deactivation, as the activity was only 60 % at 350 °C and the activity hit the highest level of about 65 % at 400 °C. However, the deactivation by Ca was negligible when anions from inorganic acids (SO_4^{2-} > PO_4^{3-} > BO_3^-) were also present. Zn was much less deactivating than Ca, but the anion effect with Zn-containing sample was not as positive as it was with Ca-containing sample. K caused the biggest deactivation resulting in less than 10 % NO_X conversion at 250 °C. Overall the results were close to those found in Chapter 3.1.

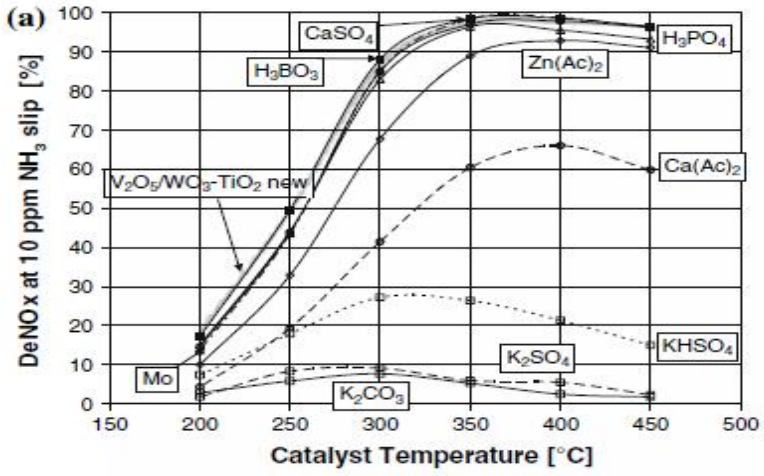

Figure 17. $DeNO_X$ activity of the poisoned and fresh V_2O_5/WO_3-TiO_2 SCR catalysts measured at 10 ppm NH_3 slip. (Nicosia *et al*., 2007)

To measure the maximum allowable K loading, two additional catalysts containing 0.2 and 0.1 mol% of K were prepared. The results are shown in Figure 18. The 0.2 mol% K containing sample showed a lot higher SCR activity at lower temperature, about 60 % at 200 °C. At 450 °C the sample showed only an activity of about 23 %. Moderate deactivation was observed only for the 0.1 mol% K containing sample over the entire temperature range. The deactivation effect of different elements and their combinations are summarized in Table 4.

The degree of N_2O production at >500 °C was not influenced by different compounds except for molybdenum which increased N_2O production a little.

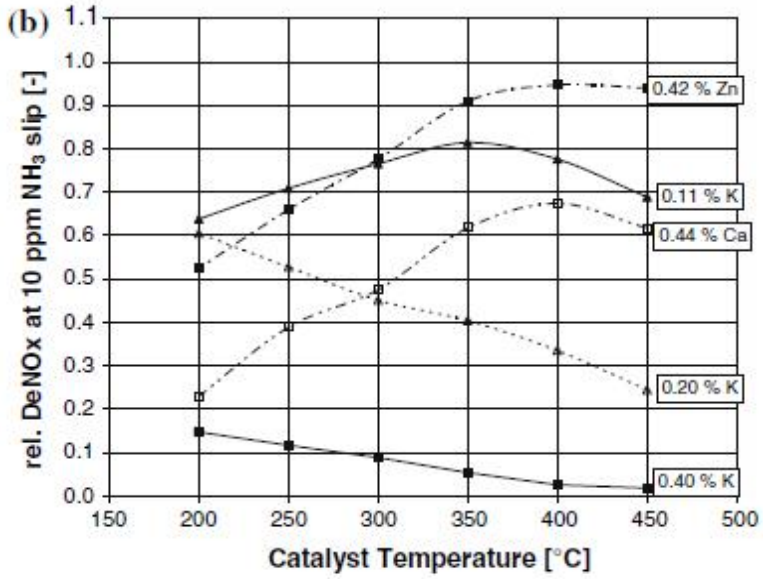

Figure 18. Influence of K concentration compared to Zn- and Ca-containing samples. (Nicosia *et al*., 2007)

Table 4. Deactivation potential of different poisoning agents and their combinations on the SCR activity. (Nicosia *et al*., 2007)

Relative $DeNO_x$ at 10 ppm NH_3 slip	Element (containing 0.4 mol%, based on catalyst; ≈20 mol%, based on vanadium)					Influence of increasing amounts of K
>95% moderate deactivation	P	B	$CaSO_4$	Mo	P/B	
75–85%	Zn	Zn/P	Zn/B	Ca/P		K (0.1 mol%)
40–70%	Ca	Ca/B	$Zn/CaSO_4$			K (0.2 mol%)
20–40%	Ca/Zn	$K/CaSO_4$				
<20% strong deactivation	K	K/P	K/B	K/Zn	K/Ca	K (0.4 mol%)

3.3.2. Temperature programmed desorption of ammonia – NH_3-TPD

One of the most important aspects of the SCR process is the adsorption of ammonia on the catalyst surface, as mentioned before. Therefore the SCR effect strongly depends on the surface acidity. Temperature programmed desorption of ammonia experiments were performed to investigate the effects of deactivation agents. In Figure 13 are shown the NH_3-TPD curves of the fresh, and the Ca and the K containing catalysts in temperature range

between 100 and 500 °C. No precise amounts of alkali metals were told in the study. All three curves exhibit two peaks corresponding to weakly and strongly bound ammonia. For all samples a large ammonia evolution was observed between 100 and 200 °C when ammonia adsorption was performed at 100 °C. The evolution in this range is very similar with fresh and K-containing samples, but noticeably lower at Ca-containing sample. Similar amounts of ammonia evolved from the K- and the Ca -containing samples at higher temperatures from 200 to 300 °C, but much less than from the fresh sample. The ammonia desorption was complete at around 450 °C for the Ca-containing sample, while ammonia was fully desorbed only between 400 and 450 °C with the K-containing sample. These results are in good agreement with the $DeNO_X$ activity trend observed in Figure 17.

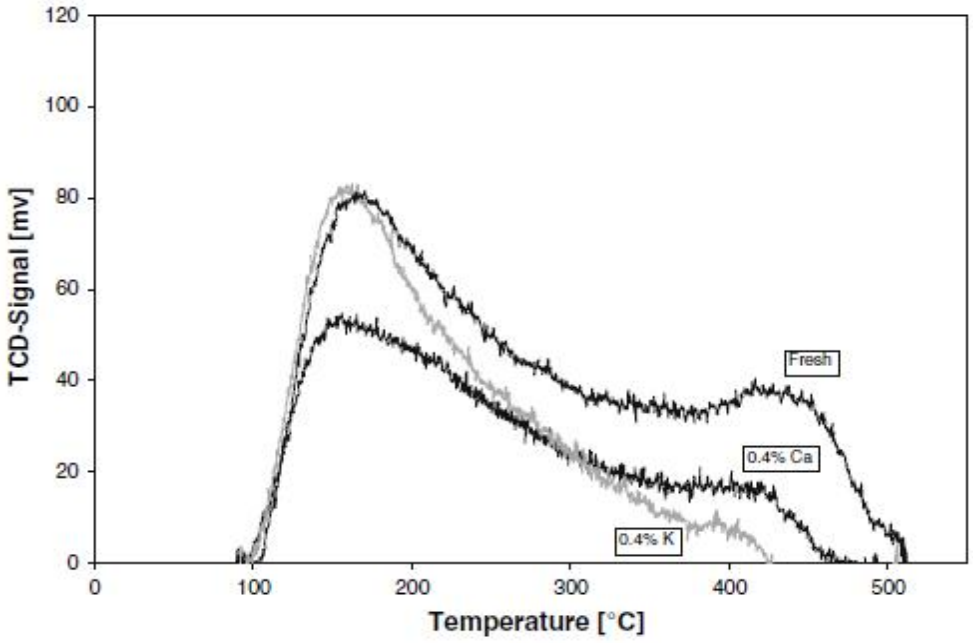

Figure 19. NH_3-TPD curve of the fresh, Ca- and K-containing catalysts. (Nicosia *et al.*, 2007)

3.3.3. DRIFT characterization of the adsorbed NH_3 species

The differential spectra of the adsorbed ammonia species on the fresh and the K-containing catalysts are shown in Figure 20. Two types of adsorbed species are shown in between the region 1300 and 1700 cm^{-1}. The band at 1425 cm^{-1} arises from the asymmetric, and 1670 cm^{-1} arises from the symmetric deformation modes of ammonium ions. This occurs upon

ammonia protonation on Brønsted acid sites. The sharp band at 1605 cm^{-1} is associated with the asymmetric deformation of ammonia species on Lewis acid sites. These bands slowly disappear upon heating, until at around 450 °C when all ammonia is desorbed from the fresh catalyst. In the presence of K the ammonia desorption was complete earlier, at 350 °C. In the Ca-containing sample the signals for the ammonium ions vanished at around 400 °C. The Ca sample is not seen in the Figures though.

It is shown in the Figures that the peak at 1425 cm^{-1} is more intense 1625 cm^{-1}. Also recognizable is that the both peaks showed comparably low intensities in the presence of K, Figure 20(b). This result shows that K strongly affects the formation of the ammonium ion, as formed by adsorption of ammonia on the Brønsted acid site.

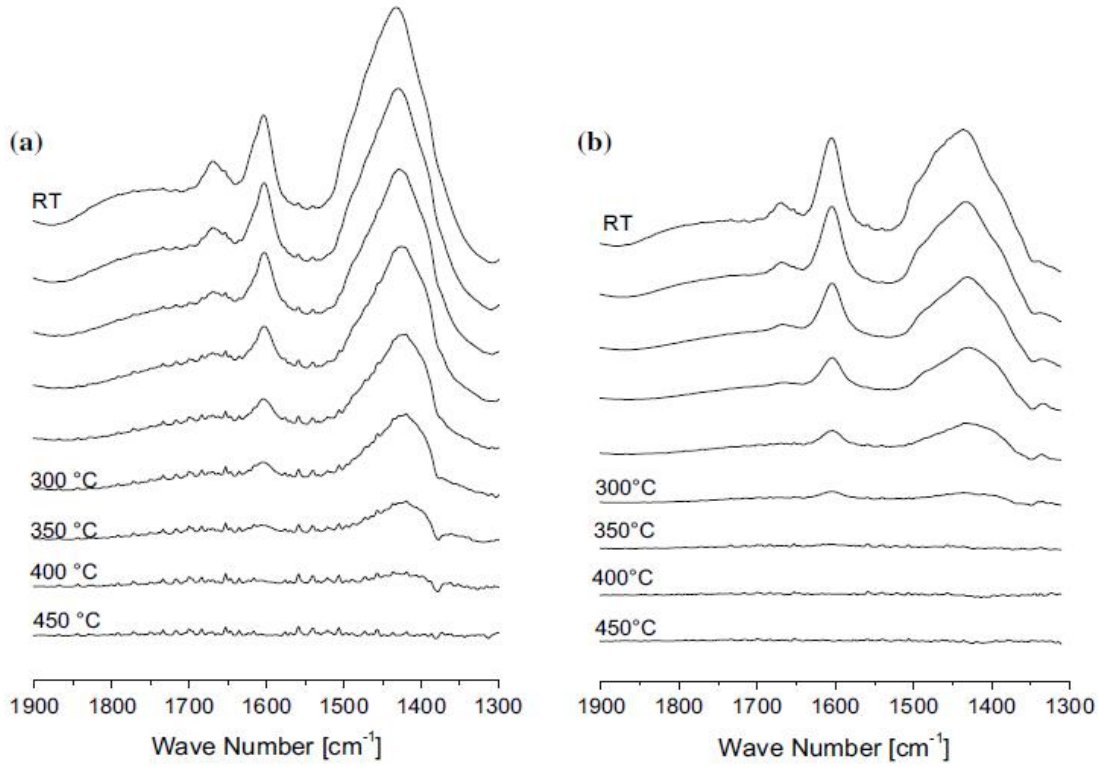

Figure 20. Drift spectra of adsorbed NH_3 species on the (a) fresh catalyst and (b) on the K-containing catalyst from room temperature to 450 °C. (Nicosia *et al.*, 2007)

These results correlate to both the catalytic activity and the NH_3-TPD experiments, and suggest that the deactivating elements strongly influence the Brønsted acidity of the SCR catalysts. It seems that the V-OH groups of the polymeric V_2O_5 were the active sites of this kind of catalyst. It is also notified that the strong poisoning effect of alkali metals is caused by their basicity, which causes the decrease of the Brønsted acidity and the ability to store NH_3. This mechanism is strongly supported by the results of this investigation.

3.3.4. Conclusions

- The catalytic and spectroscopic results suggest that small amounts of K and Ca strongly reduce the surface acidity, especially the Brønsted acidity of V_2O_5/WO_3-TiO_2 catalysts being affected. This decreases SCR catalyst activity.
- DRIFT characterization of the adsorbed ammonia species suggests that K and Ca strongly affect the Brønsted acidity of the catalyst surface, affecting the catalytic activity as well.

3.4. MORE EFFECTS OF INORGANIC ADDITIVES AND POISONS

The Chapter 3.4. with its Figures and Tables is fully based on an article written by M. Klimczak, p. Kern, T. Heinzelmann, M. Lucas and P. Claus, 2010.

Ceramic catalyst parts were either impregnated and calcined, or exposed to aerosols in order to investigate the deactivation effects of several poisons. For impregnation tests, ceramic honeycombs with cell density of 72 cpsi were chosen, supplied by Inocermic. For aerosol poisoning, catalysts with a cell density of 400 cpsi (7x7 channels) in geometry of 150 mm x 10 mm x 10 mm were prepared. The monoliths were coated with V_2O_5-WO_3/TiO_2 powder, with a powder content of 200 g/l. All parts were calcined in air at 550 ºC for 24 hours before the poisoning.

The impregnation was done separately for every channel of a monolithic honeycomb catalyst by pipetting robot. The impregnation time was 5 seconds. After drying the catalysts were calcined at 550 ºC for 24 hours. The SCR activities of every individual channel were tested. Typical feed gas composition was 1000 ppm NO, 1000 ppm NH_3, 1000 ppm CO, 5 % CO_2, 5 % H_2O and balance N_2. The experiments were done at temperatures of 250 ºC, 350 ºC and 450 ºC with space velocity of 50 000 1/h.

400 cpsi honeycomb catalysts, cut out of a serial catalyst, were poisoned by aerosols with space velocity of 50 000 1/h and at 500 ºC, 95 % air and 5 % H_2O. Three different types of catalysts were poisoned at the same time, but here are the results of V_2O_5-WO_3/TiO_2 type only. The activities were measured in a flow reactor at temperatures from 200 to 450 ºC. The simulated exhaust gas was 1000 ppm NO, 1000 ppm CO, 5 % CO_2, 8 % O_2, 5 % H_2O and balance N_2. NH_3 varied from 200 to 1200 ppm at every temperature (α = 0.2 – 1.2). After these tests the $DeNO_X$ activity at an ammonia slip of 25 ppm was searched. The reactant product analysis was done with FTIR spectroscopy with volumetric flow rate of 500 ml/min through the cell. The poison components were KNO, NaNO, $Ca(NO_3)_2$, $Mg(NO_3)_2$, $(NH_4)_2HPO_4$ and P.

3.4.1. Poisoning effect of single components

Alkaline and alkaline-earth metals proved to be highly poisonous to V_2O_5 based catalyst again. The poisoning was very clear with both impregnation and aerosol procedure. The $DeNO_X$ activities after impregnation are shown in Figure 21, and the results after exposing to aerosols are presented in Figure 22. KNO_3 was the strongest poison in both cases, giving an almost complete deactivation with a theoretical loading of 0.25 mmol/g washcoat (impregnation). Also $NaNO_3$ showed very strong deactivation effect while Ca and especially Mg being less deactivating. The results of aerosol loading were quite similar when K and Na showed very strong deactivation effect, giving the $DeNO_X$ activity of about 20 % at 350 ºC when activity of the fresh catalyst was about 65 % at the same temperature. NH_3-TPD measurements confirmed these results showing that the ammonia adsorption was very much smaller with the K and the Na poisoned catalysts, Figure 23. The poisoning was done by impregnating the catalyst powders. NH_3 adsorption temperature was 50 ºC and temperature ramp 10 ºC/min. The total results of the ammonia adsorption are shown in Table 5. The promoting effect of P and S with Ca was very interesting. In Table 6 are shown the amount of poisons adsorbed by the catalyst after 50 hours of poisoning by aerosols. Also DRIFT spectra experiments were done and they confirm the earlier results. They are not shown in detail in this thesis.

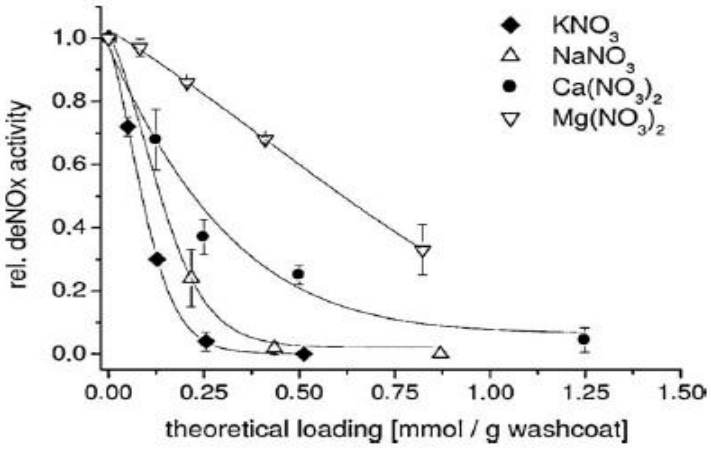

Figure 21. Relative $DeNO_X$ activity as a function of poison loading at 350 ºC. (Klimczak *et al.*, 2010)

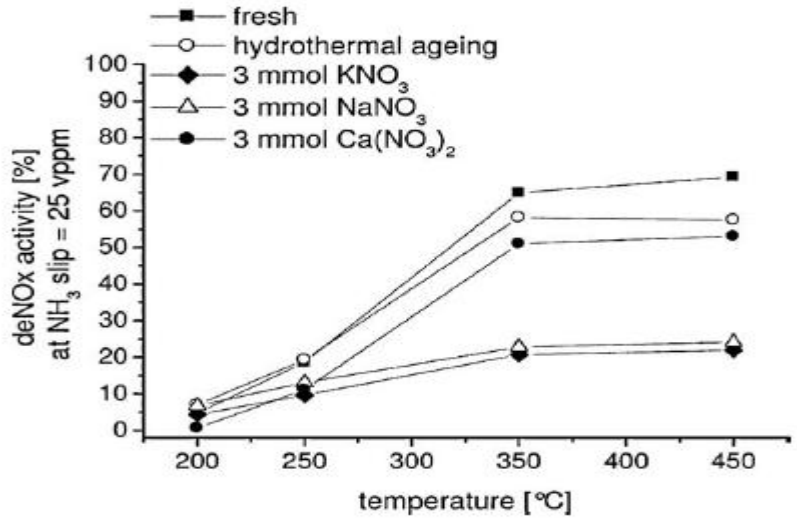

Figure 22. $DeNO_X$ activity as a function of temperature of fresh, hydrothermal aged and poisoned catalysts. (Klimczak *et al*., 2010)

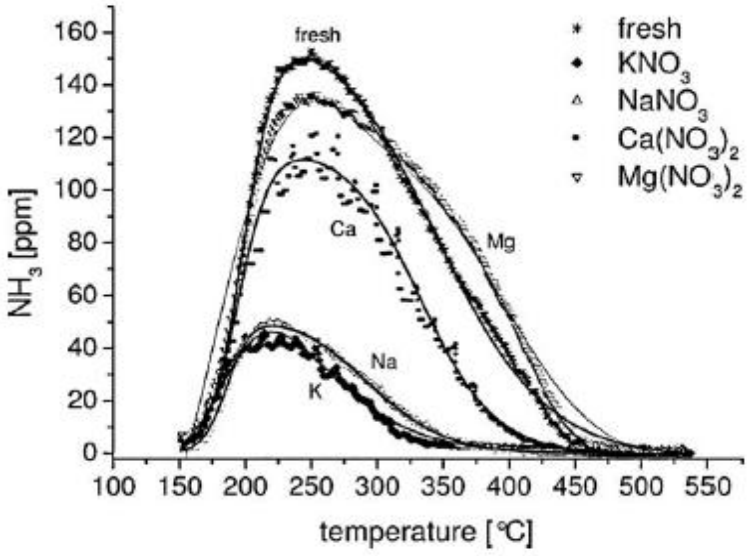

Figure 23. NH_3-TPD curve of the fresh and the poisoned catalysts. (Klimczak *et al*., 2010)

Table 5. NH_3-TPD results of the fresh and the poisoned catalysts. (Klimczak *et al*., 2010)

Catalyst/poisoning component	Adsorbed NH_3 amount [mL/g]
Fresh	1.9 ± 0.1
K	0.4
Na	0.5
Mg	2.2
Ca	1.5
Ca/P	1.7
Ca/S	2.1

Table 6. Poison loading of the catalysts and % of throughput after poisoning by aerosols. (Klimczak *et al*., 2010)

Poisoning component	Poisoning method	Content [wt.%] (washcoat)	% of throughput
3 mmol $Ca(NO_3)_2$	Aerosol	Ca: 0.26	7
3 mmol KNO_3	Aerosol	K: 0.27	7
3 mmol $NaNO_3$	Aerosol	Na: 0.2	9
3 mmol $(NH_4)_2HPO_4$	Aerosol	P: 0.2	7
11 mmol $(NH_4)_2HPO_4$	Aerosol	P: 3.9	36

3.4.2. Poisoning effect of phosphates

Poisoning with phosphates was also done with both impregnation and by aerosols. Both were done with an ammonium hydrogen phosphate solution, $(NH_4)_2HPO_4$. Both methods lead to deactivation when high enough amounts of P were used. From Figure 24 it can be seen that when 2 wt. % was exceeded the impregnation resulted in a poisoning effect. Gas phase poisoning gave similar results, as molar throughput of 11 mmol P caused a strong deactivation, Figure 25. The catalyst adsorbed 36 % of the total P amount, Table 6, and showed a $DeNO_X$ activity of 21 % at an ammonia slip of 25 ppm, Figure 25. A molar throughput of 3 mmol (0.2 wt. %) lead to a similar activity than hydrothermally aged catalyst.

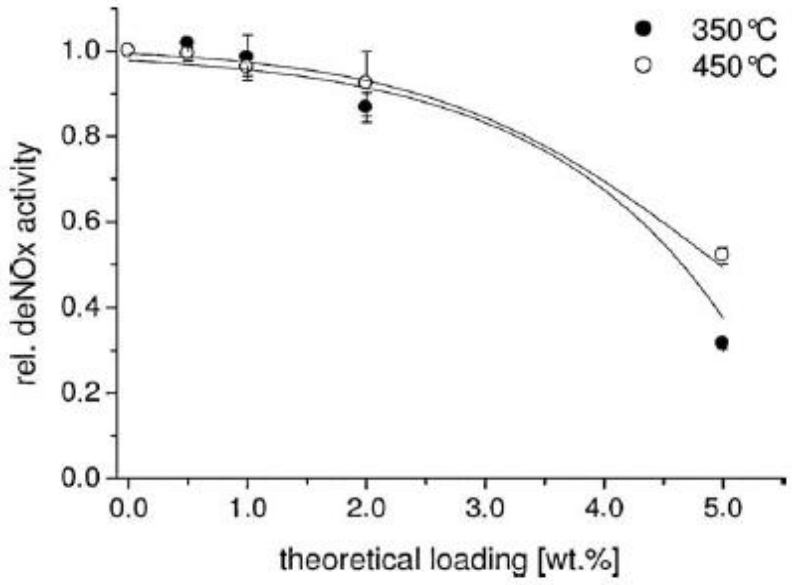

Figure 24. Relative $DeNO_X$ activity as a function of P loading, 72 cpsi monoliths. (Klimczak *et al*., 2010)

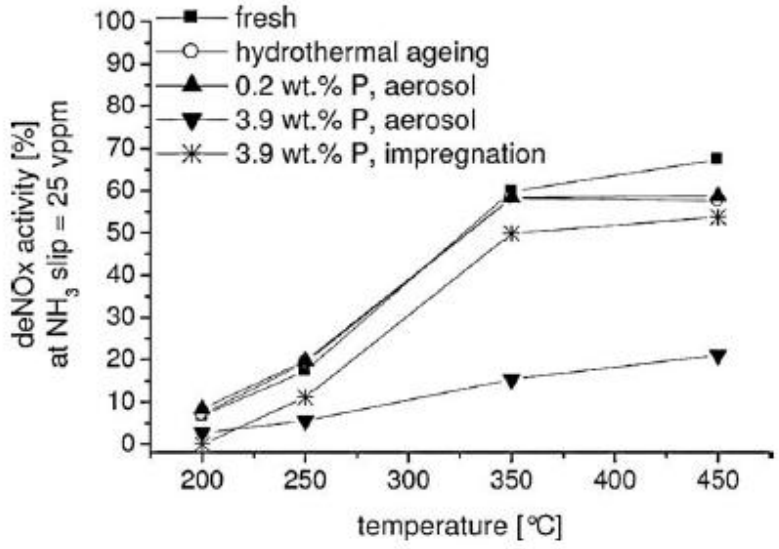

Figure 25. $DeNO_X$ activity as a function of temperature at NH_3 slip of 25 ppm. (Klimczak *et al*., 2010)

It is believed that when a certain P concentration is exceeded at the catalyst surface the formation of polyphosphates occurs. NH_3-TPD measurements of a fresh sample and a one with P concentration of 5 wt. % both show an increased amount of adsorbed ammonia with higher P loading, Figure 26. This is probably due to the increased acidity of the surface and preferred formation of surface phosphates. While increasing the acidity they also decrease the specific BET surface area of the catalysts. After aerosol loading of 3.9 wt. %, which was 122 mg P, the specific BET surface area decreased from 34 m^2/g to 20 m^2/g for non-modified hydrothermally aged catalyst sample. This indicates that the coverage of catalyst surface by P could be very deactivating. However, with smaller P loading of 0.2 wt. % (6 mg) no decrease in specific BET surface area was found. The effects of surface coverage can be seen in XPS experiments, Figure 27. The clear binding energy seen for the fresh sample is totally missing with the P poisoned sample. This means that the active vanadium sites are under the P containing layer and cannot take part in the SCR reactions. Similar results was said to be seen for W and Ti also, not shown in the Figure.

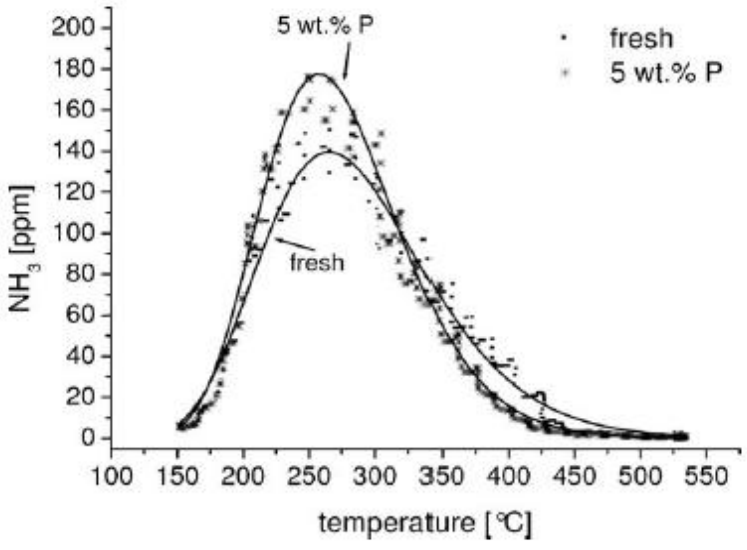

Figure 26. NH_3-TPD curve of fresh and P poisoned catalysts, adsorption temperature 50 ºC and temperature ramp 10 ºC/min. (Klimczak *et al*., 2010)

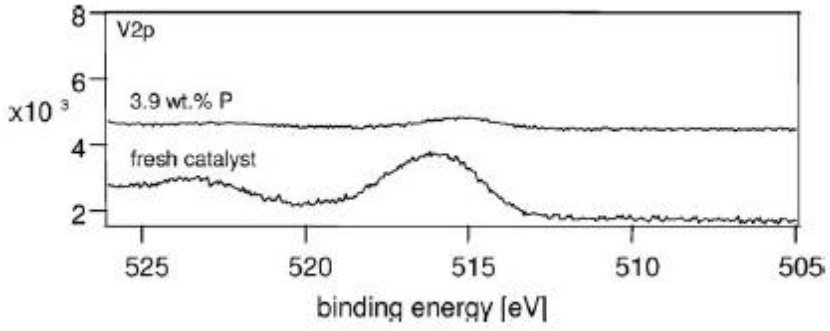

Figure 27. XPS spectra of fresh and aerosol poisoned 400 cpsi catalyst with molar throughput of 11 mmol P (3.9 wt. %). (Klimczak *et al*., 2010)

As a big difference in activity was found for impregnated or aerosol exposed samples, some further investigation was done. REM/EDX experiments were done in order to investigate the differences in distribution of P. Three parts of the catalyst were selected based on increasing flow direction and the distribution of poison in radial direction. A P/Ti ratio was selected as an indicator, as Ti is the main component in catalyst washcoat. High amounts of P were found in the middle and the front parts in complete thickness of the catalyst poisoned by aerosol P, Figure 28. Mobile particles can be sucked into the catalyst layer by capillary forces from the surface, as seen on the middle and rear parts. The rear part showed comparable results at only low penetration depths. Impregnation of the sample showed different results, as the penetration depth was very similar for all parts, Figure 29. The catalyst pores were filled with solution by capillary forces, and there was quite constant layer on the surface. Table 7 shows the final results of BET and REM/EDX experiments. These indicate that the aerosol poisoning was heavily due to the decrease in BET surface area.

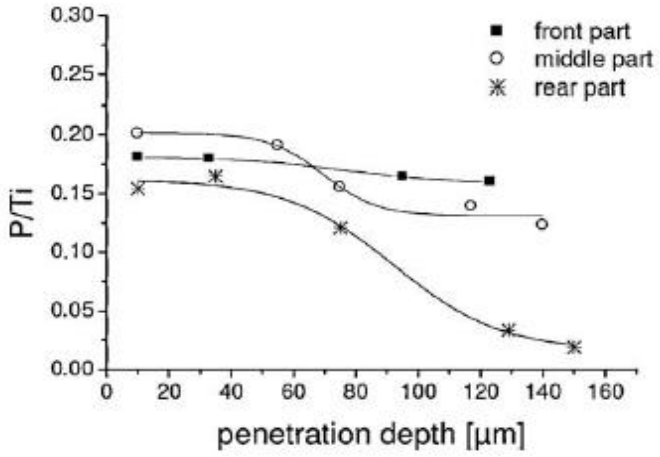

Figure 28. P/Ti ratio as a function of penetration depths of P of aerosol poisoned catalyst with loading of 3.9 wt. %. (Klimczak *et al*., 2010)

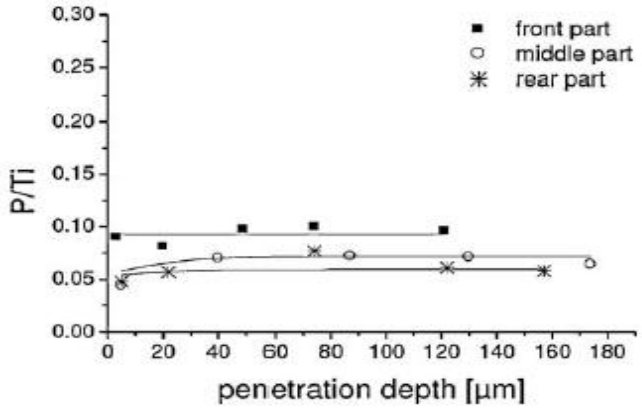

Figure 29. P/Ti ratio as a function of penetration depths of P of impregnated catalyst with loading of 3.9 wt. %. (Klimczak *et al*., 2010)

Table 7. Textural results of the hydrothermal aged and P poisoned catalysts. (Klimczak *et al*., 2010)

Catalyst/poisoning component	Poisoning method	Content [wt.%] (washcoat)	BET surface area [m^2/g]	Average pore volume [cm^3/g]	Average pore diameter [nm]
Hydrothermal aged	-	-	34	0.13	15
$(NH_4)_2HPO_4$	Aerosol	P: 3.9	20	0.09	17
$(NH_4)_2HPO_4$	Impregnation	P: 3.9	39	0.12	12

More information about aerosol poisoning effects of P can be found in an article written by Jensen, Castellino, Rasmussen, Johnsson and Fehrmann (2008). Commercial V_2O_5-WO_3/TiO_2 SCR catalysts were tested in a pilot-scale setup with natural gas burner and addition of H_3PO_4 into the flue gas. The aim was to find more realistic results than the typical wet impregnation tests. Catalysts were exposed to 10, 100 or 1000 ppm H_3PO_4 for 819, 38 and 24 hours, respectively. The relative activities of the samples were 65, 42 and 0 % after the tests. Overall the results indicated very strong effects if a lot of phosphor is in the flue gas. The polyphosphates affected in chemical way and also physically fouling and masking the catalyst surfaces. The P was also found to be very mobile on the catalyst surface, and that it could be sucked into the catalyst walls, as was found in this Chapter's article also.

Since this publication the group Jensen, Castellino, Johnsson and Fehrmann have used the same pilot-scale setup to continue the investigation of SCR catalysts. Two investigations were conducted in 2009 in order to find the effects of several poisons. Potassium phosphate (K_3PO_4) was injected in the flue gas in part 1, and in part 2 a simultaneous addition of KCl, $Ca(OH)_2$, H_3PO_4 and H_2SO_4 was carried out. K showed to be very deactivating element again, but an interesting discovery was that binding K with P and Ca might reduce its effects remarkably. More information can be found in the original publications. (Jensen *et al.*, 2008 & 2009)

3.4.3. Poisoning by transition metals

Chromium and copper were chosen to simulate the deactivation by transition metals, assumed to be from abrasion of the engine. These metals do not exist in biofuels in large scale, but are also important aspects when trying to save the SCR from deactivating. For the impregnated catalysts a small reduction in the $DeNO_X$ activity was found, Figure 30. Conditions of the tests were 1000 ppm NO, 1000 ppm NH_3, 1000 ppm CO, 5 vol. % CO_2, 8 vol. % O_2, 5 vol. % H_2O, 50 000 1/h, impregnated 72 cpsi monoliths. The small decrease in activity was attributed to an increased production of N_2O at higher poison loading and temperatures. At 2 wt. % loading the activities were 0.79 and 0.82 for Cr and Cu, respectively. More detailed information is shown in Table 8.

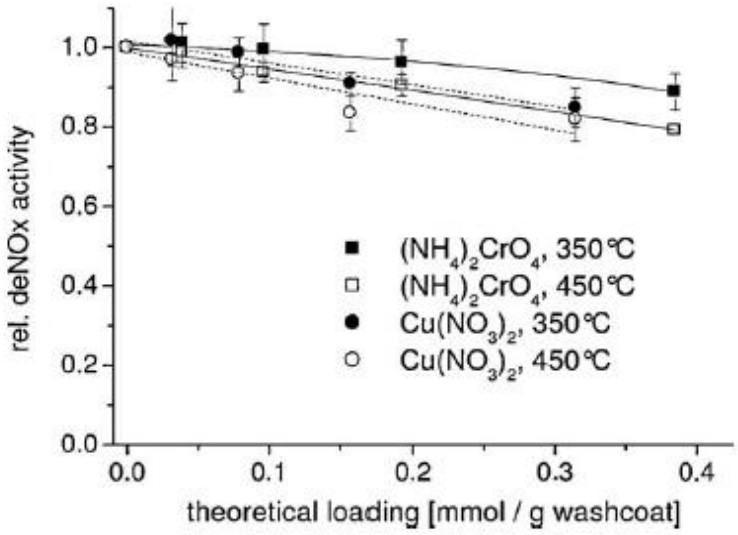

Figure 30. Relative $DeNO_X$ activity as a function of Cr and Cu loading. (Klimczak *et al*., 2010)

Table 8. Activity and selectivity data of fresh and Cu ad Cr poisoned catalysts. (Klimczak *et al*., 2010)

Catalyst	*T* [°C]	Rel. deNOx	$S(N_2O)$ [%]	N_2O [vppm]
Fresh	350	–	1	8 ± 1
0.2 wt.% Cr	350	1.01 ± 0.05	1	9 ± 1
0.5 wt.% Cr	350	0.99 ± 0.06	1	9 ± 2
1 wt.% Cr	350	0.96 ± 0.06	2	11 ± 2
2 wt.% Cr	350	0.89 ± 0.05	4	24 ± 5
0.2 wt.% Cu	350	1.06 ± 0.23	2	12 ± 3
0.5 wt.% Cu	350	0.99 ± 0.04	3 ± 1	20 ± 6
1 wt.% Cu	350	0.91 ± 0.03	5 ± 1	28 ± 7
2 wt.% Cu	350	0.85 ± 0.05	6 ± 1	34 ± 3
Fresh	450	–	1	11 ± 1
0.2 wt.% Cr	450	0.99 ± 0.03	2	14 ± 1
0.5 wt.% Cr	450	0.94 ± 0.03	4 ± 1	32 ± 7
1 wt.% Cr	450	0.90 ± 0.02	7 ± 1	61 ± 8
2 wt.% Cr	450	0.79	18	154
0.2 wt.% Cu	450	0.97 ± 0.02	3	25 ± 2
0.5 wt.% Cu	450	0.94 ± 0.04	6 ± 2	53 ± 13
1 wt.% Cu	450	0.83 ± 0.04	10 ± 1	74 ± 2
2 wt.% Cu	450	0.82 ± 0.05	10	76 ± 2

Again the tests were also done with aerosols and 400 cpsi monoliths. A molar throughput of 3 mmol of Cr and Cu was carried out. This seems to be more realistic way to do the test, because it involves the thermal decomposition of the precursors. The catalyst adsorbed 7 % and 0.7 % of the poison amount which corresponds to 0.36 wt. % Cr and 0.04 wt. % Cu in the washcoat. These had an effect on the activity and the ammonia slip, Figures 31 and 32. With 25 ppm ammonia slip the decreases in activities by poisons were about the same as with hydrothermal ageing. Regardless of the low amounts of poison adsorbed, the production of N_2O was found. The production is dependent on the temperature and NH_3 injection rate. The conditions of the tests were 1000 ppm NO, 1000 ppm CO, 5 vol. % CO_2, 8 vol. % O_2, 5 vol. % H_2O, balance N_2, at 50 000 1/h. The formed maximum amount of 30 ppm of N_2O corresponded to a selectivity of 3 %.

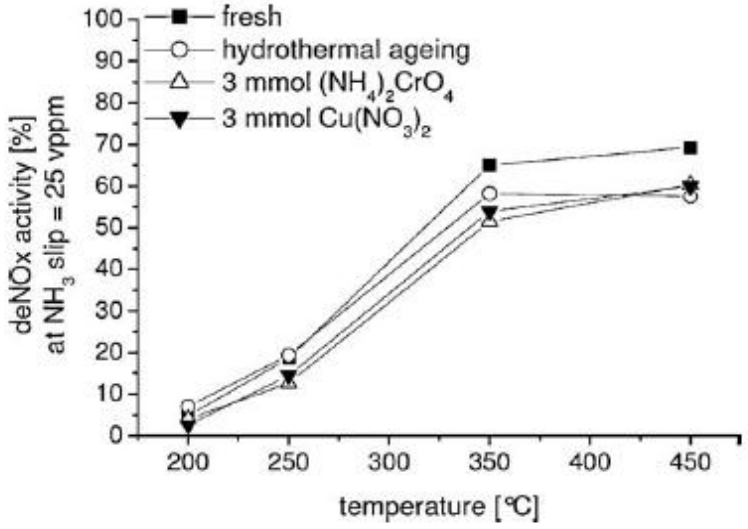

Figure 31. $DeNO_X$ activity as a function of temperature of fresh, hydrothermal aged and poisoned catalysts. (Klimczak *et al*., 2010)

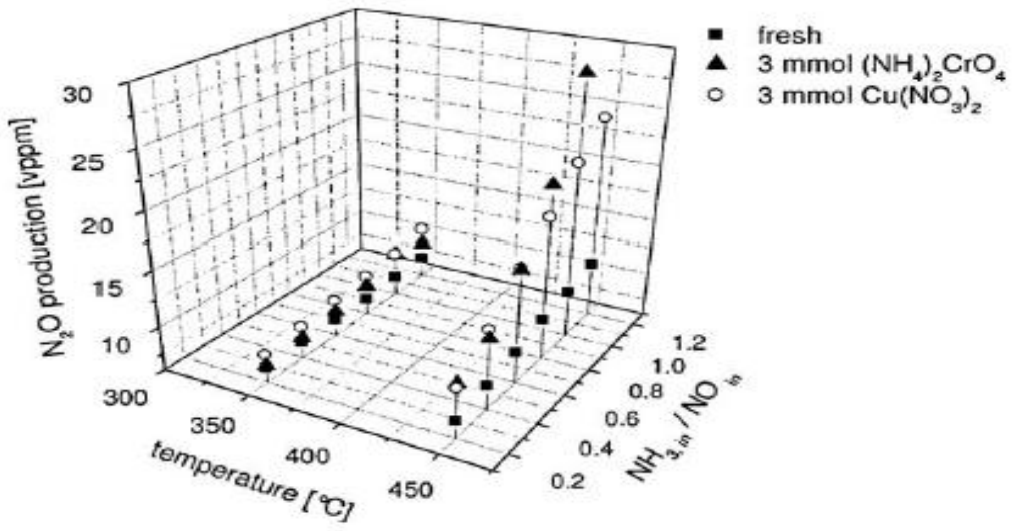

Figure 32. N_2O production as a function of temperature and NH_3/NO ratio. (Klimczak *et al*., 2010)

Also the poisoning effects in combinations of poisons were investigated, mostly by Design of Experiments (DOE). It allowed the scientist group to do fewer experiments. These experiments did not give very much further information, but confirmed the poisoning effects of K and Ca, and the regenerating effects of phosphates and sulfates when they were present in the catalyst.

3.4.4. Conclusions

- Strong deactivation was found for alkaline and alkaline earth metals even at low concentrations, due to reduced ammonia storage capacity.
- The poisoning effect was related to poison basicity, and therefore the order is K > Na > Ca > Mg of the metals investigated here. These results correlate with other studies summarized in this thesis.

- Phosphate is a strong poison, but only at very high concentrations. With smaller concentration it has an ability to increase the acidity of the catalyst surface and allow the surface to absorb more ammonia, but it also causes serious pore blocking.

- Transition metals copper and chromium are moderate poisons but they have ability to increase N_2O formation in the catalyst. Anyway, this effect was not found when simultaneous poisoning of the catalyst was done by alkaline metals and copper.

3.5. SINGLE AND COMBINED DEACTIVATING EFFECTS OF ALKALI METALS AND HCl

Chapter 3.5. with its Figures and Tables is fully based on an article written by L.Lisi, G.Lasorella, S.Malloggi and G.Russo, 2004.

Two commercial type SCR catalysts with W content of 9 wt. % and 8,5 wt. % ,and a V content of 0.55 and 1.8 wt. %, respectively, were influenced by different amounts of Na, K and HCl vapors in order to simulate poisoning by exhaust gases from MSW (municipal solid waste) incineration. Especially Na and K can also be found from liquid biofuels.

The catalysts were supplied by ENEL Produzione, Italy. They were constituted by vanadium and tungsten oxides supported on TiO_2, and they were crushed by a ceramic binder and characterized as powder before poisoning. The less V containing catalyst was called M-1 and more containing M-2.

3.5.1. Poisoning

K and Na were deposed on the catalysts by impregnation of KNO_3 and $NaNO_3$ solutions with different concentrations. After drying 3 h at 110 °C, the nitrates were decomposed at 450 °C for 3 h in flowing air. Both catalysts were poisoned with 0.3, 0.7 and 1.0 wt. % K and with 0.18, 0.41 and 0.58 wt. % Na respectively. The three values of K and Na were equivalent on molar basis, and were the same as the amount of alkali metals deposed on SCR catalysts after 600-700 h time on stream. The HCl poisoning was simulated by contacting 3 g catalyst with particle diameter of 200-300 µm, to a 10 % HCl/He gas flow mixture (900 cm^3/min) in a fixed bed reactor at 300 °C for 12 h. Both, unpoisoned M-1 and M-2, and the same catalysts that were already poisoned by maximum amount of K and Na, were treated with HCl.

The catalytic activity tests were carried out with a fixed bed quartz micro-reactor operating under atmospheric pressure in the temperature range of 200-400 °C feeding 700 ppm NO, 700 ppm NH_3, 3 % O_2 and balance of He.

3.5.2. Physico-chemical characterization

A negligible effect of poisoning agents on the surface area of the samples was observed, Table 9. Pore size distribution confirms that significant pore blocking did not occur upon poisoning. The average content of vanadium was close to the nominal especially for M-2 as seen from the Table. The tungsten content though is a lot higher. In addition to these elements, both samples contained small amounts of Ca, S and Mg. Local analysis performed on the catalyst particle gave a 10 % greater tungsten content compared to the average one for both samples, as expected since tungsten should not be present on ceramic fibers.

Table 9. Surface area and average chemical composition of pure and poisoned catalysts. (Lisi *et al.*, 2004)

Catalyst	Poisoning	Surface area ($m^2\ g^{-1}$)	Average composition (wt.%)			
			V	W	Si	Al
M-1	–	64	0.79	12.75	7.41	1.40
	1 wt.% K	62				
	0.58 wt.% Na	63				
	HCl	60				
	1 wt.% K + HCl	59				
M-2	–	59	1.88	11.81	9.84	1.51
	1 wt.% K	60				
	0.58 wt.% Na	52				
	HCl	61				
	1 wt.% K + HCl	64				

SEM/EDX analysis

SEM/EDX analysis shows that both samples were consisted of V_2O_5-WO_3/TiO_2 catalyst particles with a size range of 10 to 100 μm and by binder fibers consisting primarily of silicon and aluminum oxides, Figure 33. The analysis was also performed on the catalysts with

the maximum amount of alkaline metal. Alkaline metal content resulted higher than expected being about 1.7 wt. % K and 1.1 wt. % Na for both samples. K was said to be more uniformly distributed, but Na was more concentrated on the catalyst particle with respect to binder fibers. The Figure was not shown in the investigation. After 12 h HCl treatment at 300 °C a Cl content of 0.6 to 0.7 wt. % was found for both samples. However, a significant reduction of the vanadium content from 1.88 to 1.07 wt. % was noticed for M-2 sample, suggesting the formation of soluble vanadium chlorides (VCl_4 and VCl_2), which could be washed up by the wet flow when vanadium is present in higher amounts. The amount of Cl deposed on the surface of the catalysts enhances when the samples are pre-treated with 1 wt. % K. Cl was mainly present on the catalyst particles where the atomic ratio with K was very close to 1, suggesting that larger Cl deposition might be related to the formation of KCl KCl is discussed more in Chapter 4.1.

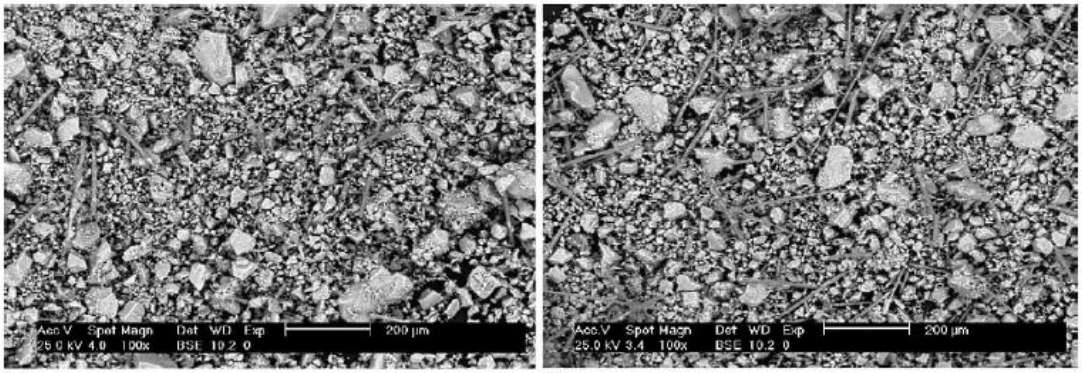

Fig. 2. Scanning electron micrograph of M-1 (a) and M-2 (b) catalysts.

Figure 33. SEM pictures of catalysts M-1 and M-2. (Lisi *et al*., 2004)

NH_3-TPD analysis

The NH_3-TPD profiles of pure and alkaline poisoned catalysts are shown in Figure 34. The amount of ammonia desorbed, evaluated from the integration of TPD curves, are shown in Table 10. No formation of N_2 or nitrogen oxides was detected up to 650 °C. Both unpoisoned samples showed a broad signal extending up to 450-500 °C, M-2 giving rise to a

higher peak at lower temperature. A further signal appears at 460-560 °C for M-1 and at 500-600 °C for M-2, absent for poisoned catalysts except with the lowest K concentration.

The deposition of alkali metals dramatically reduced surface acidity, mainly affecting the strong acid sites which were completely eliminated at the high concentration of K and Na. The effect of K was stronger than that of Na with the same molar concentration, as it can be noticed from the quantative results shown in Table 10. According to this investigation it has been reported that K decreases both the number and the strength of Brønsted sites V-OH and W-OH, and only at high loadings interacts with sites of TiO_2 support, also mentioned in Chapter 3.2. However, the results of this investigation show that a significant number of weak acid centers are still present when strong acid sites have been totally neutralized by high alkaline metal concentration. It was also reported that WO_3 protect the supported V_2O_5 from neutralization by alkali metals, to some extent. This could mean that the alkali metals neutralize desirably strong Lewis wolframyl sites with respect to weak acid sites of vanadium oxide, thus increasing poisoning resistance of vanadium.

The profiles of pure and HCl poisoned catalysts are shown in Figure 35. Also 1 wt. % K and 0.58 wt. % Na are demonstrated in the Figure. HCl modifies both M-1 and M-2 TPD curves by decreasing the contribution at low temperature and increasing it at the high temperature. This leads to a slight quantitative increase in acid sites, as reported in the Table 10. More significant quantitative recovering was found for the samples already poisoned by alkaline metals. The shape of the TPD curves suggests that the formation of new hydroxyl groups occur, instead of restoring the old ones on the surface before poisoning.

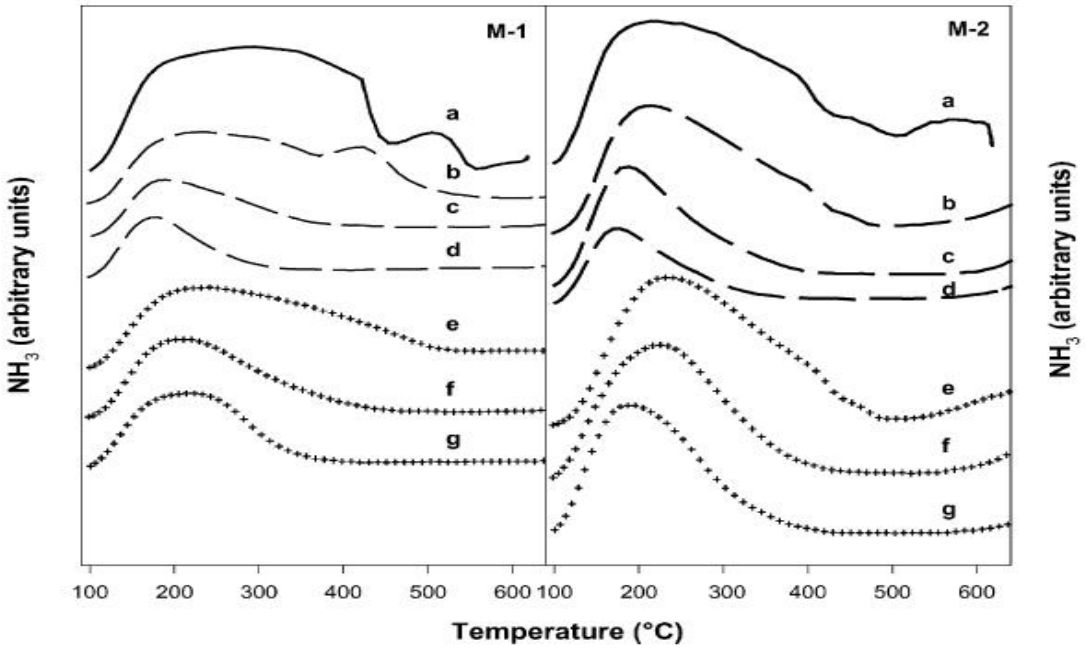

Figure 34. TPD profiles of (a) unpoisoned M-1 and M-2 and those poisoned by (b) 0.3 wt. % K, (c) 0.7 wt. % K, (d) 1 wt. % K, (e) 0.18 wt. % Na, (f) 0.41 et. % Na and (g) 0.58 wt. % Na. (Lisi *et al*., 2004)

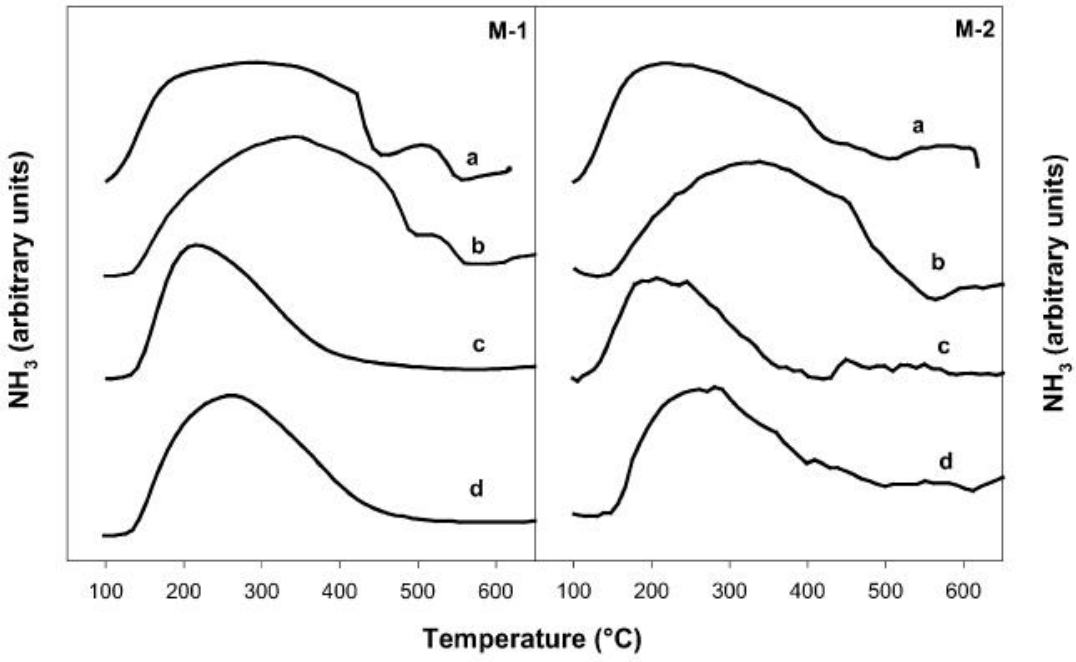

Figure 35. TPD profiles of (a) unpoisoned M-1 and M-2, (b) HCl poisoned, (c) 1 wt. % K and (d) 0.58 wt. % Na poisoned catalysts. (Lisi *et al*., 2004)

The neutralization of OH groups by alkaline metals significantly occurred at high alkali concentrations, and was confirmed by the results of unpoisoned M-1 and M-2 and on the same catalysts poisoned with maximum amount of alkali metals. Only water was released during the experiments, suggesting that the weight loss was related to physisorption of water from the catalyst surface at low temperature, and to release H_2O from OH condensation at higher temperature. In Table 10 is reported the number of evaluated OH from H_2O released after the slope change in the curve, T > 180 °C. The results confirm that alkali metals neutralize the surface hydroxyl groups and that the effect of K was stronger than Na's.

Table 10. Amount of NH_3 desorbed and OH group concentration. (Lisi *et al*., 2004)

Amount of NH_3 desorbed in TPD experiments and OH group concentration evaluated from water released in TG experiments

Catalyst	NH_3 (mmol g^{-1})	Hydroxyl concentration (mmol g^{-1})
M-1	0.222	0.690
0.3 wt.% K	0.123	
0.7 wt.% K	0.054	
1.0 wt.% K	0.046	0.188
0.18 wt.% Na	0.116	
0.41 wt.% Na	0.086	
0.58 wt.% Na	0.075	0.220
HCl	0.234	
1.0 wt.% K + HCl	0.141	
0.58 wt.% Na + HCl	0.219	
M-2	0.223	0.542
0.3 wt.% K	0.151	
0.7 wt.% K	0.102	
1.0 wt.% K	0.062	0.030
0.18 wt.% Na	0.173	
0.41 wt.% Na	0.143	
0.58 wt.% Na	0.123	0.120
HCl	0.227	
1.0 wt.% K + HCl	0.117	
0.58 wt.% Na + HCl	0.172	

3.5.3. Catalytic tests

Catalytic tests for alkali metal poisoned catalyst samples

The results of catalytic tests for alkali metal poisoned catalyst samples are shown in Figure 36. The NO/NH_3 conversion ratio was close to 1 in all experiments. No other nitrogen oxides than NO was detected, suggesting that reduction of NO to N_2 by NH_3 was the primary reaction. As expected, the activity of M-2 was greater due to the larger amount of V_2O_5. The study said that it was previously reported that WO_3/TiO2 was completely inactive below 250 °C, whereas at this temperature V_2O_5/TiO_2 gives about 90 % NO conversion. However, WO_3 increases the intrinsic activity of vanadium oxide, encouraging the formation of polyvanadates that are more active for SCR reaction. The very close WO_3 contents of the catalyst samples gives right to declare that the greater activity of M-2 is due to larger V_2O_5 content.

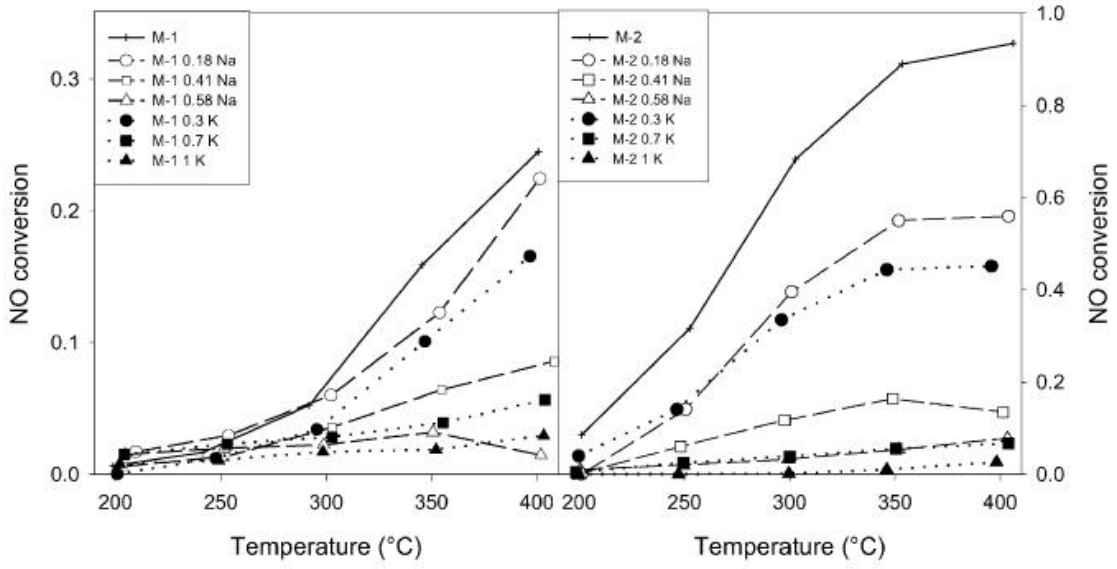

Figure 36. NO conversion as a function of reaction temperature for unpoisoned and alkali metal poisoned M-1 and M-2 catalysts. (Lisi *et al*., 2004)

Small amounts of alkali metals led to a dramatic deactivation of the catalyst samples. At the same molar concentration K was more deactivating. The values of pre-exponential factor

and activation energy were evaluated on the basis of integral activity data supposing a rate-equation $r = k_0 e^{\frac{-E_{act}}{RT}} * C_{NO}$ and an isothermal PFR model. Values of pre-exponential factor are reported in Table 11. The larger values of k_0 for the more vanadium containing M-2 for the unpoisoned samples was not linearly proportional to V_2O_5 content, confirming that polyvanadate species were more active than monomeric vanadates.

The k_0 value of the unpoisoned catalyst M-2 decreased when increasing the amount of alkali metal. This was in agreement with the hypothesis that alkali metals reduced the number of active sites. Not so uniform trend was observed for catalyst M-1, suggesting a significant interaction of non-active sites with alkali metals when vanadium was present in low amounts. A correlation with surface acidity has been tried to find by reporting the pre-exponential factor as a function of the total amount of ammonia desorbed in the TPD experiments for the unpoisoned and the alkali metal poisoned catalysts. Hypothesis is that NH_3 adsorbed on the active sites reacts with gaseous NO according to a typical Eley-Rideal mechanism, Figure 37. The expected large dispersion of M-1 suggest that at low loading the large contribution of the support WO_3 to NH_3 adsorption does not allow a direct correlation with vanadium active sites. Not linear but roughly quadratic curve was found for M-2. The ammonia desorbed in the temperature range 250-350 °C is also reported in the same Figure.

Table 11. Pre-exponential factor evaluated from experimental activity data. (Lisi *et al*., 2004)

Catalyst	$k_0 \times 10^6$ ($1h^{-1}\,g^{-1}$)	Catalyst	k_0 ($1h^{-1}\,g^{-1}$)
M-1	9.47	M-2	85.5
0.3 wt.% K	4.34	0.3 wt.% K	35.9
0.7 wt.% K	8.96	0.7 wt.% K	4.09
1.0 wt.% K	4.77	1.0 wt.% K	2.43
0.18 wt.% Na	11.6	0.18 wt.% Na	36.8
0.41 wt.% Na	5.36	0.41 wt.% Na	11.5
0.58 wt.% Na	8.66	0.58 wt.% Na	4.74

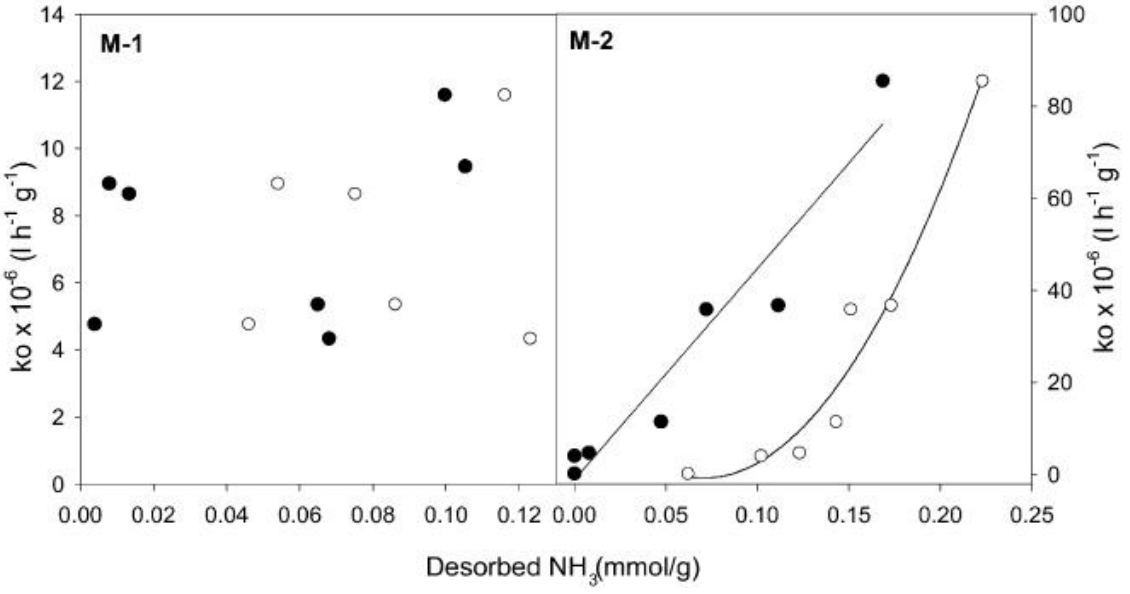

Figure 37. Pre-exponential factors as a function of total NH_3 desorbed (open dots), and NH_3 desorbed in the range of 250-350 °C (black dots) in TPD experiments. (Lisi *et al*., 2004)

Catalytic tests for HCl poisoned catalyst samples

Catalytic tests were done for HCl poisoned samples also, reported in Figure 38. N_2 was again the only N containing product detected. The effect of poison was opposite on M-1 and M-2. The treatment with HCl gave slight rise of NO conversion for M-1 at high temperature, whereas for M-2 a significant loss of activity was found, attributable to the great decrease of vanadium content. Similar findings exist in literature before this investigation, by Chen et al. This suggests that polyvanadate species are less stable than monovanadate species, being easily removed by HCl through formation of soluble vanadium chlorides. Polyvanadates are likely present in high loading of vanadium oxides, and monovanadate species are present in low vanadium content. Combined poisoning by alkali metals and HCl produced greater loss of activity than them separately. The activity decreased at the whole temperature range.

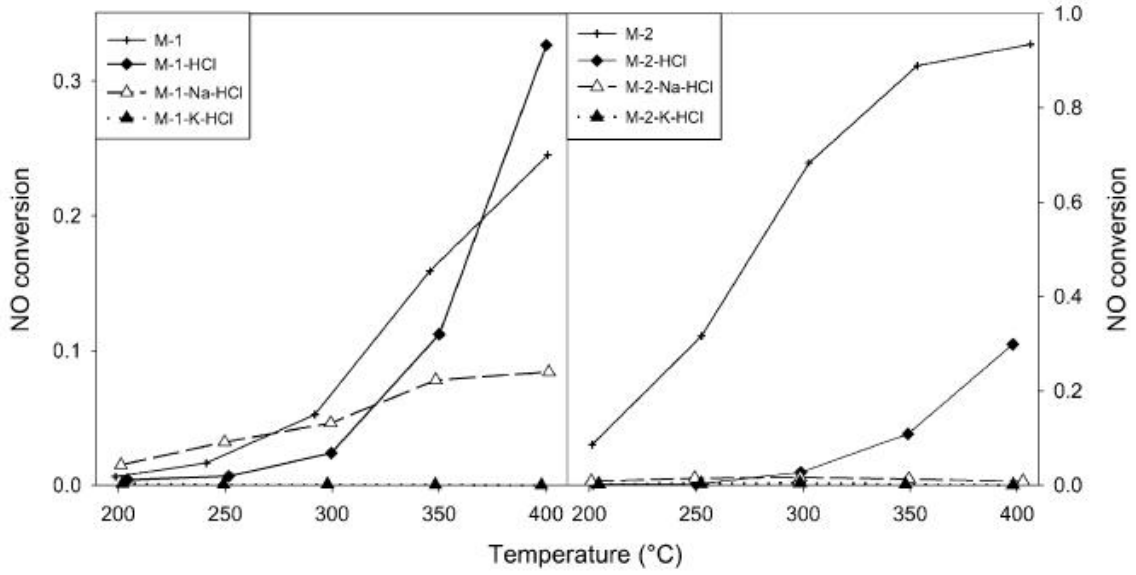

Figure 38. NO conversion as a function of temperature for unpoisoned, HCl, HCl and alkali metal poisoned catalysts. (Lisi *et al*., 2004)

3.5.4. Conclusions

- Vanadium content has a very large effect on overall catalyst activity and NO conversion.
- Alkali metal deposition on catalyst surfaces resulted in a significant loss of surface acidity.
- At the same molar concentration, K had greater impact than Na.
- A linear correlation between the activity and number of acid sites involved in reaction has been found for catalysts with higher vanadium content, M-2 in this investigation.
- Poisoning with both HCl and alkali metals together produced greater activity loss than they did separately.

3.6. DEACTIVATION OF Pt/WIRE-MESH AND VANADIA/MONOLITH CATALYSTS

Chapter 3.6. with its Figures and Tables is fully based on an article written by Morteza Sohrabi, Farokhbag Morabi and Mehri Sanati, 2007.

Some inorganic salts with high and low melting points (K_2SO_4, KCl and $ZnCl_2$) were investigated to find out their deactivation abilities in Pt/wire mesh and Vanadia/monolith catalysts. The procedure for preparing the deactivated samples of the catalysts on a laboratory scale was meant to simulate a real deactivation situation of SCR catalyst in combustion process where such aerosols are present in the flue gas. For simplicity the samples were exposed to aerosols one at a time.

Several mechanisms for deactivation of SCR catalysts may be classified as follows:

- Poisoning reactions on the catalyst surface
- Micro and macro pore blockage by salt formation or deposition of fine particles
- Masking of the catalyst surface by deposition of dust or ash and thermal degradation
- Plugging of monolith by dust and larger particles
- Decrease in the active phase of the catalyst due to erosion

As mentioned many times earlier, alkali metals are very poisoning elements for SCR catalysts. The poisoning effect is heavily related to their basicity. The severity of poisoning follows as KCl > NaCl >K_2SO_4 > Na_2SO_4. SO_2 has a promoting effect due to its ability to increase surface acidity of the catalysts, when the amount of S is not very large.

3.6.1. The experiments

Solutions of KCl, K_2SO_4 and $ZnCl_2$ salts containing 25 g/dm^3 were prepared. The aerosol particle size formation is highly dependent on the concentration of the fluid. The increase in the concentration increases the mean aerodynamic diameters of the particles. With this concentration the count mean aerodynamic diameter (CMAD) of the aerosol particles was expected to be around 70 nm.

The catalysts were deactivated by exposing to generated aerosol particles of KCl, K_2SO_4 and $ZnCl_2$ at 340 °C. Each catalyst sample was exposed to the generated aerosol particles for 31 hours, before the activity tests. This is a very short time in the case of deactivation.

3.6.2. The results of catalytic tests

The Vanadia/monolith catalyst was supplied by BASF Company. The deactivation effect of different inorganic salts can be seen in activity decreases in Figure 39. NO_X conversion increased when the temperature rose from 200 to 350 °C. Beyond this temperature the activity began to drop. However, the NO_X conversion was only about 55 % at best in this study. The deactivation effect of $ZnCl_2$ on the vanadia/monolith catalyst was stronger than the other salts, at least at temperatures from 200 to 350 °C. However, the fresh catalyst seemed to be the least active sample at 450 °C.

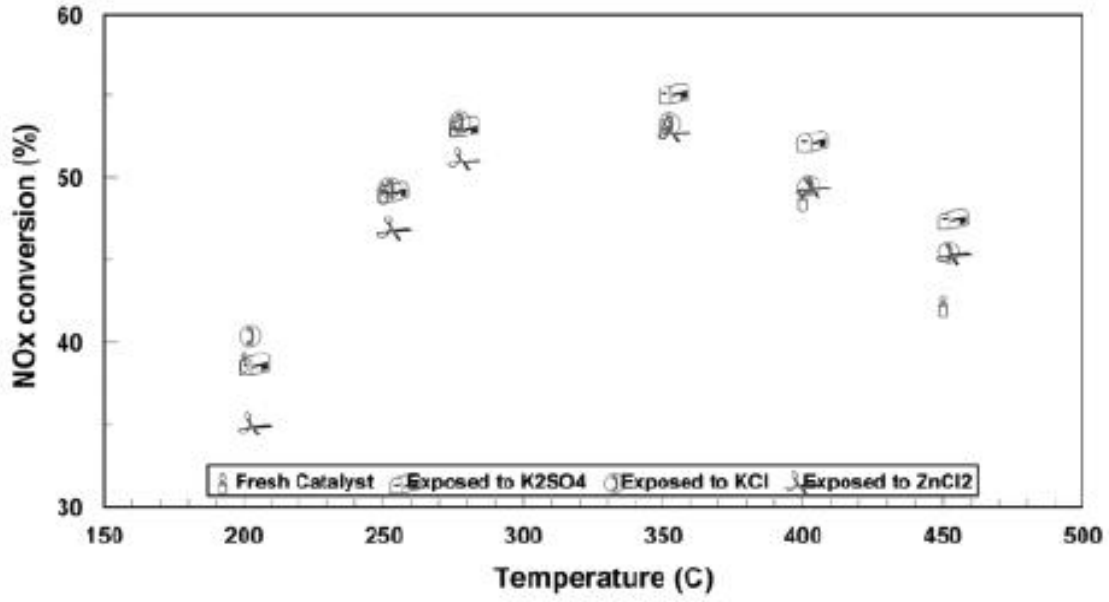

Figure 39. Effect of temperature on NO_X conversion with Vanadia/monolith catalyst. (Sohrabi *et al.*, 2007)

The Pt/wire mesh catalyst was supplied by Catator Company. Six nets of catalyst were used for every experiment. The results are shown in Figure 40. The $ZnCl_2$ aerosol was found to have the strongest deactivating effect for this catalyst as well. This could be related to a lower melting point of $ZnCl_2$ compared to other salts of this investigation. The melting point of $ZnCl_2$ is 283 °C, which means that at 340 °C it is either molten or at gas state. The catalyst was then being exposed to the liquid or the gaseous $ZnCl_2$, which could mean higher penetration ability for $ZnCl_2$ compared to that of K salts at that temperature. The results for $ZnCl_2$ were very interesting, because only a moderate deactivation was found for Zn in Chapter 3.1. It was also noticeable that KCl was also quite deactivating, but maybe not so much as it is in the study of Chapter 4.1.

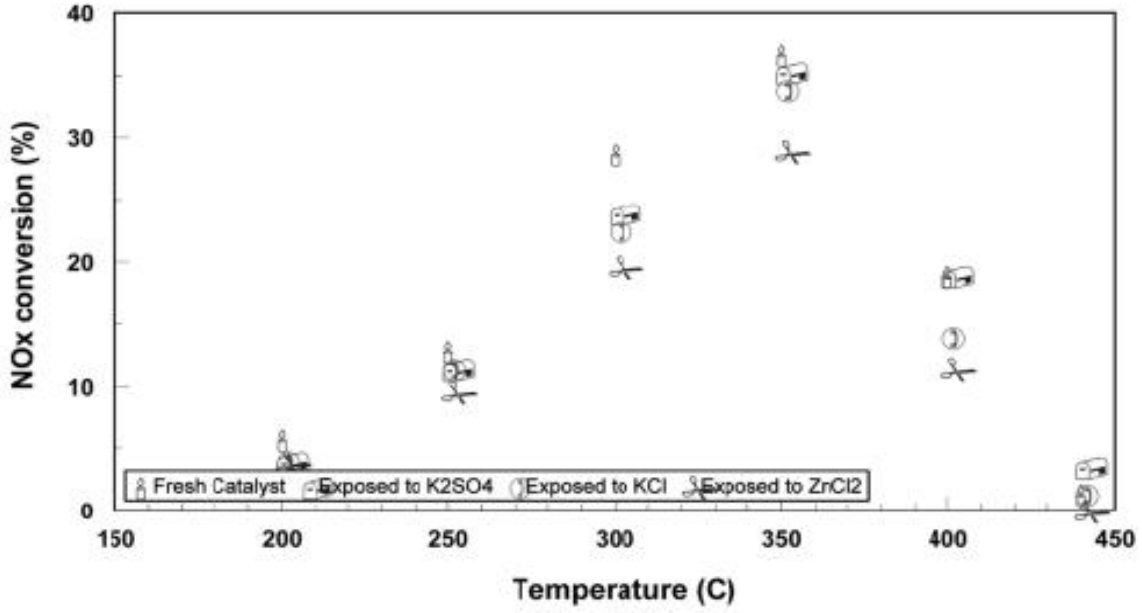

Figure 40. Effect of temperature on NO_X conversion with Pt/wire mesh catalyst. (Sohrabi *et al.*, 2007)

3.6.3. The results of SEM

The deactivation of sub-micron particles could have been due to the diffusion of the matrix of the catalyst, and blockage of the mezzo and micro pores. The electron microscopy revealed that both K salts and $ZnCl_2$ particles diffused inside the catalyst. However, the penetration of $ZnCl_2$ was deeper, as seen on Figures 64 and 65. In Figure 41, a distinct layer of KCl was approximately 2-4 µm thick, as in Figure 42 the thickness was approximately 6-8 µm for the catalyst exposed to $ZnCl_2$. This was concluded to be due to the lower melting point mentioned earlier.

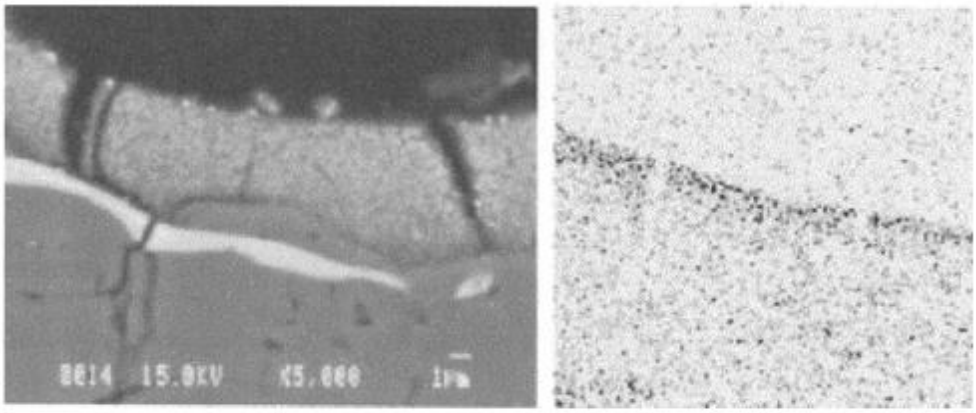

Figure 41. Left: cross section of the sample exposed to KCl. Right: X-ray mapping of K in the sample. (Sohrabi *et al.,* 2007)

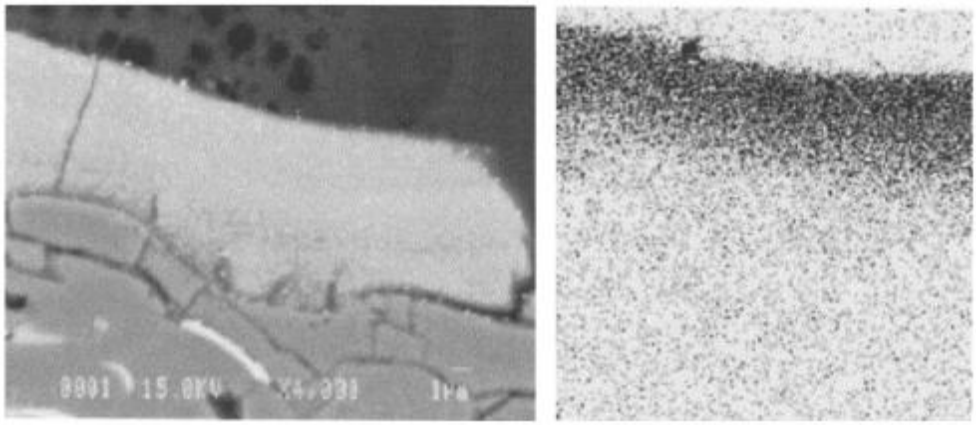

Figure 42. Left: cross section of the sample exposed to $ZnCl_2$. Right: X-ray mapping of Zn in the sample. (Sohrabi *et al.,* 2007)

In the light of this study, it seems that the aerosols generated from the low melting point salts, such as $ZnCl_2$, in the flue gas are the main sources of deactivation of the environmental catalysts. Therefore some kind of a cleaning system for elimination of these particles before the catalyst could improve the catalyst lifetime.

3.6.4. Conclusions

- $ZnCl_2$ was more deactivating than KCl ad K_2SO_4.
- $ZnCl_2$ is believed to be stronger poison due to its lower melting point, as it is at liquid or gas state when arriving to the catalyst. It can reach deeper into the catalyst pores.
- Also KCl caused noticeable deactivation.

3.7. CONCLUSIONS OF CHAPTER 3

K and other basic alkali metals, like Ca, Na, Mg and Zn are deactivating trace elements. The effect seems to be due to reducing the acidity of the surface. Especially the Brønsted acidity sites are being affected. This leads to lower ammonia adsorption and thus lower catalytic activity. Phosphate, copper and chromium can also cause some deactivation and the latter two can increase the amount of N_2O formation. Aerosol poisoning seems to be more harmful for the catalysts and so the alkali compounds with lower melting points can cause more damage. The increased vanadium content increased the amount of active sites on the catalyst surface and thus also increased the activity very clearly. Basic metals deposit on the surface and cause serious deactivation. Poisoning with HCl and alkali metals simultaneously produced greater loss in activity. $ZnCl_2$ was also very deactivating, probably due to lower melting point.

4. DEACTIVATION AT REAL BIOFUEL POWER PLANTS

4.1. DEACTIVATION AT BIOMASS FIRED POWER PLANTS

Chapter 4.1. with its Figures and Tables is fully based on an article written by Yuanjing Zheng, Anker Degn Jensen, Jan Erik Johnsson, Joakim Reimer Thøgersen, 2008.

It has been found that the SCR catalysts may deactivate much faster in biomass firing than plants firing coal, gas or oil. A full-length monolith catalyst in a slipstream high-dust reactor, installed at a straw-fired power plant was investigated. It was found that a high deactivation rate of about 1 % of the relative activity per day was observed when the power plant ran continuously. These results were compared to a laboratory-scale analysis.

K is known to be an important element for deactivation of (vanadium) SCR catalyst systems, as already established in the previous Chapters. Fly ash of biomass and also liquid biofuels can contain high levels of K. In full-scale systems K exists as an aerosol of potassium chloride and sulfate, KCl and K_2SO_4. Wet impregnation was used in this laboratory study. Results show that these compounds are strong poisons for the SCR catalyst as well as alkali oxides.

Beside KCl and K_2SO_4 the aerosol in the biomass fired flue gas contains minor amounts of Na, P and Ca, which are known poisons as well. Thus it is difficult to prove the deactivation results of a single poison.

Both types, monolith and plate V_2O_5-WO_3/TiO_2 catalysts were investigated. They were obtained from Haldor Topsøe A/S. The catalyst plates contained of 1 wt. % V_2O_5 and about 7 wt. % WO_3 on a fiber reinforced TiO_2 carrier. The dimensions of plates were 1.3 mm * 50 mm * 160 mm and were cut into 10 mm * 20 mm pieces for exposure and activity tests.

The corrugated-type monoliths were similar to the plates except they had V_2O_5 content of 3 wt. %. The monolith dimensions were 75 mm * 75 mm * 500 mm and the hydraulic diameter of the channel was 6.44 mm. The total specific outer surface area was 455 m^2/m^3 and the void factor was 0.732. The BET surface area of the fresh monolith was about 59 m^2/g.

4.1.1. Exposure to KCl aerosols

Activities of the catalyst were measured at 350 °C typically 2-3 times per day. The measurement flue gas contained 500 ppm NO, 600 ppm NH_3, 6.5 % O_2, 7 % CO_2 and about 10-15 % H_2O. The activity was then calculated by certain equations.

Exposure test for catalyst plates

Catalyst plates were exposed to a layer of commercial KCl particles with a mean diameter of 360 µm (Merck, 104936) in a lab-scale quartz reactor. About 200 ml/min compressed air passed through water bath at room temperature to be saturated with H_2O for about 3 vol. %, and was then mixed with SO_2 to get a concentration of 1000 ppm. The gas mixture passed through the reactor containing nine pieces of the catalyst plate at 350 °C. The three pieces in the middle were covered with a layer of KCl particles with a thickness of about 2 mm. The three pieces upstream were assumed to have no contact with K salts, and were used as comparison. The last three pieces downstream were used to investigate the effect of flue gas which has been exposed to K salts.

Deactivation of plate catalysts

In upper part of Figure 43 are shown the activities of plates after exposure to ash from the Masnedø power plant for 2970 h, and in the lower part of the Figure are shown the activities of plates after exposure to KCl particles for 2970 h including exposure to SO_2 in the period 0-670 h. Practically no loss was found in the activity of catalysts exposed to Masnedø ash at 350 °C for the given time. For the catalysts exposed to the KCl particles, the activities of the catalysts before and after were almost the same as of the fresh, meaning

that no or little deactivation occurred. The relative activities in the middle position were about 87 % meaning that some deactivation occurred.

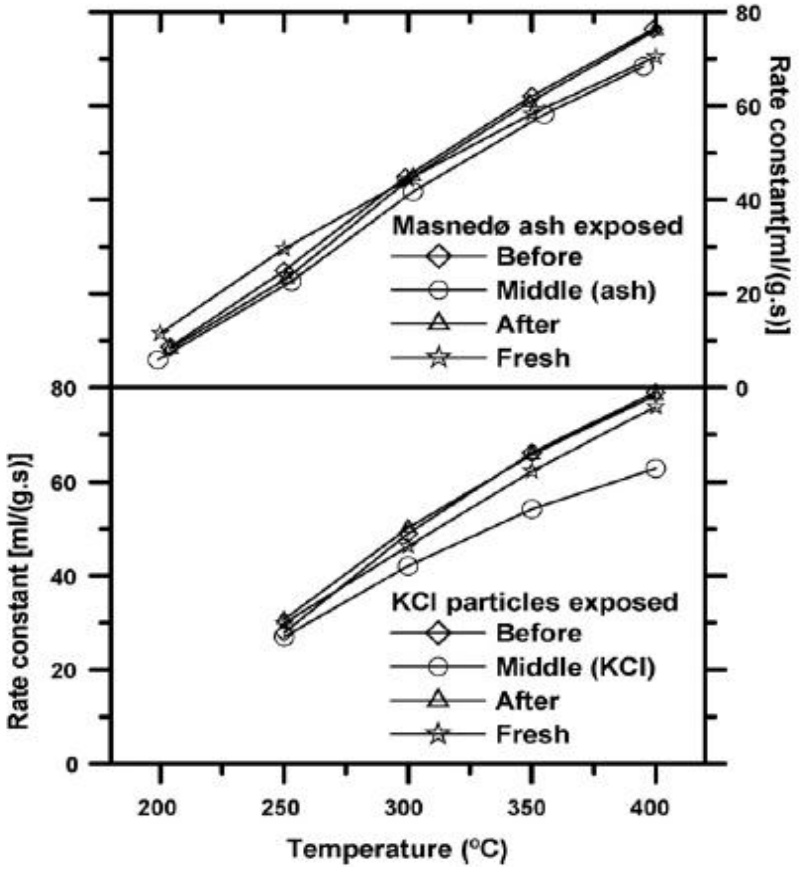

Figure 43. Catalytic activities of catalyst plates as a function of temperature. (Zheng *et al*., 2008)

Exposure test for monolith catalyst

A full-length monolith was placed in a bench-scale reactor and exposed to well-defined aerosols of KCl and K_2SO_4. Hot flue gas was produced by a natural gas burner and the NO level was adjusted by addition of NH_3 to the combustion air. A salt water that contained 7.4 g/l KCl or K_2SO_4 was prepared several days before the tests. The aerosols were produced by injecting the solution through a nozzle into the flue gas close to the burner where the temperature was between 1000 and 1150 °C. The catalyst exposure temperature was kept at

350 °C. The flow rate of 40 m^3/h through the catalyst was kept by adjusting the bypass valve, which means that channel velocity was 6 m/s at 350 °C, similar to that of a full-scale catalyst operating in a power plant.

Deactivation of monolith catalysts by exposing to KCl aerosol

Two monolith catalysts were exposed to KCl aerosols at 350 °C. The catalyst activities as a function of exposure time are shown in Figures 44 and 45. The catalyst activity was constant for the first 340 h before the KCl was added. There was a decrease of 9 % at 412 h which might be caused by the removal of the fresh catalyst from the reactor for about 130 h during maintenance of the burner. The catalyst was further removed for about 1300 h during a later maintenance of the reactor and aerosol measurement of empty reactor. There was a drop of 12 % in the activity at exposure time of 436 h when the catalyst was re-installed after the KCl had been added for 3 days to make the aerosol measurement. The KCl load then was 260 – 520 mg/m^3. The activity kept decreasing when the KCl was added continuously with an amount of 53 mg/m^3. At 750 h 1000 ppm SO_2 was added for 3 h to calibrate the system flow rate, and the relative activity increased from 51 % to 56 %. It seems that sulphation of the catalyst by the SO_2 regenerated the catalyst by increasing its acidity. The activity gain lasted for 3 days. After about 1250 h the automatic soot blowing was initiated due to high pressure drop. The soot blowing gave a rise of 5 % in the activity. After exposure to the pure KCl aerosols for about 1830 h the relative activity was only 18 %. The whole exposure time was then 2440 h.

At the end of the test the reactor was opened and both the plugged channels and the reactor system were cleared. Then the catalyst was tested for another 400 h without KCl addition and a relative activity leveled off at 20 %. The concentration of KCl aerosols in the bench-scale reactor was 10-20 times lower than in the SCR pilot plant at the Masnedø straw-fired power plant. An interesting finding in this test was that in spite of much lower volume of the pure KCl in the bench-scale reactor compared to the power plant, the deactivation rate was quite similar, about 1 % per day.

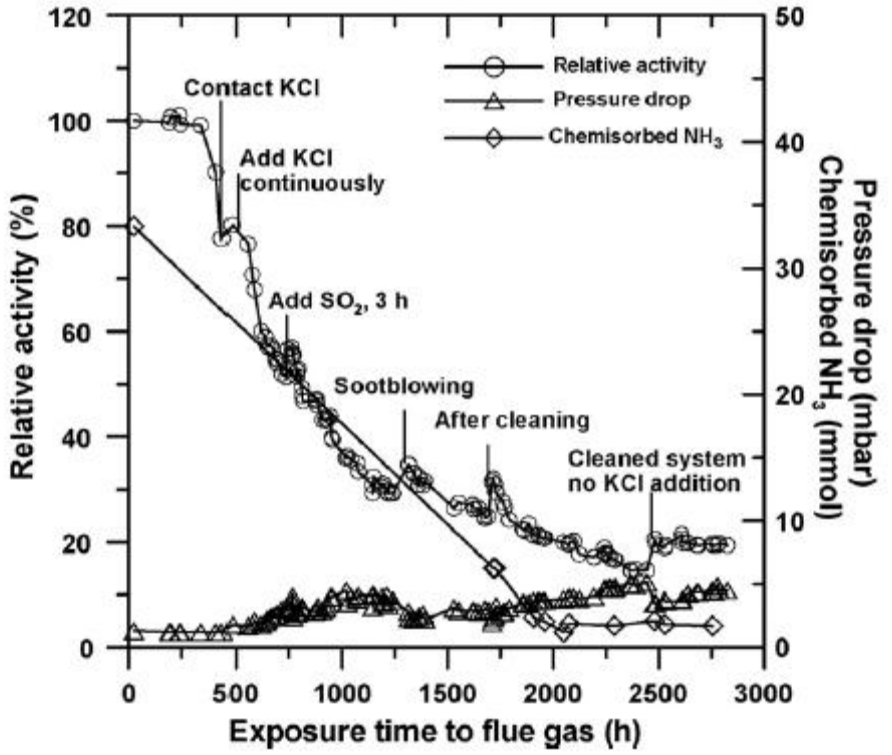

Figure 44. Activities, chemisorpted NH_3 and pressure drop on the catalyst during the first KCl aerosols exposure as a function of time. (Zheng *et al*., 2008)

The final activity level was very low in the first test. A second test was done to investigate the repeatability of the experiment, and to make sure the deactivation stops when no more KCl is being added, also in the situation where there is still a lot of activity remaining. Soot blowing and NH_3 chemisorption tests were done from the beginning of the second test. In Figure 45 can be seen that after exposing the catalyst to the KCl at 350 °C for 715 h the catalyst relative activity was 69 %, which corresponds to a deactivation of 1.0 % per day, in good agreement with the first test. Also a fast NH_3 adsorption capacity decrease is shown in the same Figure. After 715 h the system was cleaned and the catalyst was tested for another 235 h without KCl addition. The catalyst activity remained at about 69 % and the amount of chemisorpted ammonia also leveled off, meaning that the deactivation was done by KCl only.

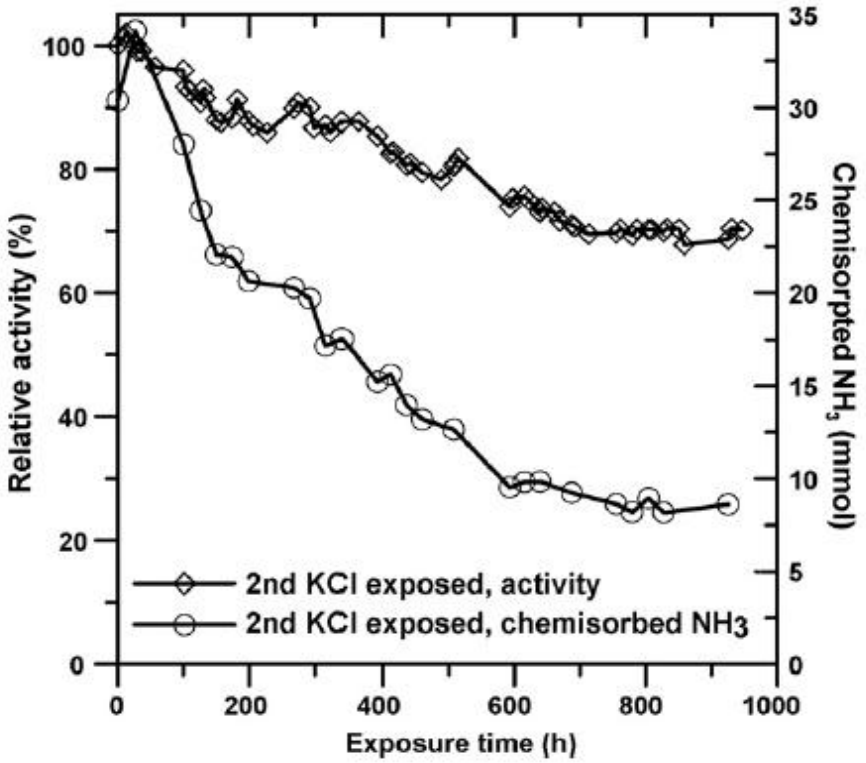

Figure 45. Activity and chemisorpted NH_3 on the catalyst during the second KCl exposure as a function of exposure time. (Zheng *et al*., 2008)

4.1.2. Deactivation of monolith catalysts by exposing to K_2SO_4 aerosol

The catalyst activity as a function of the exposure time to K_2SO_4 is shown in Figure 46. In the first 300 h the relative activity decreased to 86 %, corresponding to 1.1 % deactivation rate per day. This can be due to the deposited KCl in the system from the previous test. Elemental analysis showed that about 0.50 wt. % Cl was found in the catalytic structure. Probably the system was not cleaned carefully enough between the tests. The next 200 h the relative activity fluctuated at around 90 %. The relative activity kept decreasing at a rate of about 0.40 % per day, which could be assumed to be more truthful rate for the K_2SO_4. The rate was only 40 % of the deactivation rate observed for the catalysts exposed to the KCl at a similar aerosol load and at the Masnedø power plant. The pressure drop during the test was almost constant 1.6 mbar except a slight increase at the end, which informs that there was no plugging, or only a very small plugging in the catalyst (not shown in Figure).

The catalyst capacity for NH_3 chemisorption decreased faster than the relative activity. The active sites within the catalyst structure, although not participating in the SCR reaction, do react with K. This results in a faster decrease in the catalyst capacity for NH_3 chemisorption than the observed activity which is damped by the mass transfer resistances. The deactivation rate did not increase, although there was a higher aerosol load in the last exposure period. The precise load increase wasn't informed in the investigation though.

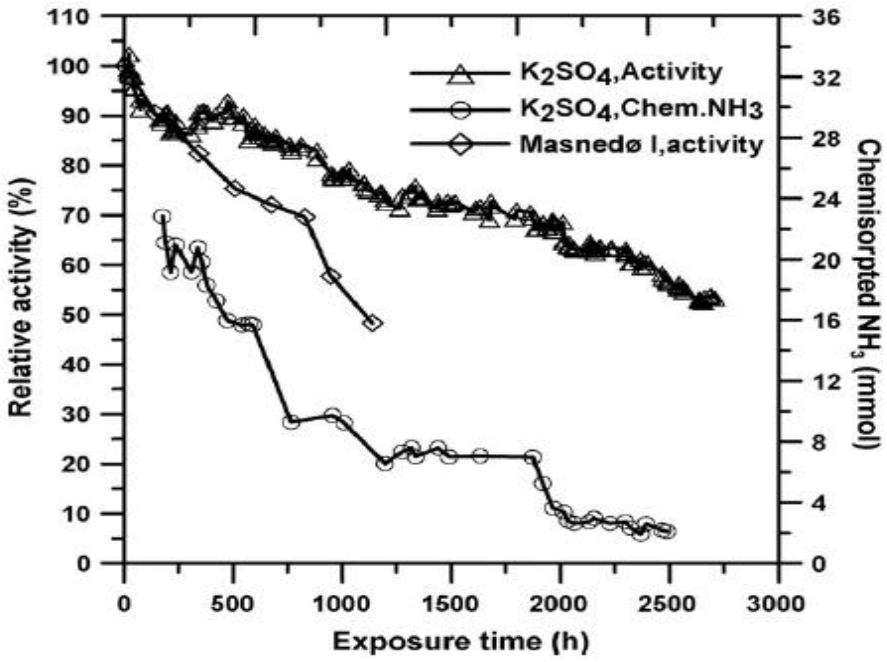

Figure 46. Activities and chemisorpted NH_3 on the catalyst during the second KCl aerosols exposure test. (Zheng *et al.*, 2008)

4.1.3. BET and hg-porosimetry measurement

The BET surface area was slightly smaller with the KCl exposed catalysts compared to the fresh samples. The Hg-porosimetry measurement showed that both total pore volume and average pore diameter both decreased after exposing to the KCl aerosols, meaning that some macropores were plugged by the KCl aerosols. Results are shown in Table 12.

Table 12. BET and Hg-porosimetry results. (Zheng *et al*., 2008)

	Fresh	KCl aerosol exposed
Surface area (m^2/g)	59.43	55.13
Total pore volume (BET) (cm^3/g)	0.17	0.19
Total pore volume (Hg) (cm^3/g)	0.84	0.48
Average pore diameter (BET) (nm)	11.5	13.9
Average pore diameter (Hg) (nm)	97.6	81.7

4.1.4. SEM-EDX analysis

SEM – Scanning Electron Microscope

Figure 47 (a) and (b) shows the SEM images of the upper and the undersurface of the catalyst plate exposed to a layer of the KCl particles for 2397 h, with 1000 ppm SO_2 for 670 h. Few particles were found from the undersurface, Figure (b). These particles were probably from the catalyst material during the cutting of the sample before analysis, because the elemental analysis showed that there was no K or Cl on the undersurface or in the dispersed particles, confirming that the few particles were from the catalyst matrix. On the upper surface, Figure (a), can clearly be seen that there were sintered KCl particles. There were some big particles with diameter of 2-4 µm and many small particles accumulated on the surface, even as the average diameter size of a KCl particle being 360 µm. The KCl layer was pressed onto the catalyst to avoid blowing it away by the air stream. There was almost no Cl in the catalyst structure, and KCl was sulfated to K_2SO_4.

Figure 47 (c) presents the surface analysis of the catalyst exposed to the pure KCl aerosols for 1830 h with total exposure time of 2440 h in the bench-scale reactor. Large pores were partly filled and there were some loose particles deposited on the surface.

In Figure 47 (d) is shown the surface of the catalyst exposed to K_2SO_4 aerosols for 2707 h in the bench-scale reactor. Some loose particles were deposited on the surface.

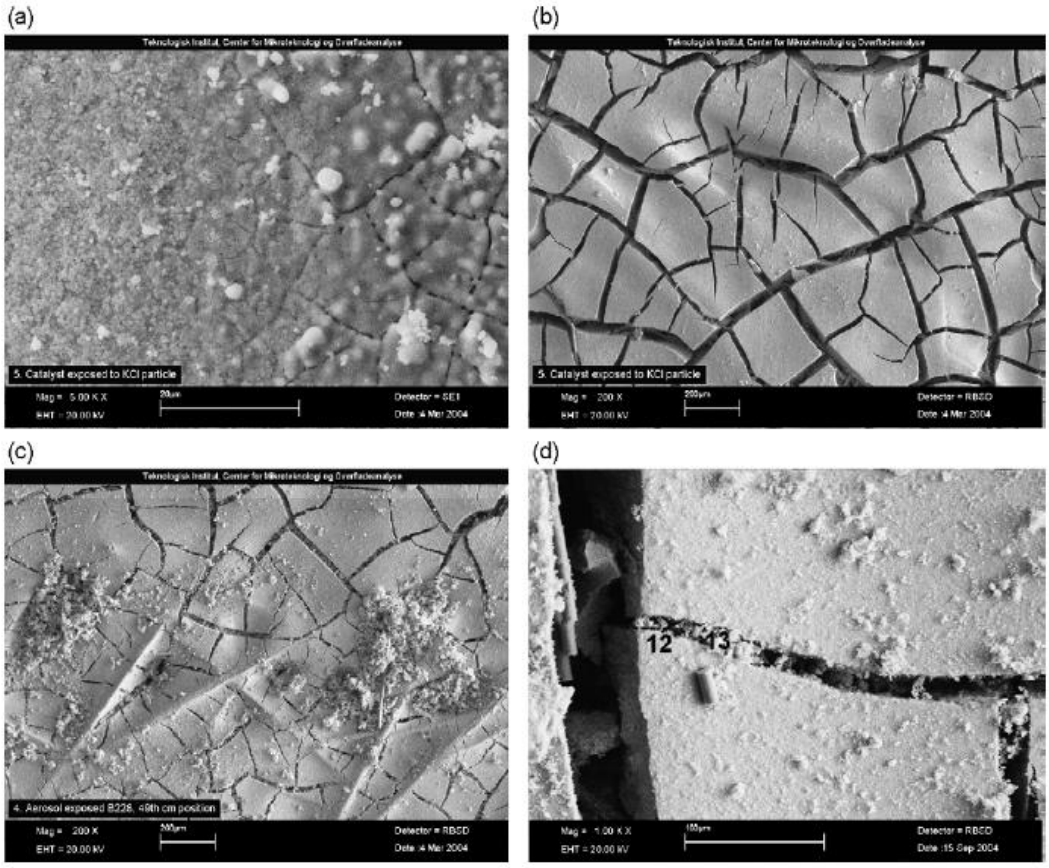

Figure 47. SEM pictures of the exposed catalysts: (a) upper surface plate in the middle position exposed to KCl particles, (b) undersurface of the catalyst plate in the middle position exposed to KCl particles, (c) surface of monolith catalyst exposed to KCl in bench-scale reactor, and (d) surface of monolith catalyst exposed to K_2SO_4 aerosol in the bench-scale reactor. (Zheng *et al*., 2008)

EDX – Energy-dispersive X-ray spectroscopy

Figure 48 shows the K distribution along the catalyst thickness. It can be seen that the K penetrated into about 10 % of the wall thickness. For the catalyst exposed to the ash collected at Masnedø, no K was found on either upper- or the undersurfaces.

The EDX analysis showed that the aerosols deposited on the first KCl aerosol exposed catalyst were mainly in the form of K_2SO_4. The average S content at the surface, down to a depth of 73 µm, was 3.35 wt. % on carbon and oxygen free basis, while the average trough the thickness of the wall was about 0.9 wt. %, and the content in the fresh catalyst being 1 wt. %. Considerably the S addition to the catalyst by exposing to 1000 ppm SO_2 for 3 h was

negligible. Still, the effect of surface sulfates was significant as the catalyst activity increased from 51 % to 56 % during those three hours. Sulfate species on the catalyst support interact with adsorbed water to form Brønsted acid sites, promoting the adsorption of ammonia. It is suggested that the presence of SO_2 affects the molecular structure of the catalysts with low vanadia coverage through driving the dispersed vanadia species in a state of high surface density, providing more closely related V sites for activation of NH_3 in SCR reaction conditions. In contrast with S, the contents of Cl at the surface and in the catalyst structure were similar with an average content of about 0.33 wt. %.

Figure 48 shows the profile of K/V molar ratio along the wall thickness of the first KCl aerosol exposed catalyst. There was a fast decrease of the ratio from the surface into the catalyst. At a depth of 200 µm there was an average K/V ratio of about 0.75 in the catalyst structure with both the plate and the monolith. Such a ratio is high enough for a significant chemical deactivation. The previous investigation of this scientist group (Zheng, Jensen, Johnsson. 2004) showed that the remaining activity of a 3 wt. % V_2O_5 catalyst doped with a K/V ratio of 0.8 was about 10 %. The remaining activity of 18 % after exposure to pure KCl aerosols for about 1830 h is in reasonable agreement with the lab-scale data.

For the catalyst exposed to K_2SO_4 the elemental analysis showed that the sulfur content on the catalyst surface was 0.94 wt. %, and in the deposit 3.16 wt. %. This indicates that S level within the catalyst did not increase due to the expose to K_2SO_4. The average K/V ratio was about 0.49, which was lower than that in the catalyst exposed to the KCl. There was about 0.3 -0.5 wt. % Cl in the catalyst structure, which could be due to the exposure to the KCl before the K_2SO_4 test because of the difficulties in cleaning of the reactor.

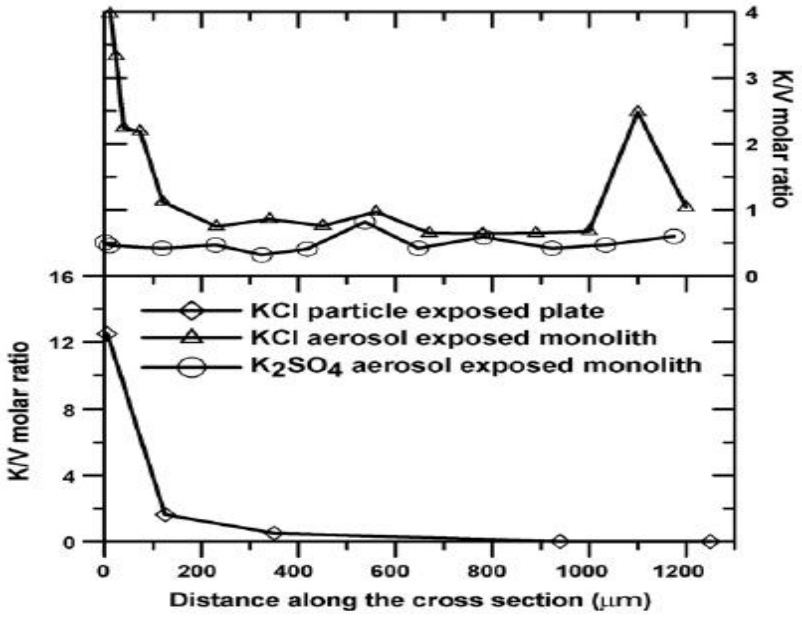

Figure 48. K distribution along the thickness of the catalyst. (Zheng *et al.*, 2008)

Deactivation by fouling and channel plugging

The experiment and SEM analysis showed that the catalyst had a high risk of fouling and channel plugging, and therefore powerful and frequent soot blowing was necessary to keep the catalyst clean. Fouling seems to be a more severe problem in biomass-firing than coal-firing power plants. This could be due to the fine KCl and K_2SO_4, or alike, aerosols produced in the bench-scale reactor, which causes more particles to deposit by Brownian and turbulent diffusion. There are no big particles in the flue gas to sand blast the catalyst surface. In this study it was observed that plugging of the channels takes place mainly close to the inlet. This may be caused by impaction of the particles against the edge of the channel, which accelerates the building of deposits. Lower melting point of the KCl and the K_2SO_4 compared to typical coal fly ash may enhance particle sticking on the catalyst surface. When a channel is plugged it is obvious it does not work at maximum activity. This can be severe deactivation mechanism especially in full-scale SCR catalyst systems where soot blowing cannot be carried out as frequently as in this experiment. Channel plugging was not major problem in these studies, but fouling may have contributed to an unknown but rather small extent.

Deactivation by poisoning and mechanisms of K penetration and accumulation

From SEM-EDX analysis can be pointed that K penetrated into the catalyst wall and the NH_3 chemisorption measurement revealed that the Brønsted acid sites had reacted with poison and caused inactiveness for NH_3 adsorption and subsequent reaction with NO. This poisoning has been proposed by the same scientist group in their previous investigation, same as above mentioned (Zheng et al. 2004). In situ Raman spectroscopy revealed that K changes the vanadium surface species in the SCR reaction by lengthening the V=O bond. The mechanisms by which the K penetrates the catalyst active sites are still unknown.

Deactivation by diffusion of K vapor into the catalyst was excluded since the calculated vapor pressures of the KCl and the K_2SO_4 at 350 °C are too low for this mechanism. It is pointed out that the deactivation of the monolith catalysts due to the K salt fouling layers do not occur without aerosols in the flue gas. The effect of K vapor was further excluded by the fact that there was no deactivation found at the “after” positions at the lab-scale exposure tests, Figure 43.

The formation of liquid potassium-vanadium-pyrosulfates could in principle be formed in systems used in this investigation and be involved in destroying active sites in the SCR reactions. Figure 44 showed that the catalyst activity does decrease from exposure to pure KCl aerosols in the absence of SO_2, meaning under conditions where the pyrosulfate mechanism could not have been active. The 1 % deactivation rate per day is similar to full–scale, indicating that the pyrosulfate mechanism did not affect on full-scale tests either.

The little deactivation of the catalyst plates by direct contact with the pure KCl or ash indicates that the deactivation by deposits on the catalyst is a slow process. The relative activity and ammonia chemisorptions settled when the KCl addition was disrupted, both at a low and high level of poisoning. Also in earlier findings were observed that when the power plant ran for few hours per day the catalyst activity stabilized. It would be expected that deposits on the catalyst surface would cause continuous deactivation if the pyrosulfate mechanism was active. The results show that without an aerosol in the flue gas no more deactivation occurs. This indicates that the K accumulated in the deposits on the catalyst

wall is not capable of penetrating and deactivating the catalyst, or the deactivation is very slow.

A continuous flow of aerosol through the catalyst is needed for the deactivation. The deposits of Merck KCl that contain large particles only causes slow deactivation of about 0.1 % per day in relative activity with only one side contacting the deposit. This points out that only the finest fraction of the aerosol is involved in the reaction. These particles are easily deposited due to their high diffusion coefficient, and their contact area to the wall per mass of aerosol is large.

Figure 49 shows the aerosol diffusion coefficient at 350 °C in 10^{-8} cm^2/s, the distribution of the catalyst pore size in ml/kg and the size distribution of the K_2SO_4 aerosol created in the bench reactor in mg/m^3. The fine aerosol particles may diffuse into the catalyst structure since there is some overlap between pore sizes of the catalysts and size distribution of the fine aerosols. It is suggested that mainly alkali in ultra fine particles, <100 nm, in the flue gas caused the alkali accumulation on the catalyst samples exposed to flue gas from biofuels and peat. The catalyst investigated in this work used fiber reinforced TiO_2 as carrier and had large pores compared to extruded or plate type catalysts. It is assumed that fine particles diffuse into large >1 µm pores of the catalyst in this investigation. In the catalyst wall K catalyst reacts with the V-OH group and turns the active sites to –V-O-K and through surface diffusion these are distributed all over the wall.

The results of this investigation show clearly that the deactivation of this type of catalysts by the KCl aerosol is much faster than that by the K_2SO_4 aerosol, though the previous lab-scale investigation of this scientist group with deactivation of SCR catalyst by wet impregnation, showed that K_2SO_4 would be only slightly weaker poison compared to KCl. For K in the form of aerosol, the different mobility in "Tamman and Hüttig temperatures" of the KCl and the K_2SO_4 could be the reason of difference between the deactivations. The so-called Hüttig and Tamman temperatures indicate the temperature at which sintering starts. For KCl the $T_{Hüttig}$ and T_{Tamman} temperatures are 40 °C and 249 °C, and for K_2SO_4 they are 129 °C and 397 °C, respectively. The temperatures are clearly higher for K_2SO_4, which

means that the mobility of KCl is better and that it penetrates the catalyst faster. Another reason could be the mass mean diameter of K_2SO_4 aerosols being bigger than KCl's. Bigger particles have difficulties to penetrate into the catalyst and less is deposited on the surface.

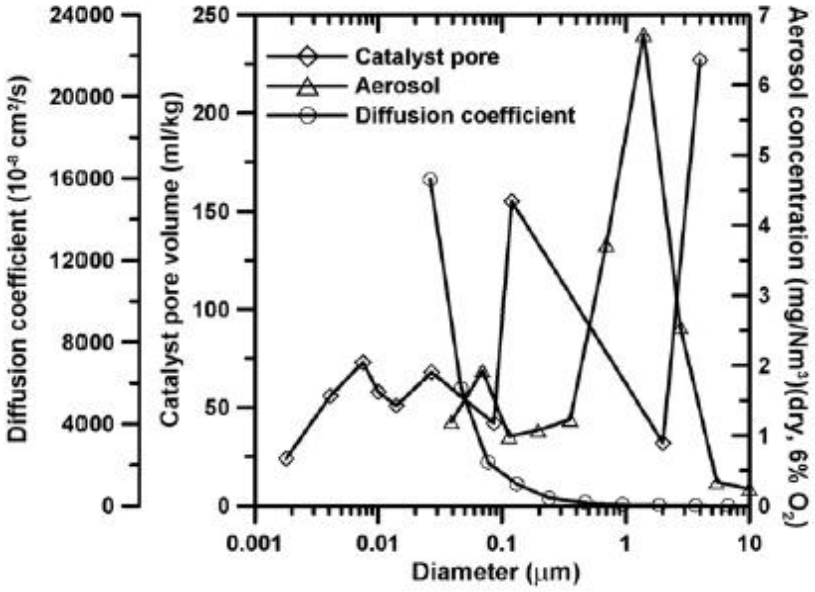

Figure 49. Aerosol mass size distributions of K_2SO_4, pore size distribution of the monolith catalyst and the diffusion coefficient at 350 °C. (Zheng *et al*., 2008)

4.1.5. Conclusions

- The chemical poisoning of the active sites is the dominating deactivation mechanism when catalyst is exposed to KCl and K_2SO_4, physical blocking being a secondary mechanism.

- After 1970 exposure hours no deactivation was found for the catalyst plates exposed to ash collected from a SCR pilot plant installed in a straw-fired power plant.

- Slow deactivation of 10 % was found for the catalyst plates exposed to a layer of KCl particles for 2397 hours with addition of SO_2 for 670 hours.

- A fast deactivation was found for the catalysts exposed to pure KCl and K_2SO_4 particles, deactivation rates being 1.0 % and 0.4 % per day, respectively.

- The deactivation caused by K_2SO_4 is less than that found in Chapter 3.1., probably due to the smaller amount of the matter. The precise amount was not told in ppm in this investigation.

- K penetrates into the catalyst structure. In this investigation the K/V molar ratios were 0.5-0.75 and high enough to explain most or all of the activity loss by chemical deactivation.

- S can increase the acidity of the catalyst surface and therefore increase conversion activity, at least momentarily.

4.2. DEACTIVATION AT 100 MW-SCALE BIOFUEL AND PEAT BOILERS

Chapter 4.2. with its Figures and Tables is fully based on an article written by Åsa Kling, Christer Andersson, Åse Myringer, David Eskilsson and Sven G. Järås, 2007.

Three different 100 MW-scale boilers running on different biofuel compositions and peat were investigated in order to find about alkali deactivation of SCR equipment. The deactivation of the catalyst samples was correlated to the corresponding flue gas composition. Also the effect of sulphation was investigated by adding S into the furnace during the tests. The combustion method was found to have strong impact on overall deactivation rate, the deactivation was more severe during pulverized fuel combustion than with during circulating fluidized bed combustion. The temperature at SCR equipment was the same in all cases. This indicates that only specific forms of K causes the deactivation or it is at least more severe in some forms. This fact has been introduced earlier in this thesis at earlier Chapters.

In biomass K is usually bound as salts or organically bound in ion-exchangeable form, which means high volatilization in the combustion. Depending on the fuel the K is usually bound mainly to sulfate or chloride in the flue gas. From 300 to 400 ºC only low amounts of K vapor are thermodynamically stable. However the smallest particles, <0.5 µm, will mostly be K, S and Cl.

4.2.1. Exposure of the catalysts

Three types of honeycomb V_2O_5/TiO_2-WO_3 catalysts were used, called A, B and C. The difference between these was mainly the vanadium content. Type A was a typical catalyst for coal-fired power plants with high SO_2 content in the flue gas, with low vanadium content and low $DeNO_X$ activity per m^3. Type B was a “bio-optimized” catalyst with higher vanadium content for applications with low amounts of SO_2 in the flue gas. Type C was a

very high vanadium content catalyst for high alkali metal environments. No more specific information was given about the catalysts.

The samples were exposed from 100 h to 3000 h using a sample bench. The sample bench was placed so that the temperature was 300 - 400 ºC in “high-dust” position before dust collection. The pressure drop over the catalyst makes the flue gas flow through the samples. Exposure of short samples usually results greater deactivation than of full-length catalyst, mainly because of turbulence at the inlet of the catalyst before a laminar flow is achieved.

Three full-scale CHP plants were used for the tests. “Johannes” had a thermal capacity of 90 MW with bubbling fluidized bed combustion with bark and demolition wood fuel mix. The combustion temperature was about 800 ºC. “Brista” had a thermal capacity of 120 MW with circulating fluidized bed combustion with forest residues as fuel. The combustion temperature was 850-880 ºC. The Uppsala CHP plant had a thermal capacity of 400 MW with pulverized fuel combustion with a mix of peat and wood powder. The different boilers, combustion principle etc. are listed in Table 13. The samples were exposed during 5 year-period but only during the cold time of the year, from December to April, called the combustion season, seasons named A, B, C and D. Table 14 represents the contents of potential poisons in the fuel mixes. They are just average and not exact.

Table 13. Basic information of the boilers and combustion circumstances. (Kling *et al.*, 2007)

Name	Season[a]	Boiler type	Maximal thermal capacity (MW)	Fuel	Furnace additive	SCR-sample temperature (°C)	Flue gas velocity (m/s)	Sample space velocity (h^{-1})
Johannes	A	BFB[b]	90	Bark + 15% demolition wood (B + 15% DW)		270	3.9	156000
Johannes	B	BFB[b]	90	Bark + 30% demolition wood (B + 30% DW)		270	3.9	156000
Brista	A	CFB[c]	120	Forest residues (FR)		370	3.2	128000
Brista	B	CFB[c]	120	Forest residues (FR)		370	3.2	128000
Brista	C	CFB[c]	120	Forest residues (FR)	Sulphur (S)	370	3.2	128000
Brista	D	CFB[c]	120	Forest residues (FR)	Sulphur (S)	370	3.2	128000
Uppsala	A	PC[d]	400	Peat + 30% wood (P + 30% W)		370	10	400000
Uppsala	B	PC[d]	400	Peat + 20% wood (P + 20% W)		370	10	400000
Uppsala	C	PC[d]	400	Peat (P)		370	10	400000

[a] The cold period of the year from December until April.
[b] Bubbling fluidised bed.
[c] Circulating fluidised bed.
[d] Pulverised combustion.

Table 14. Contents of potential poisons in the fuels. (Kling *et al.*, 2007)

Fuel	K (mg/kg ds)	Cl (mg/kg ds)	S (mg/kg ds)	Na (mg/kg ds)	Ash content (%)
Peat + 15% wood (1)	434	100	2300	218	5.4
Forest residues (11)	1500 ± 480	211 ± 66	384 ± 130	275 ± 190	3.1
Demolition wood (32)	1165 ± 580	641 ± 550	788 ± 790	665 ± 300	5

4.2.2. Deactivation results

The catalytic activity decreased from 5 to 50 % after 100 – 3000 h of exposure to the flue gas. No or little plugging was found. The deactivation of the samples cannot be directly compared to the deactivation of full-length catalysts. However the deactivation rate with different fuels and combustion principles can be compared. To compare the different samples the loss of activity was calculated as a linear decrease from various samples and interpolated to 1500 h. Results are introduced in Table 15.

During peat combustion the deactivation was 5 – 15 %, and the increased wood co-combustion up to 30 % did not increase the deactivation. The loss of activity when burning forest residues was two to three times bigger than in peat combustion after 1500 h. Even stronger deactivation was found for bark and demolition wood combustion in bubbling fluidized bed. The effect of S addition was only small. Figure 50 shows the losses in catalytic activity per 1500 h of exposure to the different flue gases at a temperature of 300 ºC.

Table 15. The effects of combustions to relative catalytic activity. (Kling *et al*., 2007)

Fuel	Boiler type	Additive	Season	Exposure time (h)	Relative catalytic activity (%)		
					Type B	Type A	Type C
Peat + 30% wood	PC[a]		A	864	91 ± 1 (4)		
Peat + 30% wood	PC[a]		A	1340	92 ± 1 (2)		
Peat + 30% wood	PC[a]		A	2850	93 ± 6 (3)		
Peat + 15% wood	PC[a]		B	768		88 ± 2 (2)	
Peat + 15% wood	PC[a]		B	1488	85 ± 2 (4)	80 ± 2 (2)	
Peat	PC[a]		C	526	96 (1)	91 (1)	
Peat	PC[a]		C	929	93 (1)	84 (1)	
Peat	PC[a]		C	1455	95 (1)		
Forest residues	CFB[b]		A	1230	70 (1)		
Forest residues	CFB[b]		A	1650	71 ± 4 (4)		
Forest residues	CFB[b]		A	2880	55 ± 3 (4)	46 (1)	81 ± 8 (4)
Forest residues	CFB[b]		B	120	83 (1)		
Forest residues	CFB[b]		B	864	88 (1)		105 (1)
Forest residues	CFB[b]		B	1584	64 ± 6 (2)	49 (1)	89 ± 6 (2)
Forest residues	CFB[b]		C	648		73 ± 2 (2)	
Forest residues	CFB[b]		C	984	79 ± 3 (4)		
Forest residues	CFB[b]	Sulphate	C	1320	73 ± 5 (4)	56 ± 2 (2)	
Forest residues	CFB[b]	Sulphate	C	2820	55 (1)		
Forest residues	CFB[b]	Sulphate	D	502	84 ± 1 (2)	71 ± 1 (2)	
Forest residues	CFB[b]	Sulphate	D	1038	76 ± 1 (2)	60 ± 1 (2)	
Forest residues	CFB[b]	Sulphate	D	1540	71 ± 2 (2)	54 ± 1 (2)	
Bark + 15% demolition wood	BFB[c]		A	720	72 ± 1 (2)		97 (1)
Bark + 15% demolition wood	BFB[c]		A	1150	95 ± 11 (2)		94 (1)
Bark + 15% demolition wood	BFB[c]		A	1870	66 ± 3 (3)		87 ± 19 (2)
Bark + 30% demolition wood	BFB[c]		B	100	93 ± 3 (3)		93 ± 4 (3)
Bark + 30% demolition wood	BFB[c]		B	500	86 ± 7 (3)		85 ± 4 (3)
Bark + 30% demolition wood	BFB[c]		B	1000	67 ± 5 (3)		88 ± 4 (2)
Bark + 30% demolition wood	BFB[c]		B	1400	59 ± 4 (2)		
Bark + 30% demolition wood	BFB[c]		B	1500	58 ± 0 (3)	48 ± 1 (3)	79 ± 4 (2)

All the activity analyses were conducted at a temperature of 300 °C.

[a] Pulverised combustion.

[b] Circulating fluidised bed.

[c] Bubbling fluidised bed.

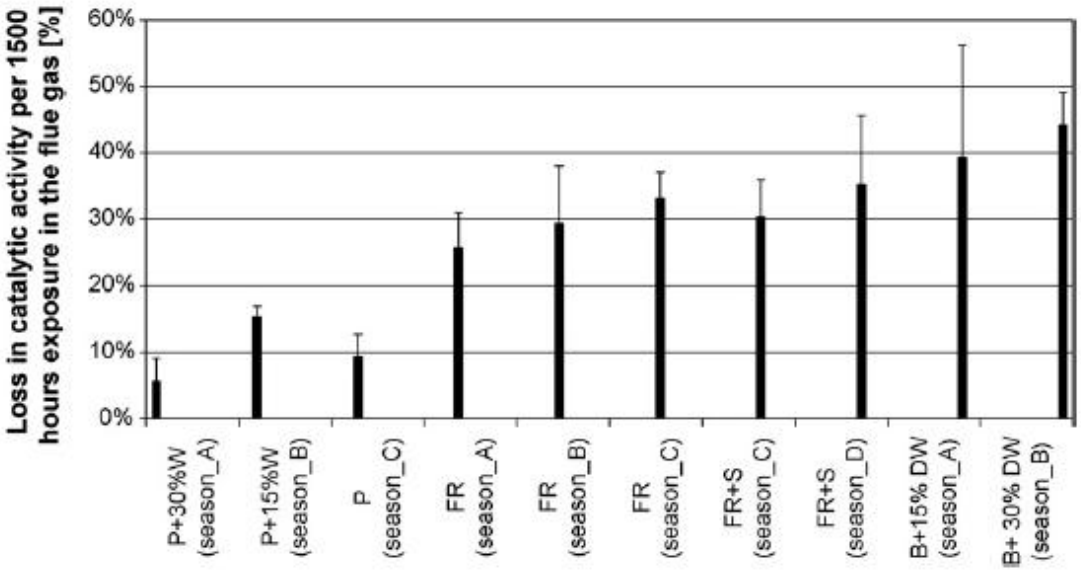

Figure 50. The loss of catalytic activity of type B catalyst samples per 1500 h. (P = Peat, W = Wood, FR = Forest Residues, B = Bark, DW = Demolition Wood). (Kling *et al*., 2007)

The deactivations of different types of catalysts are shown in Figure 51. The deactivation of type B "bio-optimized" catalyst was 1.2-1.9 times faster than of type A, the low vanadium catalyst. Deactivation of type C sample was 0.4-0.7 times the deactivation of type B after 1500 h of exposure at 300 ºC. These results indicate that the bio-optimized catalysts would not only be more active but also more durable with biofuels.

The elementary analysis by SEM-EDX on the samples showed increased amounts of mainly K but also Na. Also lead (Pb) was found on the samples exposed to demolition wood flue gases. The amounts of poisons were bigger at the inlet than the outlet of the samples. The results of SEM-EDX were not very accurate and they are not introduced in more detail in this thesis.

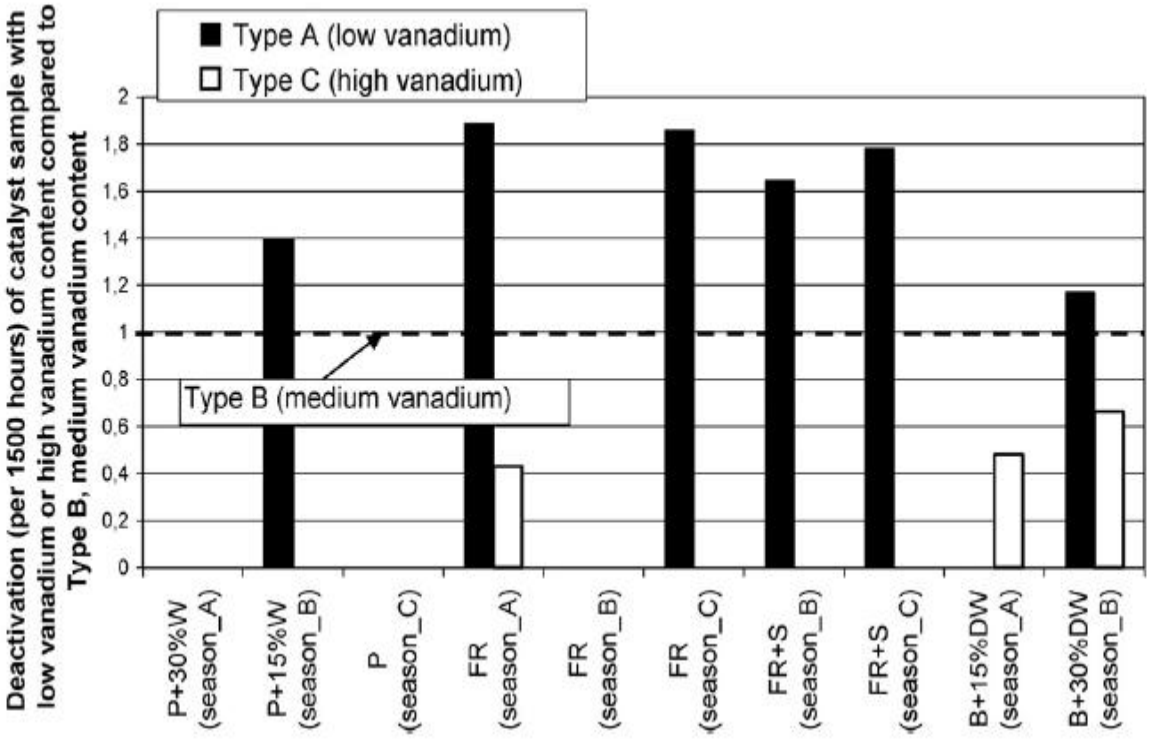

Figure 51. Loss of activity of different types of catalysts. (Kling *et al*., 2007)

Wet chemical analyses were carried out on the samples from Uppsala, seasons B and C, Brista, seasons C and D and Johannes seasons A and B. The results are shown in Figure 52. K and Na were accumulated quite linearly on the catalyst samples. After 1500 h the accumulation of K was highest, about 0.2 wt. %, in co-combustion of bark and demolition wood. The accumulation of K from forest residues was about 0.10 – 0.13 wt. % with and without S additive, and from peat about 0.05 wt. % after 1500 h. The accumulation of Na was low, less than 0.05 wt. % in all samples. The amount of S was about 1.5 wt. % in the fresh samples. During combustion of peat and co-combustion with bark and demolition wood it decreased by about 0.10 - 0.15 wt. %. During combustion of forest residues with or without sulfate additive the amount of S decreased by about 1 wt. %. The accumulations of Zn, Cl and Pb were all very low, and basically only from bark and demolition wood.

Surface area and pore-size distribution were also measured for two samples exposed to bark and 30 % demolition wood, and for fresh sample. The average pore-size of fresh sample was 13 nm. 85 % of the pores were in the range of 10-23 nm and 99 % of the pores were smaller than 100 nm. The BET analysis showed a decrease of about 6 % in the surface area for bark and demolition wood exposed samples, Table 16.

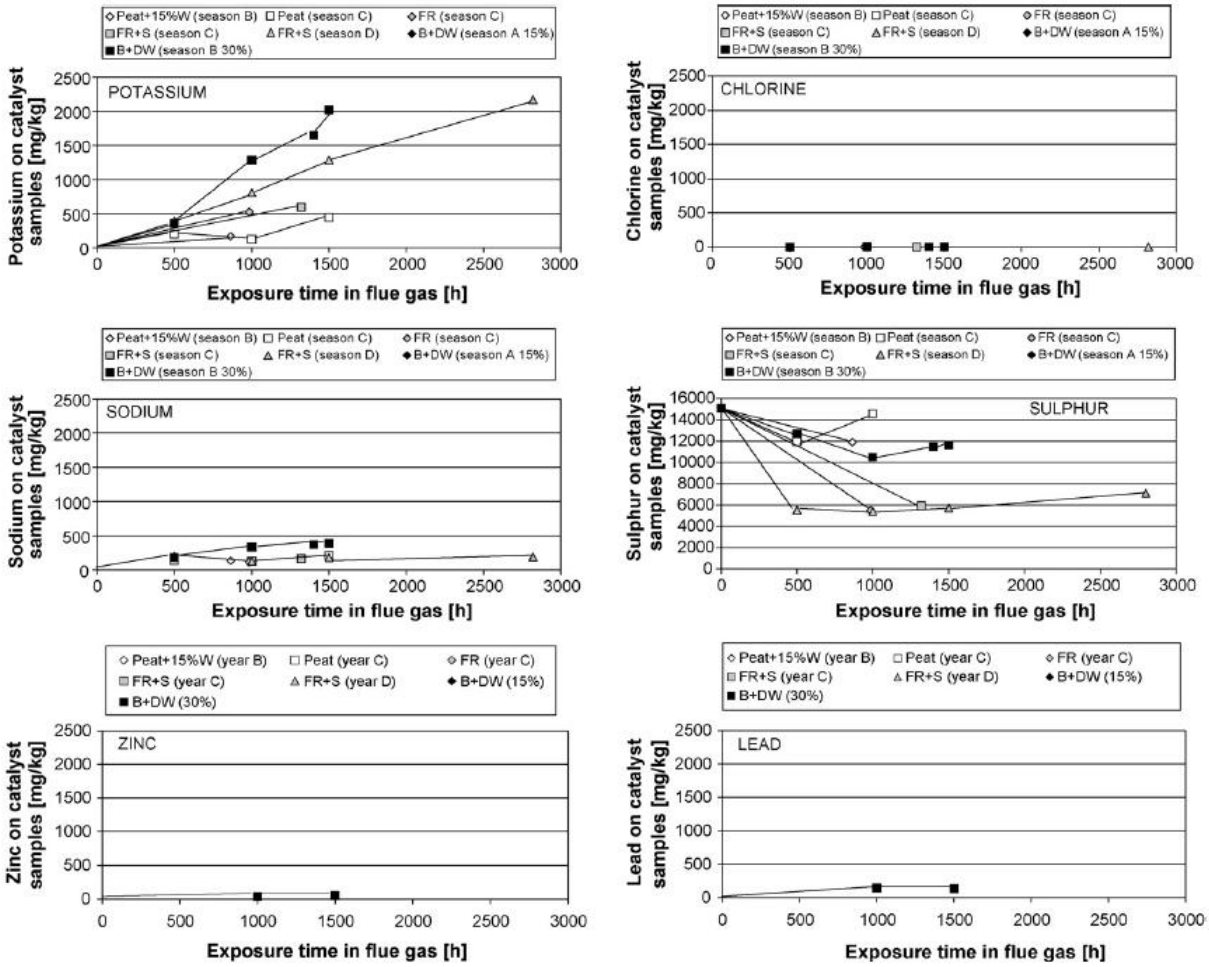

Figure 52. Accumulation of different poisons on catalyst samples as function of exposure time. (Kling *et al*., 2007)

Table 16. Results of BET surface area analysis. (Kling *et al*., 2007)

Catalyst. type	Fuel	Relative catalytic activity (%)	Surface area (m^2/g)	Micro pore volume (cm^3/g)	Average pore diameter (Å)
Type B	Fresh	100	66.8	0.0016	128
Type B	Bark + 30% demolition wood	79	62.7 ± 1.7	0.0024	138

4.2.3. Flue gas analysis

The S content in the flue gas varied a lot, from 200 ppm_{wg} in peat combustion to 3-10 ppm in co-combustion of bark and demolition wood. The alkali chloride content was continuously measured from the forest residue flue gas. The amounts of Cl and SO_2 were very little, 1 – 7 ppm_{wg}.

Impactor measurements were carried out in all locations. The amount of particles varied between boilers and size fractions, Figure 53. The biggest amount of smaller than 1 µm particles was found for co-combustion of bark and demolition wood. The least of these particles was found for co-combustion of peat and wood. A big difference was found in total amount of particles smaller than 2 µm with and without S additive during the combustion of forest residues. At times of S addition larger amounts were found. The amount of ultrafine particles smaller than 100 nm was the same with and without the additive.

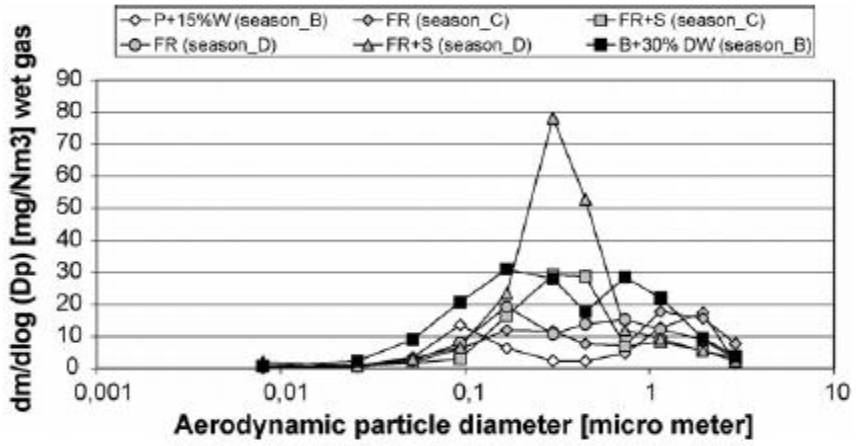

Figure 53. Fly ash mass size distribution. (Kling *et al*., 2007)

The amounts of K, Na, Cl, S, Pb, Zn, P and Ca were calculated from the results of DLPI (Dekati Low Pressure Impactor) and SEM-EDX. Results are shown in Table 17 and Figure 54. In ultrafine particles the dominating chemical compounds were K, Na, Cl, S and oxygen. Also Ca and P was found in particles larger than 0.5 µm. The amount of ultrafine K particles was highest during the combustion of bark and demolition wood. The amount did not change greatly with sulfate additive. The alkali content in peat combustion was low. The amount of K was bigger than Na's with every fuel. The highest Na content was found during bark and demolition wood combustion. A significant decrease for Cl content was found when S additive was included.

Table 17. Fly ash mass size distribution of particles smaller than 100 nm. (Kling *et al*., 2007)

	Peat + 15% wood	Forest residues (season C)[a]	Forest residues (season D)	Forest residues + sulphate (season C)	Forest residues + sulphate (season D)	Bark + 30% demolition wood (season B)
Potassium (mg/N m^3)	4.4	10.5	6.7	6.2 ± 0.2[a]	6.8	16.7
Sodium (mg/N m^3)	0.8	1.1	1.3	0.9 ± 0.1[a]	2.5	5.8
Chlorine (mg/N m^3)	0.6	2.5	1.1	0.0 ± 0[a]	0	4.3
Sulphur (mg/N m^3)	2.7	4.9	2.8	3.3 ± 0.3[a]	3.8	2.1
Lead (mg/N m^3)	0	0	0	0[a]	0	0
Zinc (mg/N m^3)	0	0	0.1	0[a]	0.2	0.1
Phosphorous (mg/N m^3)	1.1	0	0	0[a]	0	0.1
Calcium (mg/N m^3)	2.2	0	0	0[a]	0	0
Total particle amount (mg/N m^3)	17.9	8.6 ± 5.0[a]	11.6	6.0 ± 0.9[a]	12.5	32.7
(K + Na)Cl (ppm_{wg})		5.2	8.0	1.6	2.4	
SO_2 (ppm_{wg})		5.4	0.0	7.1	6.3	

[a] Average of two measurements during the same day.

Five fuel samples of forest residues from Brista were analyzed for Cl content, and then compared with the corresponding amount of alkali chloride in the flue gas. There was a strong correlation between the Cl in the fuel and alkali chloride concentration in the flue gas, Figure 55.

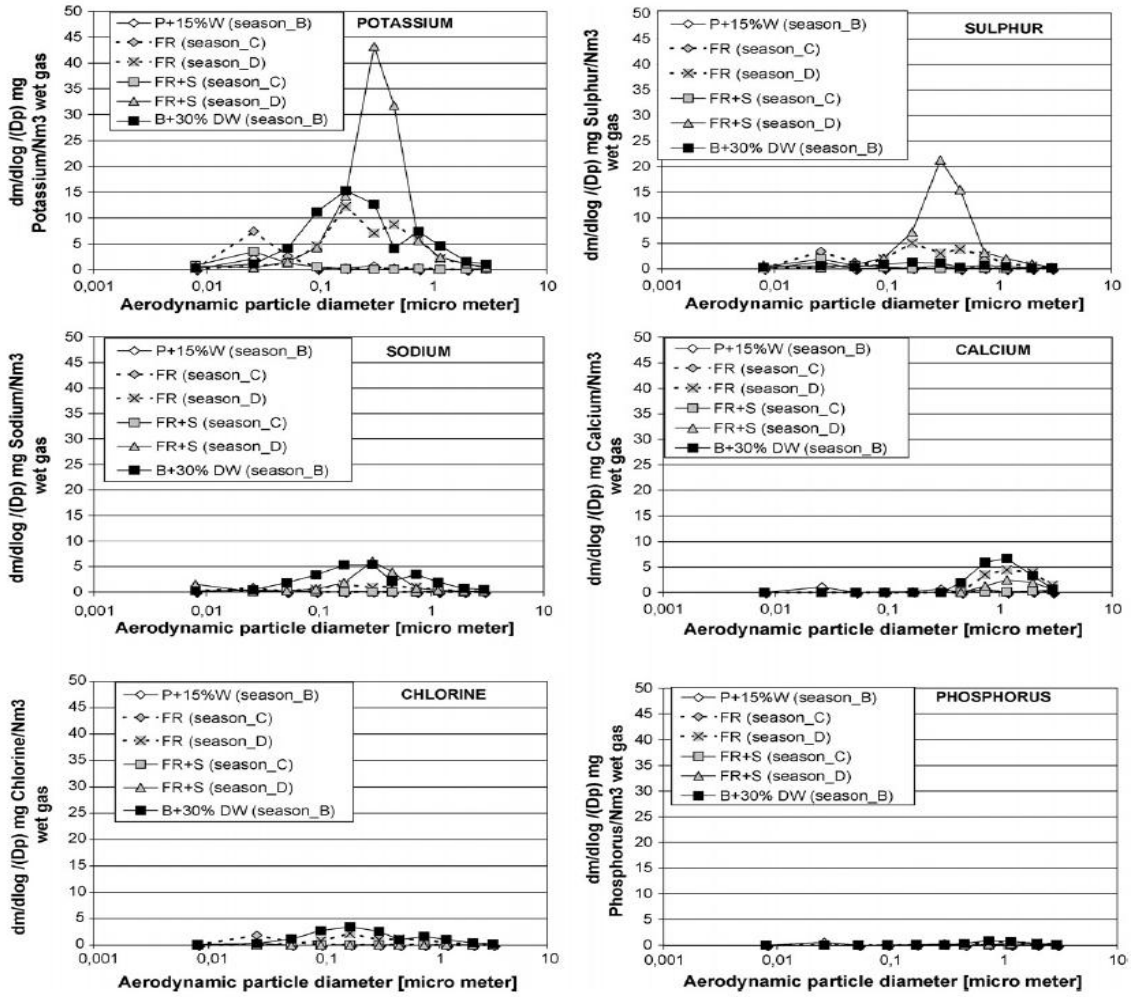

Figure 54. Fly ash mass size distribution with different fuels. (Kling *et al*., 2007)

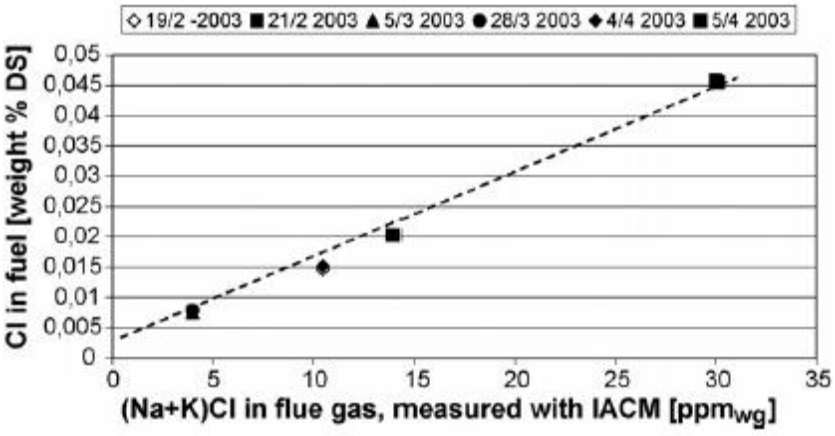

Figure 55. Cl content in fuel and alkali chloride in flue gas. (Kling *et al.*, 2007)

4.2.4. Catalyst deactivation

K and Ca were the main components accumulated in and on the catalyst samples. A strong correlation between the accumulation of those and the relative catalytic activity was found, Figure 56. This prefers that the cause of the deactivation was very likely alkali poisoning. This is in line with all the other studies investigated in this thesis. No clear conclusion could be done about what forms and compounds of alkali metals penetrate into the catalyst. However, K was quite evenly distributed throughout the catalyst material, and not only on the outer surface, which suggests that K is probably transported into the material in gas phase and as small particles.

S was found to be a regenerating agent in the SCR catalysts. The decrease of S in samples exposed to low S flue gas was probably a part of the catalyst deactivation.

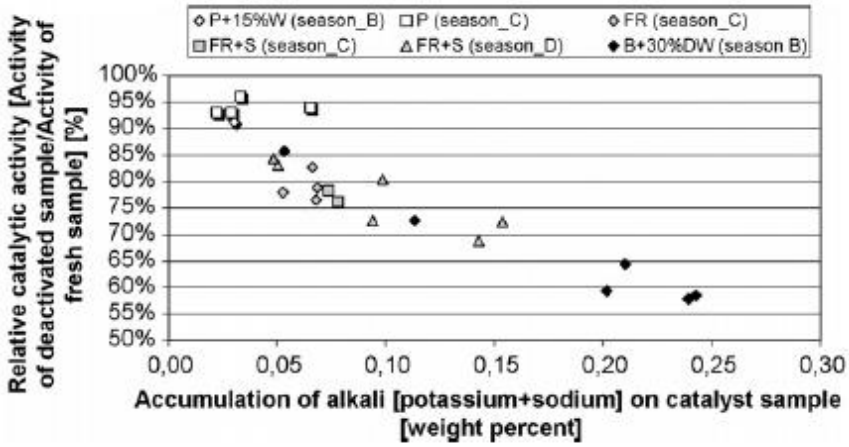

Figure 56. Accumulation of alkali as a function of relative catalytic activity. (Kling *et al*., 2007)

A linear correlation between the alkali content in the ultrafine particles and the alkali accumulation was found, Figures 57 and 58. These show the accumulations of <100 nm and <450 nm particles in the catalyst. The largest catalyst pores were about 100 nm, so larger components than that must be transported in by solid-state diffusion. This should lead to higher accumulation on the outer side of the catalyst, but this effect was not found in this study. However, the impactor measurements were very short comparing to total combustion time, and the variation in fuels' quality might have been quite significant during the tests.

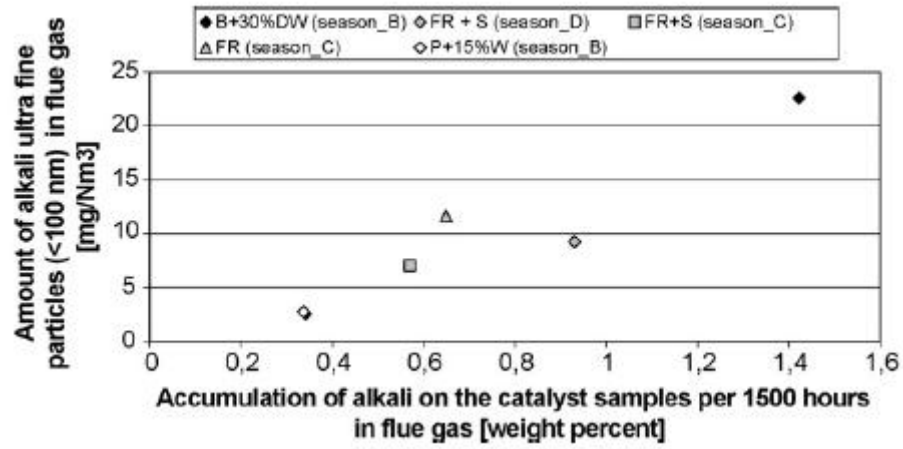

Figure 57. Accumulation of under 100 nm particles on the catalyst samples. (Kling *et al*., 2007)

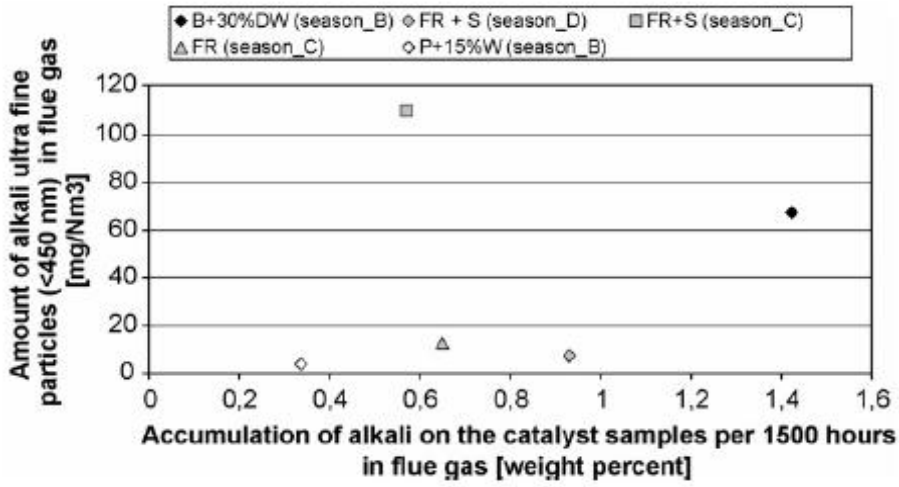

Figure 58. Accumulation of under 450 nm particles on the catalyst samples. (Kling *et al*., 2007)

4.2.5. Conclusions

- Alkali, mainly K, accumulate on catalyst surface and causes strong deactivation.
- An increased vanadium content in the catalyst material decreased deactivation rate.
- Great amount of ultrafine particles accumulate in the catalyst and probably cause deactivation.

4.3. CONCLUSIONS OF CHAPTER 4

The chemical poisoning was the dominating deactivation mechanism in actual power plants as well as in the laboratory experiments seen in the Chapter 3. Physical blocking and fouling was not as bad but still have some effect. Ash does not seem to harm the chemical activity of the catalyst but only block the inlet. Aerosol particles deposit into the pores of the surface and cause severe chemical deactivation. The smaller the particles are, the deeper they can get into the pores. K was the strongest poison as also in Chapter 3. The increase in vanadium content increased the effectiveness of the catalyst.

5. PHOSPHOUROUS POISONING OF AUTOMOTIVE SCR CATALYST

Chapter 5 with its Figures and Tables is based on an article by Karl Henrik Bergquist, unless otherwise stated.

V_2O_5-WO_3-TiO_2 SCR catalyst of 24 liters, supplied from Haldor Topsøe, was deactivated by accelerated poisoning. The catalyst was based on a fiber reinforced ceramic structure with a high cell density, and was designed to automotive use. The catalyst was deactivated for 40 hours in an engine rig, with tributyl phosphate (TBP) doped fuel. No specific amount of P was given. A length wise sample was taken from the deactivated catalyst and divided into 9 parts, part 1 being the inlet and part 9 being the outlet.

5.1. BET surface area and pore size measurements

There was a linear relationship between the BET surface area and the P concentration, see Figure 59. The amount of P had a great impact on the surface area. The surface area of the fresh sample was 78 m^2/g, and that of part 1 was 39.6 m^2/g. The surface area decreased very linearly from the fresh to part 1. In part 9, which had the lowest P concentration of about 2.3 wt. %, the BET surface area was decreased by 29.5 %. For part 1, which had a P concentration of about 3.7 wt. %, the decrease was 50 %.

The P concentration also had an impact on the average pore size, see Figure 60. The change in the average pore size was probably due to P forming substances that closes the smaller pores. This leads to an increase in the average diameter.

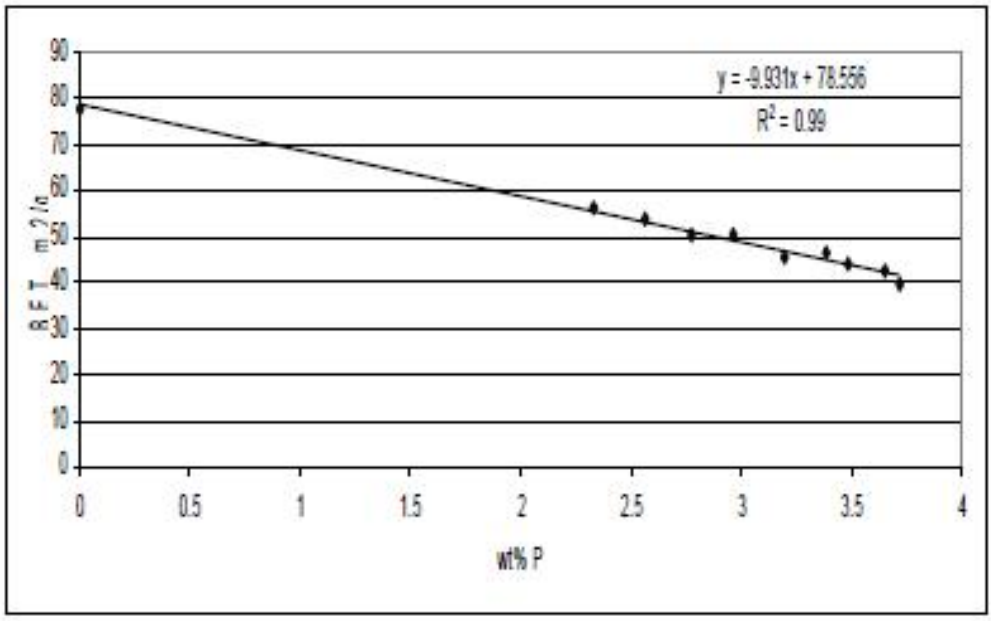

Figure 59. The BET surface area as a function of P concentration. (Bergquist)

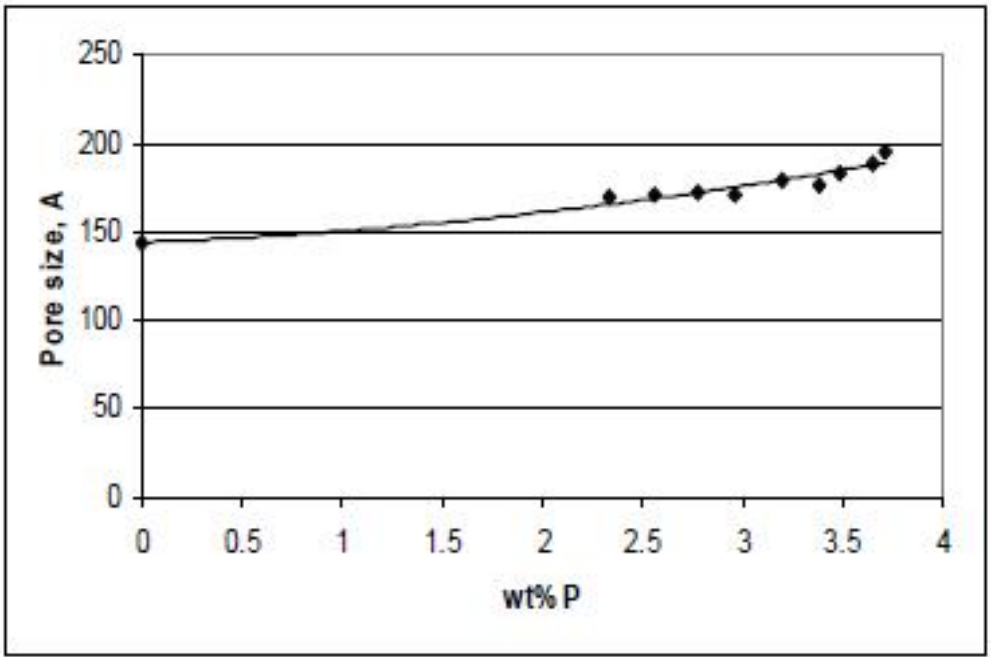

Figure 60. The average pore size as a function of P concentration. (Bergquist)

5.2. X-ray Diffraction results

All the other noticeable peaks belong to TiO_2, expect the small peak at $2\theta = 7.4$ that is seen for part 1, Figure 61. There was no difference in the peak widths for the other peaks, suggesting that the size of the TiO_2 crystallites on the surface had not been affected by the coverage of P. The small peak at 7.4 in parts 1 and 2 was highly likely an unknown formation of a P species, according to the writer.

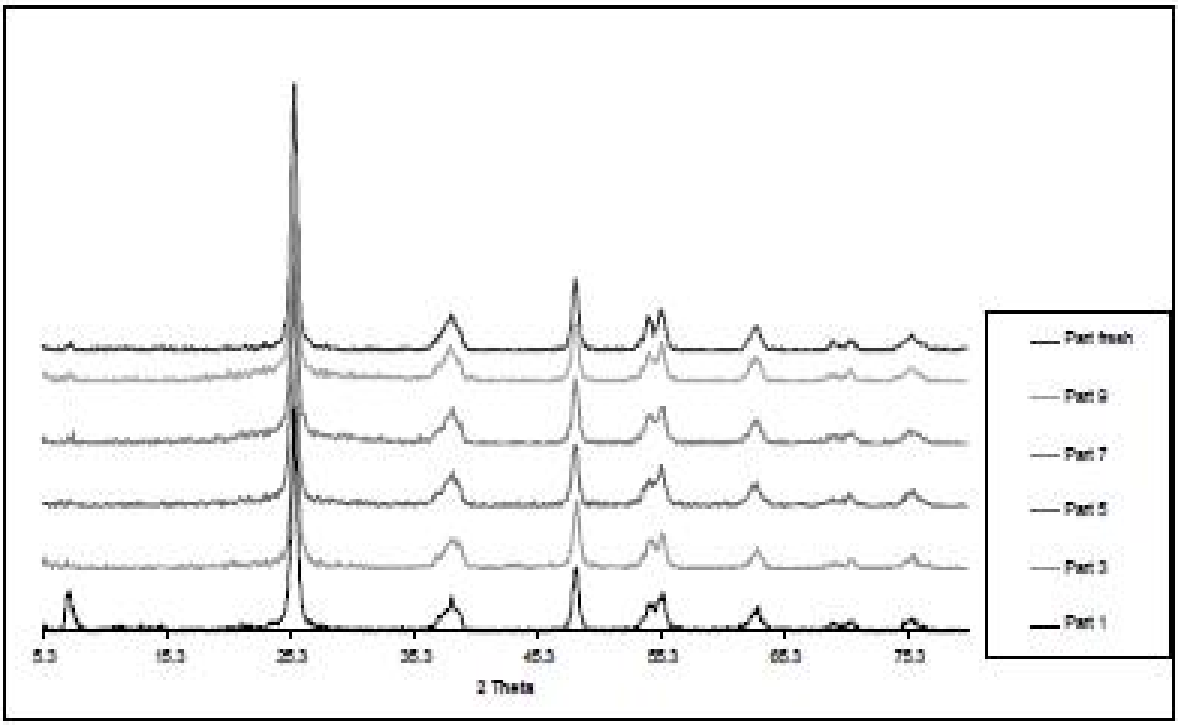

Figure 61. XRD spectra from the samples tested. (Bergquist)

5.3. TPD measurements

The results of TPD measurements are shown in Tables 18 and 19. Table 18 shows the amount of acid sites per a gram of sample. The amount of acid sites was dependent of the concentration of P. The fresh part and part 9 had almost the same amount of acid sites, but

when the concentration increased, the amount of acid sites decreased, leading to a decrease in capability of adsorbing NH_3.

Table 19 shows the number of acid sites per BET surface area. The number of the acid sites did not change in the deactivated parts. The result was the same for parts 1 and 9. Thus can be assumed that P primarily selectively poison the active sites, and secondarily block the pores of the catalyst. The P also increased the number of acid sites per BET surface in comparison with the fresh part.

Table 18. Acid sites in tested samples. (Bergquist)

Part	µmole/g
1	169
5	192
7	211
9	240
Fresh	238

Table 19. Number of acid sites, µmol/m^2 BET surface area. (Bergquist)

Part	µmol/m^2 BET
1	4.27
5	4.20
7	4.18
9	4.27
Fresh	3.05

Figure 62 shows the distribution between the strong and the weak acid sites. P did affect the distribution, as at higher P concentration the weaker acid sites dominated, but when the concentration decreased the fraction of strong acid sites increased.

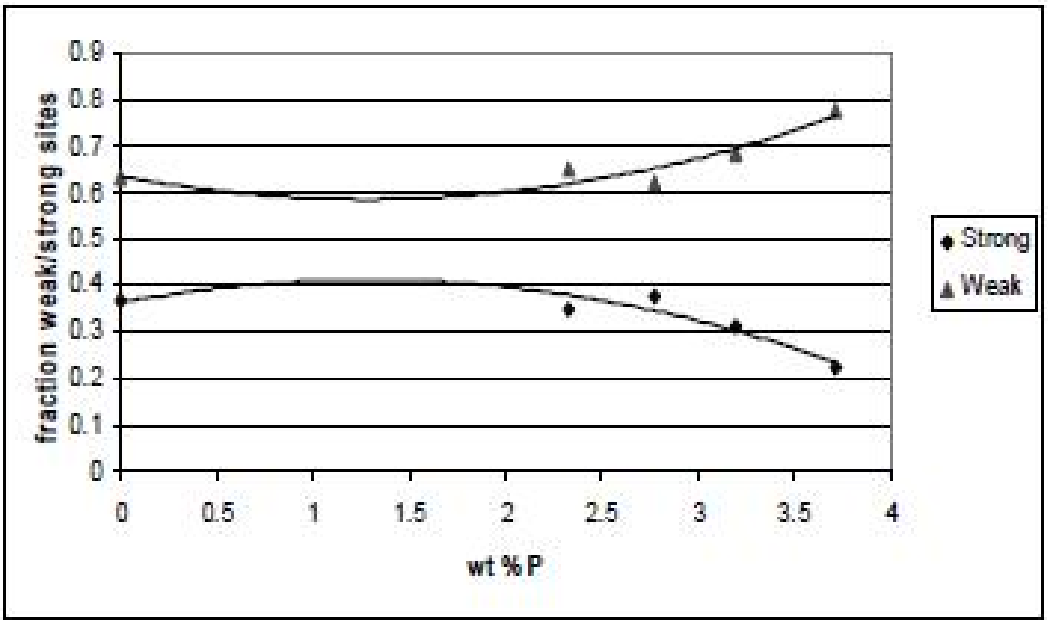

Figure 62. Fractions of weak and strong acid sites with different P concentrations. (Bergquist)

5.4. ICP

Results from the Inductively Coupled Plasma (ICP), that is used to find trace metals from samples, are shown in Figure 63. The P concentration was highest in part 1 with 3.72 wt. %, and the concentration decreased down to 2.33 wt. % in part 9. The difference of P concentration along the catalyst was 60 %. These results showed that 61.86 % of the added P in the fuel was collected on the catalyst surface. This suggests that the running conditions must have been quite optimal for P collection. Also, there were no other poisons included, so the catalyst could collect as much P as possible.

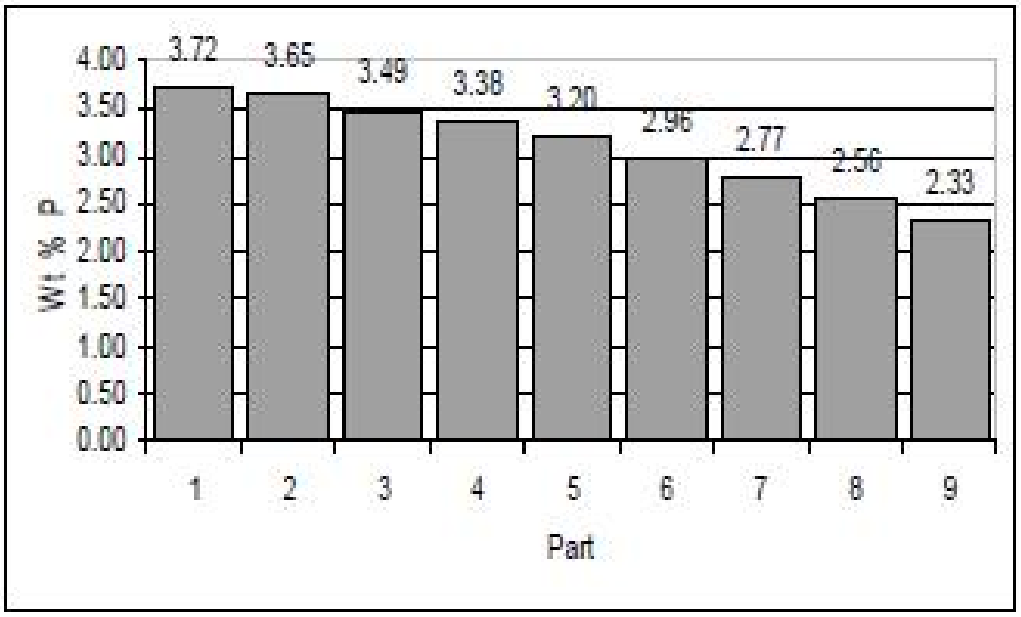

Figure 63. Distribution of P in the deactivated catalyst samples. (Bergquist)

5.5. Catalytic activity test

The catalytic tests were done with conditions of 500 ppm NO, 400 ppm NH_3, 10 % O_2, 5 % H_2O and balance with He, at space velocity of 30 000 1/h. There was a clear decrease in activity for the poisoned catalyst samples, Figure 64. At 300 °C the NO conversion was 80 % with the fresh catalyst and only 50 % with the catalyst sample part 1. No higher than 80 % conversion could be achieved in this study. The conversion was 76 % with the catalyst part 9 at 300 °C. The maximum activity was reached at higher temperatures with the poisoned samples compared to the fresh. Usually this type of catalyst is at its best at around 350 °C, but with the poisoned ones the activity reached their maximum levels at 400 °C. However, even there they did not reach the activity level of the fresh sample. The higher the P concentration the higher temperature was needed for the maximum conversion. Since the curves both changed shapes and moved to the right, a combination of selective poisoning and masking was the cause of the deactivation.

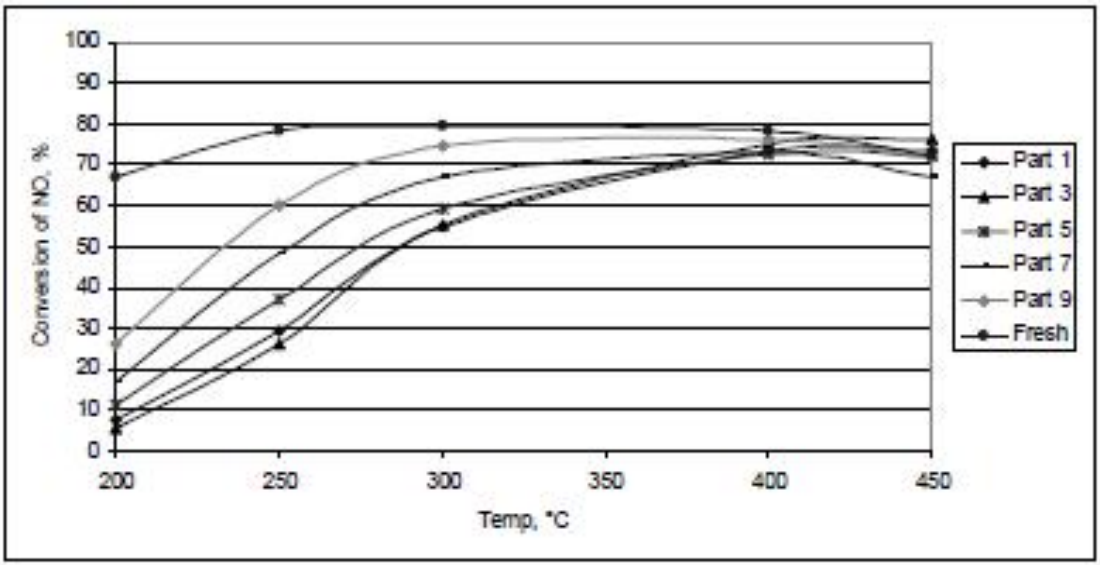

Figure 64. NO Conversion of different samples. (Bergquist)

Figure 65 shows the activation energy as a function of P concentration. The activation energy was calculated from the three lowest temperatures. P concentration affects the activation energy by changing the active sites by covering or poisoning. The correlation between the P concentration and the activation energy was linear. At the lowest P concentration an activation energy of 38 kJ/mol was measured, and at highest P concentration that was 60 kJ/mol.

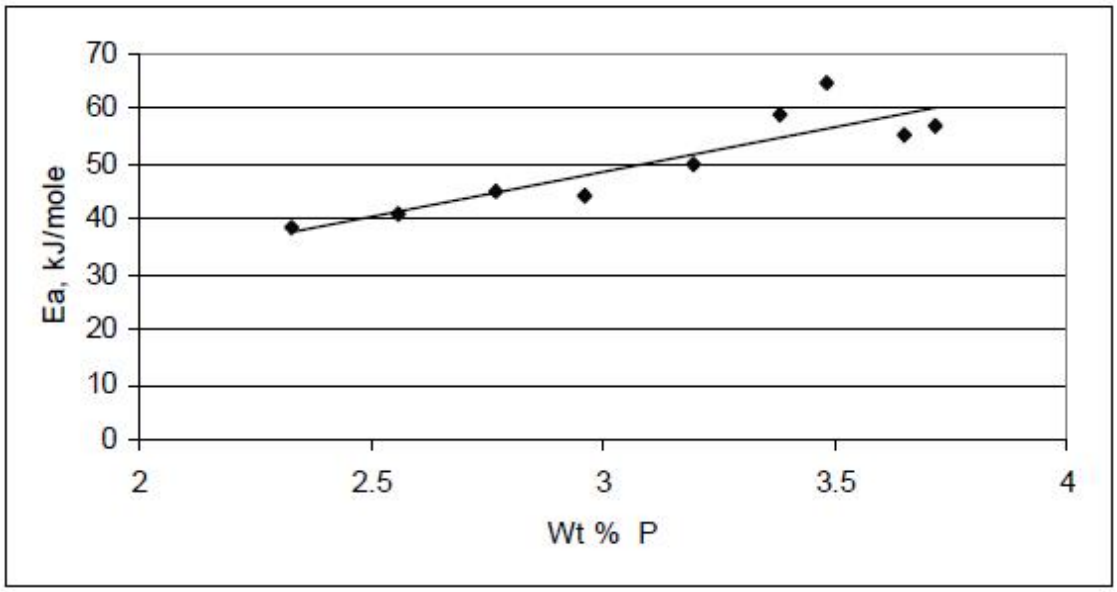

Figure 65. The activation energy as a function of P concentration. (Bergquist)

5.6. Conclusions

- The concentration of P decreased from inlet to outlet, being the highest at the inlet and lowest at the outlet of the catalyst.
- Total collection efficiency was 62 % of the P added to the fuel, which could be considered very high.
- P caused a decrease in the number of active sites on the catalyst surface through selective poisoning and masking.
- P affected both the amount and the distribution of the acid sites of the automotive catalyst.

6. DEACTIVATION OF Fe-ZEOLITE CATALYSTS

Chapter 6 with its Figures and Tables is fully based on an article written by P. Kern, M. Klimczak, T Heinzelmann, M. Lucas, P. Claus, 2010.

This study is the second part of the study summarized in Chapter 3.4.

Zeolites are gaining popularity little by little as the technology improves. So far the temperatures have been higher for them to work well compared to vanadium based catalysts. This Chapter shows that there are some similarities and also some exceptions in deactivation processes of these two main SCR technologies.

High Fe content Fe-zeolite powder was provided by Südchemie AG. Fe-MFI and Fe-BEA consist of 5.5 wt. % Fe_2O_3, Si/Al = 25-27 and were supposed to be close to industrially applied material. Two kinds of SCR catalysts were made for the tests, a 72 cpsi ceramic honeycomb cordierite for high-throughput experiments and 400 cpsi in case of catalytic tests close to industrial conditions. They were coated with the powder. Zeolite contents were adjusted to 90 g/l in the case of 400 cpsi honeycombs and, 30-45 g/l for the high-throughput investigations.

Blocks of 150 mm x 10 mm x 10 mm, 7 x 7 channels, were cut off from a serial catalyst, (VWT, 1 l, 400 cpsi, 200 g/l washcoat, cordierite), or of honeycombs representing a serial catalyst (Fe-MFI zeolite, 1 l, 400 cpsi, 90 g/l washcoat, cordierite. They were calcined in air at 550 ºC for 24 h prior the measurements. Catalytic tests were carried out at GHSV of 50 000 1/h, with flue gas containing 1000 ppm NO, 0 – 1200 ppm NH_3, 1000 ppm CO, 5 vol. % CO_2, 8 vol. % O_2, 5 vol. % H_2O and balance N_2. The measurements were done at several temperatures from 175 to 450 ºC and with different NH_3/NO ratios to get the ammonia slip curves. The poisonings were done by 10 s impregnation or by exposure to aerosols.

6.1.Chromium and copper

The activities of undoped catalyst samples are shown in Table 20. The Fe-MFI catalyst with thinner coating showed a lot higher NO conversion at 450 ºC. This may be due to material properties and the catalytic coating properties such as surface/volume and coating density.

Table 20. Activity of undoped Fe-zeolites in high-throughput experiments. (Kern *et al*., 2010)

Catalyst, washcoat (g)	*T* (°C)	NO conversion unpoisoned cat.	DeNOx unpoisoned cat.	S_{NO}	S_{NH_3}
Fe-BEA (45 g/L)	350	28.5 ± 2%	26 ± 2%	94 ± 2%	81 ± 8%
Fe-BEA (45 g/L)	450	58 ± 4%	56 ± 4%	98 ± 2%	79 ± 8%
Fe-MFI (30 g/L)	350	30 ± 4%	27 ± 4%	95 ± 2%	81 ± 5%
Fe-MFI (30 g/L)	450	76 ± 7%	73 ± 7%	99 ± 1%	92 ± 2%

The first poisoning tests were done by impregnation with $Cu(NO_3)_2$ and $(NH_4)_2CrO_4$. Both combinations increased the relative $DeNO_X$ activity at temperatures lower than 350 ºC, but the increase was negligible at temperatures of about 450 ºC. The copper combination showed bigger increase. Cu-zeolites tend to produce N_2O, and also in these impregnation tests both poisons caused an increase in N_2O production. This increase could have been bigger if HC containing flue gas would have been used. In Table 21 it can clearly be seen that N_2O production increased with both catalysts at both temperatures. The conditions of the tests represented in Tables 20 and 21 were 1000 ppm NO, 1000 ppm NH3, 1000 ppm CO, 5 vol. % CO_2, 5 vol. % H_2O, 8 vol. % O_2, balance N_2 at GHSV of 50 000 1/h.

Table 21. Effects of chromium and copper to activity and N_2O production. (Kern *et al*., 2010)

Catalyst	Y_{N_2} (%)		S_{NO} (%)		S_{NH_3} (%)		N_2O (vppm)	
	350 °C	450 °C	350 °C	450 °C	350 °C	450 °C	350 °C	450 °C
Fe-BEA (45 g/L)	26 ± 2	56 ± 2	92	98	84	80	9	10
Fe-BEA/2 wt.% Cu	30 ± 3	58 ± 4	91	95	88	75	16	23
Fe-BEA/2 wt.% Cr	28	62 ± 1	88	89	71	63	28	68
Fe-MFI (30 g/L)	30 ± 4	76 ± 7	95	98	81	92	10	9
Fe-MFI/2 wt.% Cu	62 ± 8	79 ± 3	96	97	91	85	14	20
Fe-MFI/2 wt.% Cr	39 ± 3	82 ± 1	95	96	85	87	15	26

6.2.Alkali- and alkaline-earth metals

All alkali- and alkaline-earth metals showed strong deactivation potential, shown in Figure 66. The metals used in the impregnation tests were K, Na, Mg and Ca. As known, for vanadium based catalysts the basicity of metals very much orders the rate of deactivation. Therefore the order of poison strength for vanadium catalysts would be K > Na > Ca >Mg. This was not the case for Fe-zeolites. For zeolites Mg was the most severe poison, and the order is Mg > K ~ Ca > Na.

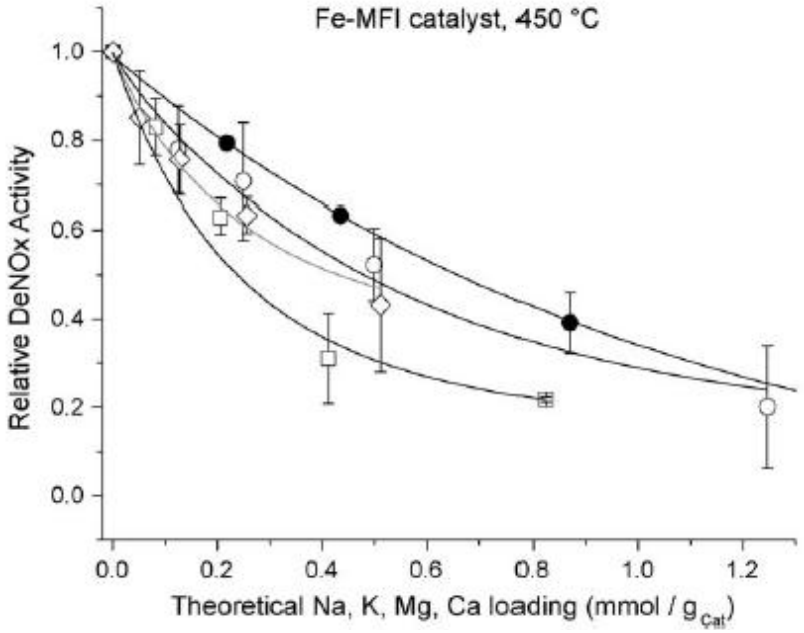

Figure 66. Deactivation of Fe-MFI catalysts by: (●)$NaNO_3$,(◊) KNO_3, (□) $Mg(NO_3)_2$ and (○) $Ca(NO_3)_2$. (Kern *et al*., 2010)

The impact on chemisorbed ammonia is shown in Figure 67, and the comparison of chemisorptions between zeolites and vanadium catalysts is shown in Figure 68. The K did have the biggest effect on the ammonia desorption, but the activity rate did not follow straightly. The relative surface coverage of ammonia is very important aspect in catalyst function, so

the lack of coverage could lead to deactivation and increase in ammonia slip. The ammonia slip –DeNO_X curves of 400 cpsi honeycomb catalysts are shown in Figure 69. The contents of flue gas were 1000 ppm NO, 200 - 1200 ppm NH_3 (α = 0.2, 0.4, 0.6, 0.8, 1.0, 1.2), 1000 ppm CO, 5 vol. % CO_2, 5 vol. % H_2O, balance N_2 and GHSV of 50 000 1/h. It can be seen that the KNO_3 poisoned catalysts did not achieve even close the activity results of the un-poisoned catalyst, even with the ammonia slip of 600-700 ppm. The poisoned catalyst reached its full potential at about 300-400 ppm slip at 450 ºC, as the unpoisoned reached its at lower than 100 ppm. Further characterization of the influences of K and Ca are shown in Table 22. The BET surface area and microspore surface areas were noticeably lower in K-influenced catalyst.

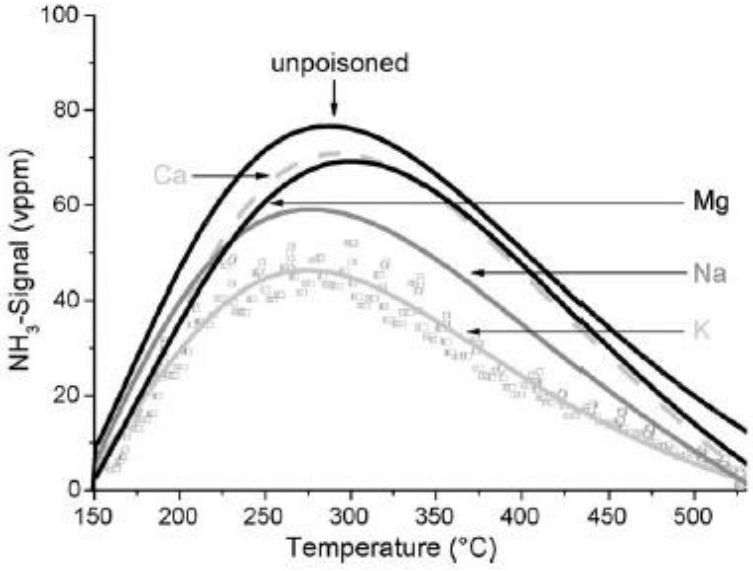

Figure 67. NH_3-TPD profiles of poisoned Fe-MFI zeolite catalysts. (Kern *et al*., 2010)

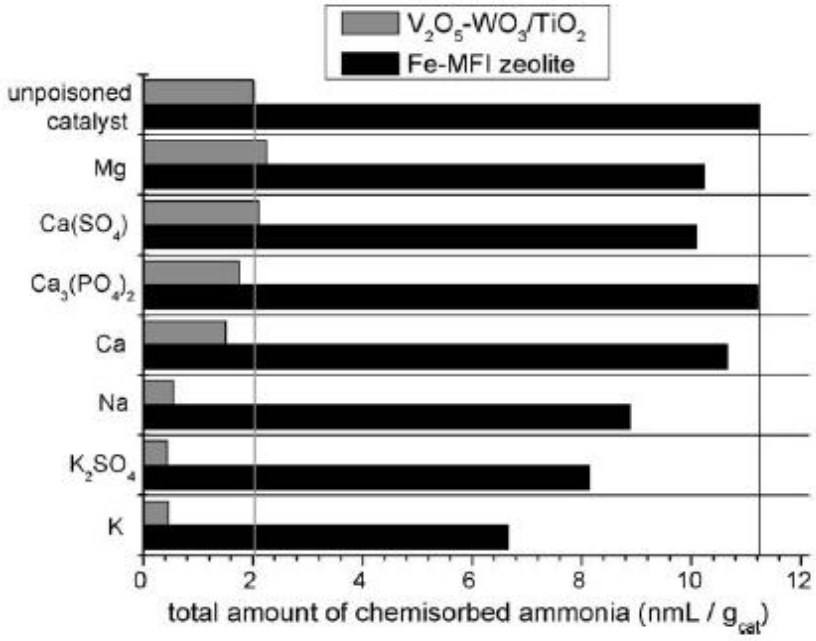

Figure 68. Integral ammonia storage capacity of Fe-MFI catalysts in comparison to V_2O_5-WO_3/TiO_2 catalysts. (Kern *et al*., 2010)

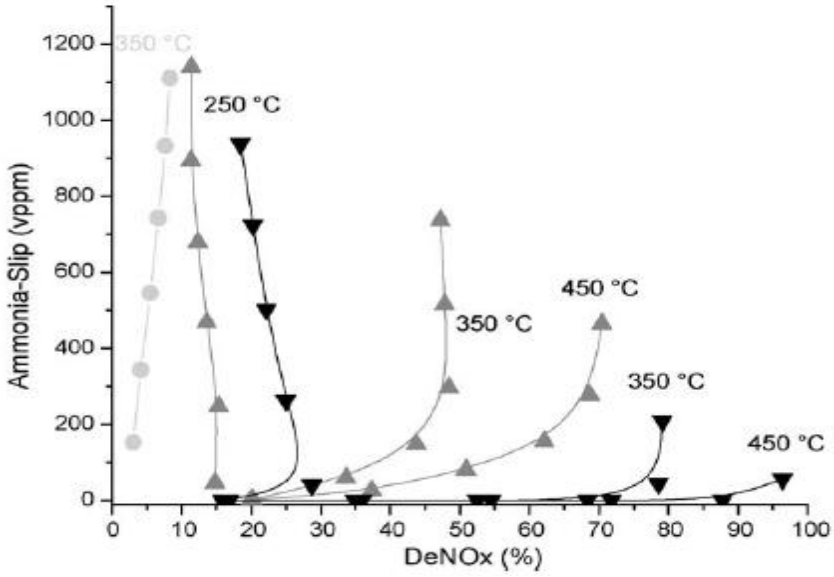

Figure 69. NH_3 slip curves: (▼) Fe-MFI impregnated with water, then thermally treated, (▲) Fe-MFI impregnated in aqueous 0.3 mmol K/g washcoat KNO_3 solution, (●)V_2O_5-WO_3/TiO_2 MFI impregnated in aqueous 0.3 mmol K/g washcoat KNO_3 solution. (Kern *et al*., 2010)

Table 22. Characterization data of Fe-MFI zeolites poisoned with KNO_3 and $Ca(NO_3)_2$. (Kern *et al.*, 2010)

Catalyst: Fe–MFI	$T_{50,NO}$ (°C)[a]	UV–vis-DRS: relative signal intensity I/I_{total}			N_2 physisorption	
		<400 nm	400–500 nm	>500 nm	BET surface[b] (m^2/g)	Micropore surf. area[b] (m^2/g)
Unpoisoned	290	0.29	0.34	0.37	308	525
0.3 mmol K/g[c]	295	0.33	0.34	0.33	268	<404
0.3 mmol Ca/g[c]	320	0.32	0.35	0.33	295	<480

[a] Quartz glass laboratory flow reactor, packed bed, 75 mg catalyst (d_{Grain} = 100 nm–10 μm), 500 mg SiC, volume flow: 700 mL/min, 1000 vppm NO, 1000 vppm NH_3/7 vol.% O_2, N_2.
[b] N_2 physisorption, BET analysis and Horvath–Kavazoe analysis.
[c] Incipient wetness using water or aq. precursor solution (nitrates) of the poison to contain 0.3 mmol/g K/Ca; then calcined in air (550 °C/24 h).

6.3. Zinc, phosphates and borate

Zn and phosphor are known poisons especially to automobile catalysts, but also to SCR catalysts at least in large amounts, as already notified in this thesis. The results of impregnation tests are shown in Figure 70, and of gas-phase poisoning in Figure 71. All three poisons caused severe deactivation effect on impregnation tests. In the gas-phase poisoning P caused stronger deactivation effect than Zn especially at 350 ºC. In the impregnation test the flue gas contained of 1000 ppm NO, 1000 ppm NH_3, 1000 ppm CO, 5 vol. % CO_2, 5 vol. % H_2O, 8 vol. % O_2, balance N_2 and GHSV of 50 000 1/h, and in the gas-phase poisoning NH_3 was 200 – 1200 ppm and H_2O content of 5 vol. %. The hydrothermal treatment of gas-phase poisoning was carried out at 550 ºC, 5 vol. % H_2O and Air for 50 h and GHSV of 50 000 1/h.

More results of poisonings are shown in Tables 23 and 24. In Table 23 the interesting thing is the decrease of BET and micropore surface areas of P and Zn influenced catalysts, them still remaining the NH_3 adsorption ability almost perfectly. The results in Table 23 are from impregnation tests. In Table 24 are introduced the $DeNO_X$ activities of hydrothermally treated and HCl poisoned catalysts at α = 1 and 25 ppm NH_3 slip. At 450 ºC the poisoned catalyst was actually better at both circumstances. Cl induced dealumination of a zeolite catalyst is still possible threat when operated over temperatures of 600 ºC.

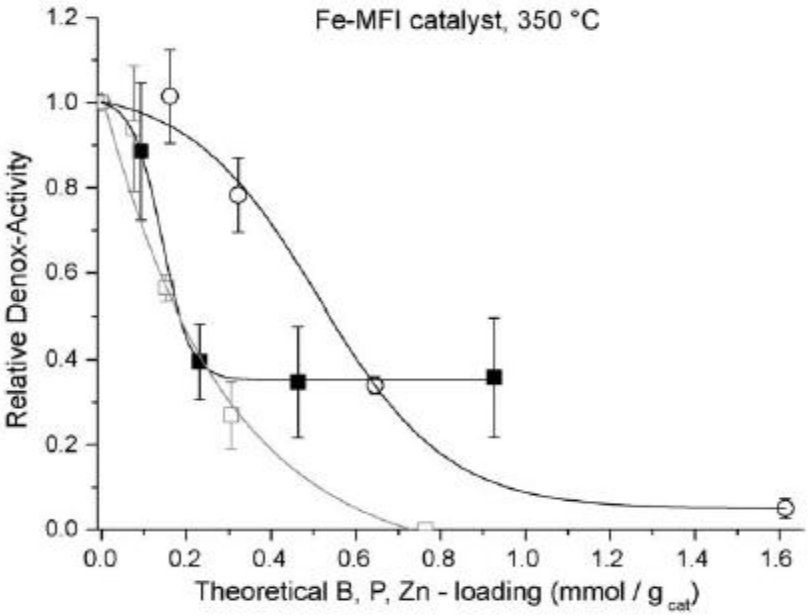

Figure 70. Deactivation of Fe-MFI zeolite by impregnation of: (■) H_3BO_3, (○) $(NH_4)_2HPO_4$, (□) $Zn(NO_3)_2$ at 350 ºC. (Kern *et al*., 2010)

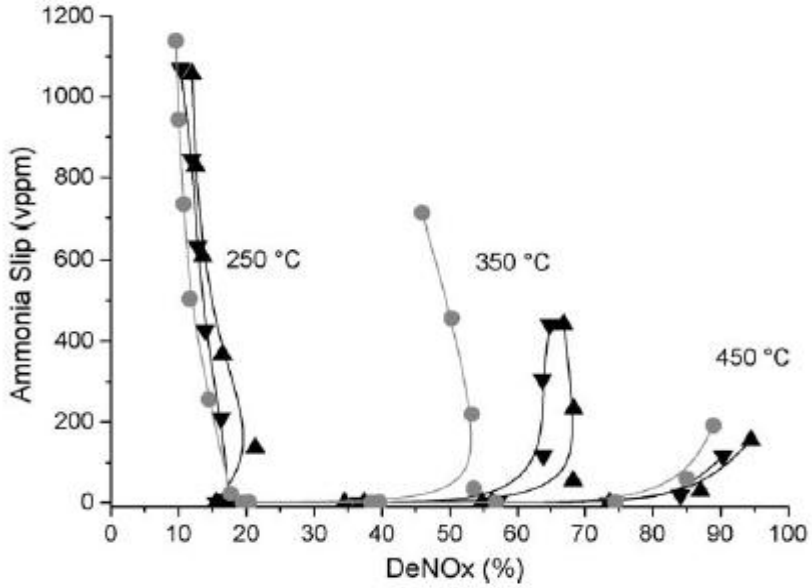

Figure 71. Gas-phase poisoning of 400 cpsi 90 g/l Fe-MFI zeolite honeycomb catalysts by (▲) hydrothermal treatment, (●) hydrothermal treatment + 3 mmol P from $(NH_4)_2HPO_4$, (▼)hydrothermal treatment + 3 mmol Zn from $Zn(NO_3)_2$. (Kern *et al*., 2010)

Table 23. Characterization data of Fe-MFI zeolites poisoned with $(NH_4)_2HPO_4$ and $Zn(NO_3)_2$. (Kern *et al*., 2010)

Catalyst: Fe–MFI	$T_{50,NO}$[a] (°C)	NH_3 chemisorbed[b] [nmL/g]	NO_2 chemisorbed[b] [nmL/g]	BET surface[c] [m^2/g]	Micropore surf. area[c] [m^2/g]
Unpoisoned[d]	290	11.5 ± 1	2.6	308	525
1 wt.% P[d]	315	10	2.0	n.a.	n.a.
2.2 wt.% P[d]	325	10.5	1.1	263	< 445
0.3 mmol Zn/g[d]	335	11.5	n.a	221	<306

[a] Quartz glass laboratory flow reactor, packed bed, 75 mg catalyst (d_{Grain} = 100 nm–10 μm), 500 mg SiC, volume flow: 700 mL/min, 1000 vppm NO, 1000 vppm NH_3, 7 vol.% O_2, N_2.
[b] Integration of TPD-concentration profiles after saturation at 150 °C.
[c] N_2 physisorption, BET analysis and Horvath–Kavazoe analysis.
[d] Incipient wetness using water or aq. precursor solution ($(NH_4)_2HPO_4$, $Zn(NO_3)_2$) of the poison; then calcined in air (550 °C/24 h).

Table 24. Activity of HCl treated 400 cpsi Fe-MFI zeolite honeycomb. (Kern *et al*., 2010)

Catalyst	DeNOx at 250 °C		DeNOx at 350 °C		DeNOx at 450 °C	
	$\alpha = 1$	NH_3 slip: 25 ppm	$\alpha = 1$	NH_3 slip: 25 ppm	$\alpha = 1$	NH_3 slip: 25 ppm
Hydrothermally treated	12%	17%	68%	68%	87%	86%
Hydrothermally treated + 3 mmol HCl	11%	16%	57%	66%	89%	90%

6.4. Conclusions

- Compared to vanadium based catalysts, Fe-zeolites were much more resistant to alkali and alkali earth metals.
- When using fuels with high alkali metal contents found in some biodiesels, the use of Fe-zeolite should be considered.
- Pore plugging seems to be the dominant deactivating mechanism over poisoning for Fe-zeolites, even though reduced acidity and ammonia storage capacity were observed.
- Inorganics like P, Zn and B present a strong risk of deactivation for Fe-zeolites.

7. TESTS CONDUCTED WITH INTERNAL COMBUSTION ENGINES USING BIO-FUELS

Marleena Laine presented the results of four SCR catalyst elements aged with rapeseed oil (RSO) in her Bachelor's Thesis. The investigation was conducted at the engine laboratory of Turku University of Applied Sciences in 2012. First the right parameters had to be determined for the spraying of the urea solution AdBlue. This study was also a part of the Cleen Ltd's FCEP-program. Chapters 7.1. to 7.4. with Figures and Tables are fully based on this thesis.

7.1. The testing procedure

Four catalysts were investigated and aged with raw rapeseed oil. The catalysts were named A, B, C and D. No more specific information was given about the catalyst elements. The test engine was a modern non-road common rail diesel engine, Agco Sisu Power 49CWA. The injectors' holes were larger than in the normal version to ensure the flowing of the viscous oil. In the exhaust piping set all the catalysts were aged simultaneously. The exhaust gas was divided into all four catalysts. The set is shown in Figure 72. The NO_X levels and temperatures were measured before and after the elements.

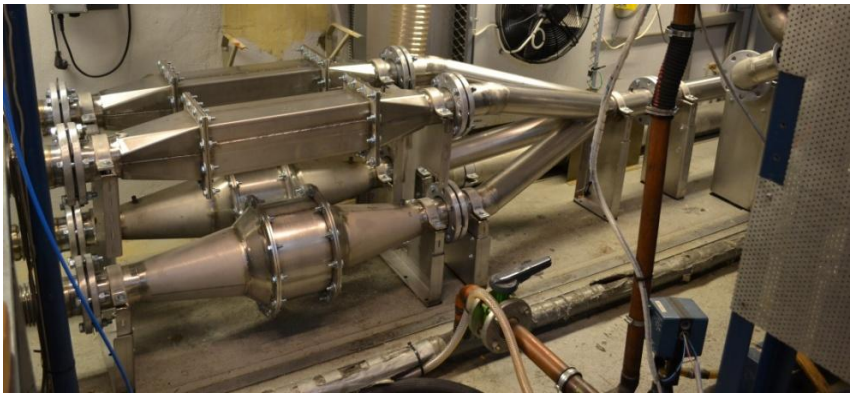

Figure 72. The piping set and the four catalysts. (Laine, 2012)

Before the ageing the injection parameters had to be determined. A NO_X decrease of 80 % was the target level without NH_3 slip. This was achieved with two catalyst elements, A and B. C and D showed very different results the D being the least favorable. The conversions and the test loading points are shown in Figure 73. For comparison the conversions of diesel fuel are shown in Figure 74. The lowest loading did not produce high enough temperature so no urea solution was injected. RSO demanded a little more AdBlue compared to standard diesel. The target temperature 350 °C for ageing was achieved with heaviest loading with both diesel and RSO. There were no significant differences in temperatures between the catalysts, and the before and after temperatures were very similar for every catalyst. The NO_X levels were slightly higher with RSO, possibly due to the higher oxygen level. The differences were quite small and noticeable only at the highest and the lowest loads. The levels were between 8 and 16 g/kWh.

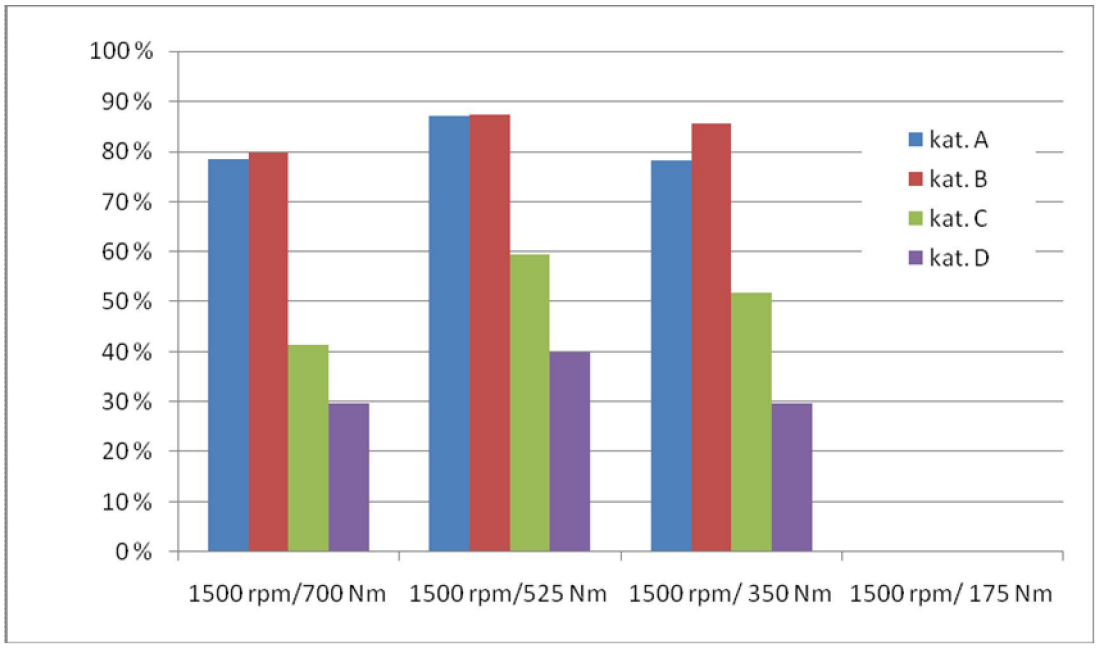

Figure 73. NO_X conversions with RSO. (Laine, 2012)

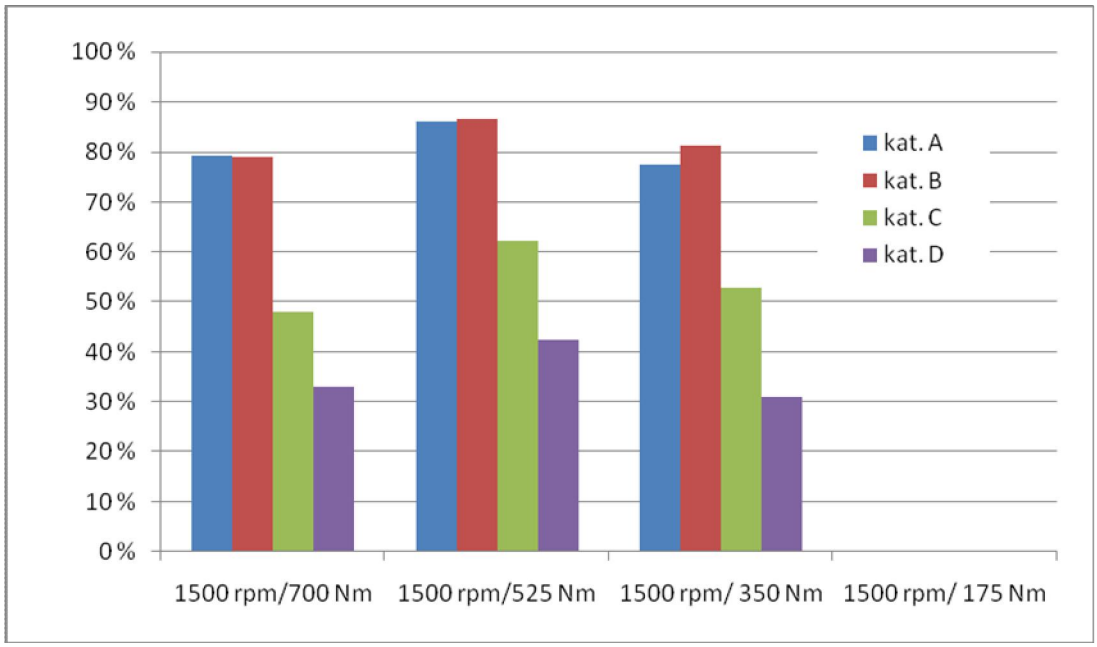

Figure 74. NO_X conversions with diesel. (Laine, 2012)

7.2. The ageing tests and results

Each day the tests began and ended with diesel, to make sure that the engine started well and the pipes were cleaned from traces of ammonia and RSO. The engine was driven approximately 4 to 6 hours per day and the levels were measured every half an hour. The results of NO_X and Filter Smoke Number (FSN) are shown in Figure 75 ("savutus" means smoke). The peaks in the Figure were always in the morning, when the catalyst probably was not warm enough. NO_X and smoke tended to increase with time. FSN was usually higher when NO_X levels were lower.

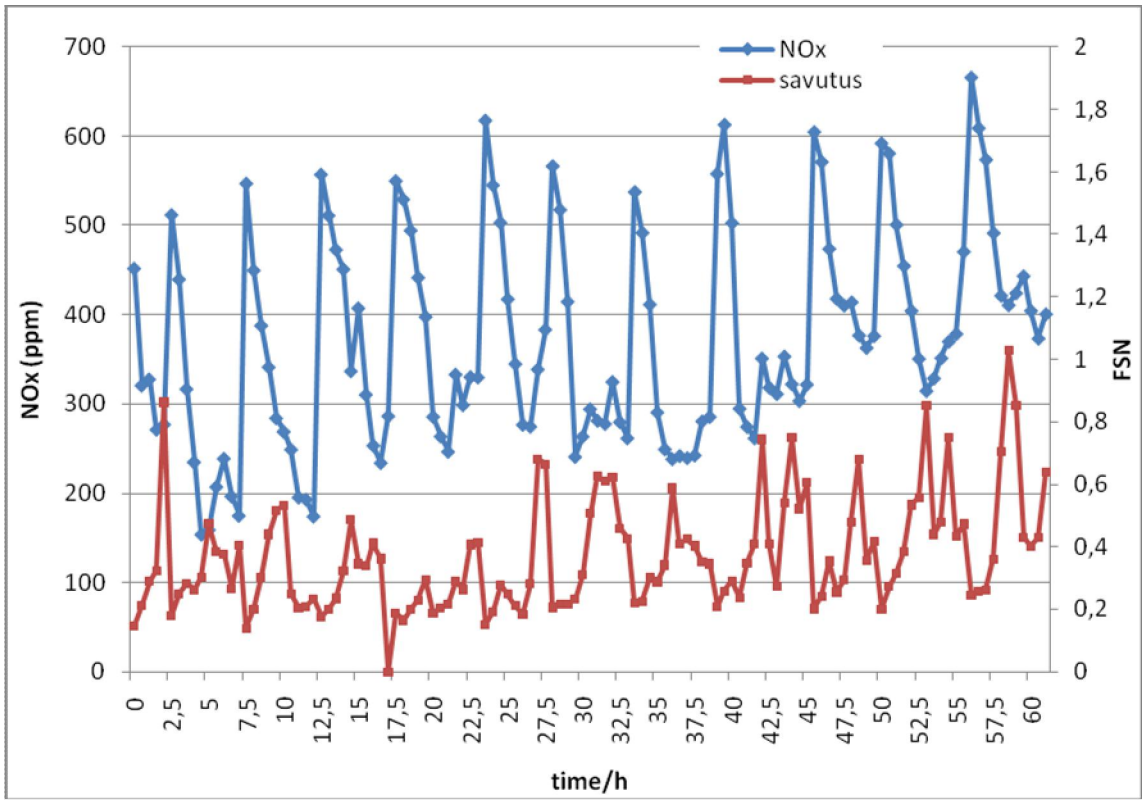

Figure 75. NO_X and FSN levels as function of time. (Laine, 2012)

The tests had to be stopped at 61 hours due to engine problems unrelated to the ageing tests. The comparison to the reference measurements could be performed at only one loading point, at 350 Nm. The results before and after the 61 hours with all the catalysts are shown in Figure 76. “Ikäytetty” means aged. The real NO_X levels before and after the catalysts are shown in Figure 77. It is very clear that catalysts A and B were affected considerably more than especially the catalyst C and even D. They seem to have been much more vulnerable to the RSO’s trace elements and ash. Relatively the activity loss for catalyst A was about 80 %, for B about 60 %, for C about 23 % and for D about 50 %.

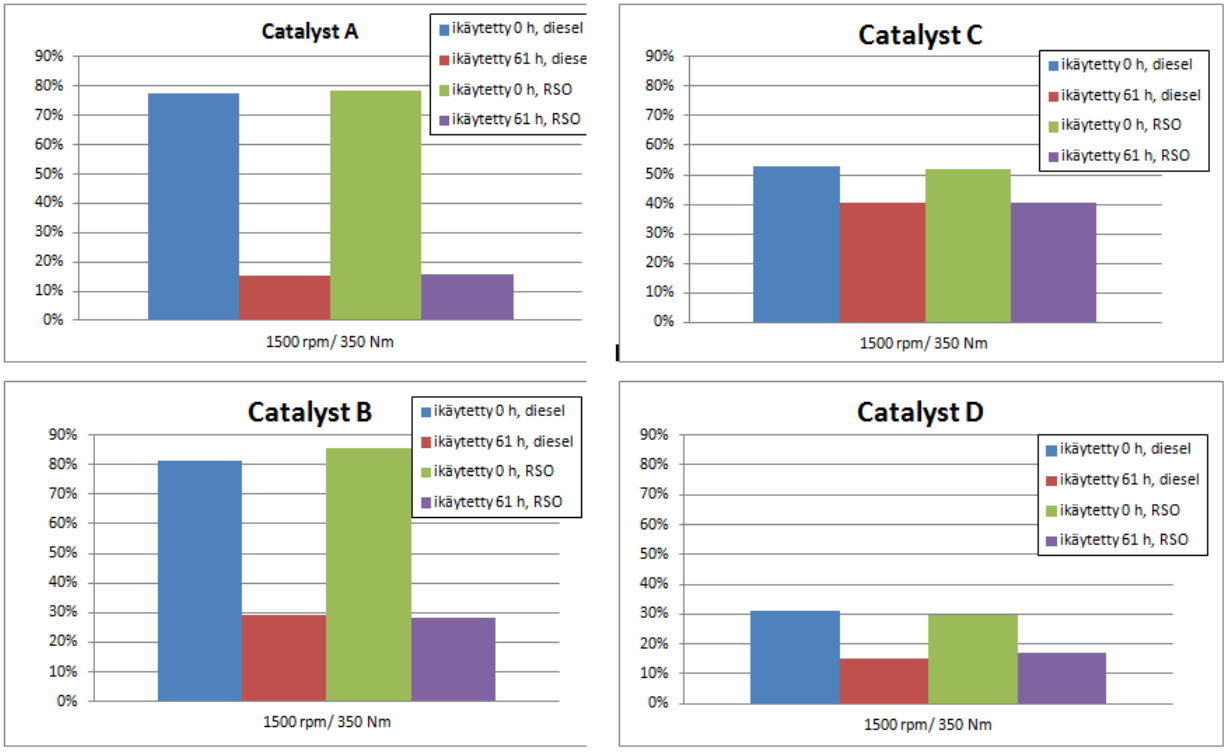

Figure 76. Conversion results of the ageing for 61 hours with RSO. (Laine, 2012)

The results in the form of g/kWh are shown in Figure 77. It shows the raw and treated emissions of NO_X with diesel before and after the ageing test. The raw emissions ("raakapäästö" in Figure) were close to those before ageing, indicating that the engine did not suffer from the use of RSO. Catalysts A and B were damaged much more than catalysts C and D. Figure 78 shows raw and treated emissions with RSO, and the results were very similar to diesel's.

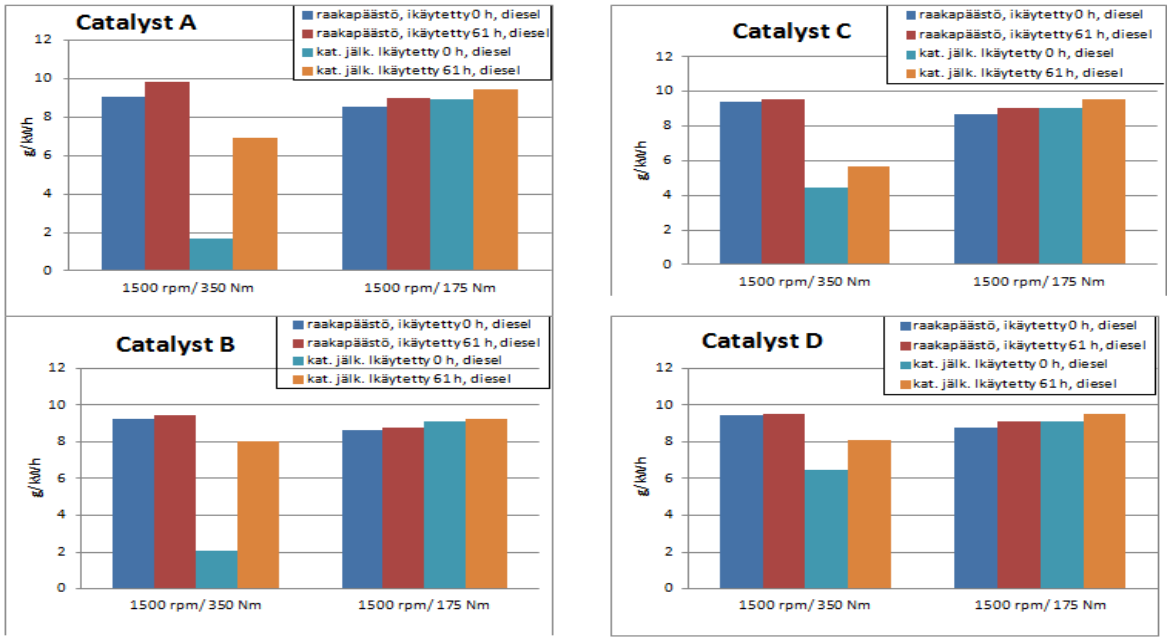

Figure 77. Raw and treated NO_X emissions with diesel. (Laine, 2012)

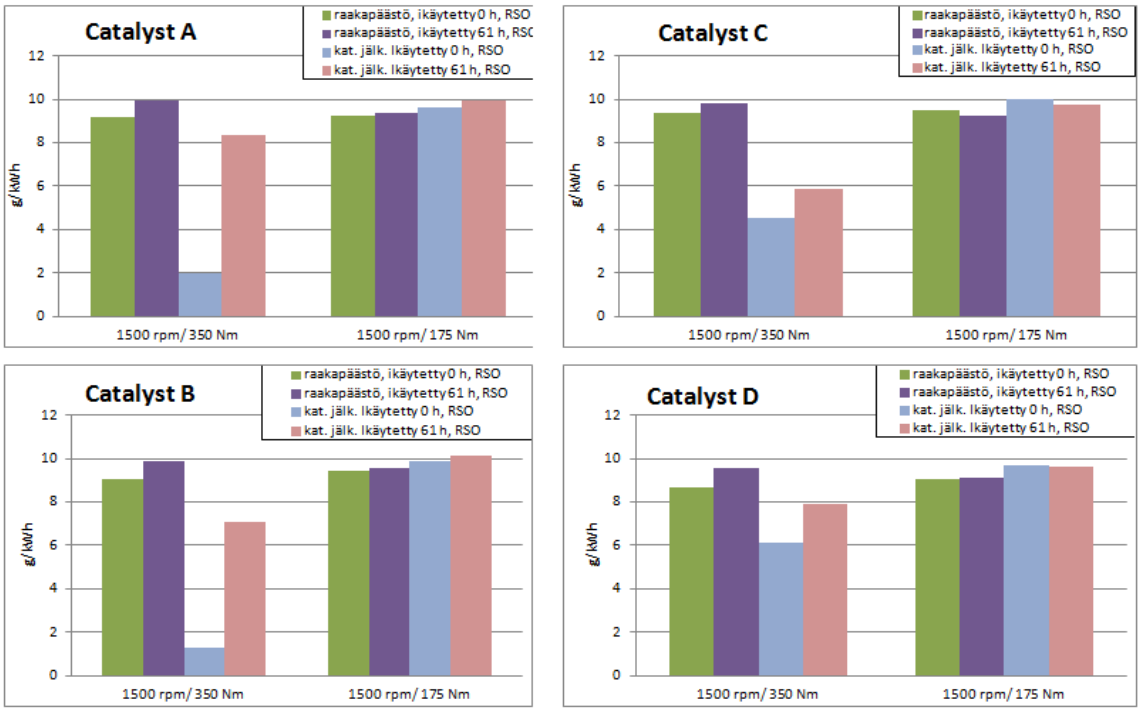

Figure 78. Raw and treated NO_X emissions with RSO. (Laine, 2012)

7.3. Other emissions and measured values

Back-pressure

The increase in back-pressure indicates that something accumulated somewhere in the exhaust line. In Catalyst A the back-pressure had doubled from the beginning of the test. For catalyst B the increase was about 70 %. The back-pressures were also higher with these catalysts at the beginning. Catalysts C and D behaved in a completely opposite way, as their back-pressures decreased by 85 % at best. This phenomena has not been introduced in earlier findings of the present thesis. According to earlier findings, for Catalysts A and B the increase could possibly be due to accumulation of ash in front of the catalysts or inside the catalysts.

Smoke

Overall higher smoke values were measured with RSO than diesel, but the level was quite low in both cases. All catalysts had almost similar behaviors. The FSN (Filter Smoke Number) increased with diesel and decreased with RSO. The results were noticeable only at load point 1500 rpm / 350 Nm. With all catalysts the number with diesel was roughly 0.2 before the ageing and 0.5 after it. With RSO the number was roughly 0.7 before and 0.5 after with all the catalysts.

Fuel consumption

There were no differences in fuel consumption before and after the ageing.

Others

The flue gas rate was exactly the same before and after ageing with all catalysts, as were the temperature levels. HC levels rose by about 0.2 g/kWh with both diesel and RSO. The levels were slightly lower with RSO. CO levels rose with all catalysts after ageing. The levels were higher with RSO.

The Turku University of Applied Sciences continued the investigation by using the same catalysts again (Karhu, Cappelli 2012). This time the exhaust gas was not divided, but each catalyst was aged at a time and one new element was also studied. The focus of this investigation was a little different, and at the time of writing the current thesis it was not yet published. However, the results showed again that high-ash RSO had deactivating effects on the catalysts.

7.4. Conclusions

- The catalysts A and B, which had better NO_X conversion rates at the beginning, lost more of their activity than Catalysts C and D.
- The relative activity loss was between 23 and 80 % after ageing of 61 hours, which can be considered fast poisoning.
- Back-pressure increased in Catalysts A and B but decreased with Catalysts C and D.

Another similar investigation was published by SAE International at 2011. The study was made by A. Williams, R. McCormick, J. Luecke, R. Brezny, A. Geisselmann, K. Voss, K. Hallstrom, M. Leustek, J. Parsons and H. Abi-Akar. The objective was to find out what effects B20 biodiesel blend would have on several exhaust gas control systems. B20 is a fuel blend where there is 20 % biodiesel and 80 % fossil diesel. The study covered multiple types of DPF substrates, DOC and SCR catalysts, but in this thesis only the relevant results concerning SCR catalysts are introduced.

7.5. The experiment

The investigation team wanted to expose the emission control systems during 150,000 and 435,000 miles of ash from the biodiesel blend. These are about 241,000 and 700,000 km respectively. To achieve these numbers in reasonable amount of time, an accelerated test was developed by the team. They created a soy-based B20 blend containing about 27 times more metals than allowed by the ASTM standards. This way the time needed became greatly shorter. Another very important aspect was the regeneration temperature and time of the DPF substrates. To achieve somehow realistic results, the DPFs were at regeneration temperature almost continuously. The regeneration temperature was about 650 °C about 90 % of the time, and about 850 °C for 10 % of the time to represent uncontrolled temperature spikes that can occur while burning the soot out of the filter. The high temperatures in the DPF may result in vaporization of K and other metals that are harmful for the SCR equipment. Earlier it has been revealed that the vapor can be much more harmful than ash that accumulates on the SCR inlet.

The test engine was a Caterpillar 2008 C9 ACERT, 8,8 L, 300-hp (≈221 kW), calibrated to Tier 3 off-road emission limits. In its base configuration it does not have any emission control devices. The engine was turbocharged and used direct injection of the fuel. The engine was pre-conditioned with a 60-hour break-in method supplied by Caterpillar. Some modifications were made to the engine in order to achieve the needed temperatures. Additional fuel injectors were assembled to exhaust line. The order of emission control devices was DOC – DPF – SCR. There was a 4,3 m distance between the DPF and SCR to ensure that the temperature at the SCR would not exceed 650 °C. There were two similar SCR bricks in series, named SCR-1 and SCR-2. The diameter was 26,7 cm and the length was 15,24 cm (10,5” x 6”) and the CPSI was 300.

The parameters of the steady-state test are shown in Table 25. The test consisted of three phases where there was low and high temperature regeneration and soot loading. In the soot loading phase the accumulation of soot was about 2,4 g/l. The temperature increase between soot loading and high temperature regeneration was kept at 1 °C/sec to avoid unin-

tentional and uncontrolled regeneration. The three phases and their transition phases created a 7-hour test cycle. The SCR equipment was only used in the longer, 435,000 miles equivalent tests. The tests were done with the modified B20 and ultra-low-S diesel (ULSD) for comparison. In this testing the high temperature regeneration –phase was skipped until the first 150,000 mile equivalent was full and the DOCs were changed. The fuel trace element analysis of the modified B20 fuel is shown in Table 26. For comparison, the ASTM standards allow 5 ppm of Na+K and 5 ppm of Ca+Mg in 100 % biodiesel.

Table 25. Ash loading test cycle. (Williams *et al*., 2011)

Engine mode	Time (h)	Speed (rpm)	Load (Nm)	DPF temp (°C)
1 Low temp regen.	4,5	2000	1080	650
2 Soot loading	2,0	2000	272	<300
3 Hihg temp regen.	0,5	1200	1180	850

Table 26. Modified B20 fuel trace element analysis. (Williams *et al*., 2011)

Metal	Blended fuel (ppm)	Filtered fuel (ppm)
Ca	24	21
Mg	<1	<1
Na	21	19
K	7	6
P	<1	<1

7.6. Results

After the ageing the SCR equipment was assembled to another engine in order to carry out Heavy-Duty Diesel Transient (HDDT) test cycle. This engine was 8,3 liter Cummings, 223 kW. Also the DOC and DPF used in this test were different than the ones in the ageing, but these were aged independently in similar way. The emission testing itself was carried out with ULSD only. Temperature range over the test cycle in the SCR was from 202 to 305 °C

and peak space velocity was 65,000 hr^{-1}. The urea solution was injected to exhaust gas in NH_3 to NO_X molar ratio of 1.

After three hot-start repeats of the HDDT test cycle the averaged reduction percentages of the two bricks are shown in Figure 79. With both ULSD and B20 aged catalysts the first catalyst reduced greater part of the NO_X, but SCR-2 also did have additional effect. With ULSD the reductions were 85,7 % after first and 92,1 % after the second brick. With B20 the percentages were 78,0 % and 87,2 %. Thus can be seen that B20 had a small deactivation effect, but rather small especially after the second SCR bricks. With ULSD aged catalyst the second catalyst increased the percentage by 6,4 %, and with B20 the increase was 9,2 %. In the light of earlier findings, this could be due to ash accumulation at the inlet of the first catalyst, and so the other SCR brick would be rather unharmed.

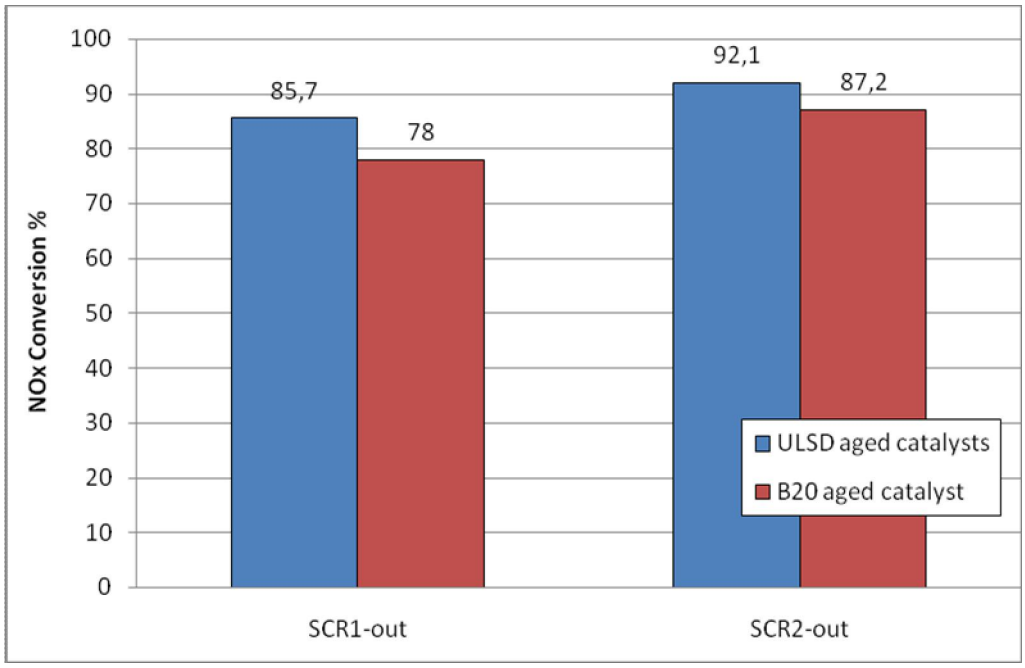

Figure 79. Averaged NO_X conversion percentages of aged catalysts. (Williams *et al.*, 2011)

The cumulative NH_3 slip levels of one test cycle are represented in Figure 80. The third test cycle gave the largest slips. The slips were higher after the first catalyst than the second catalyst, as expected. It is noticeable that the slip levels were considerably lower with B20

aged catalysts. In the test the peak slip was about 50 ppm, which can be controlled with ammonia oxidation catalyst. The ammonia slip levels were 1,09 g for the ULSD aged catalysts and 0,82 after the B20 aged catalysts.

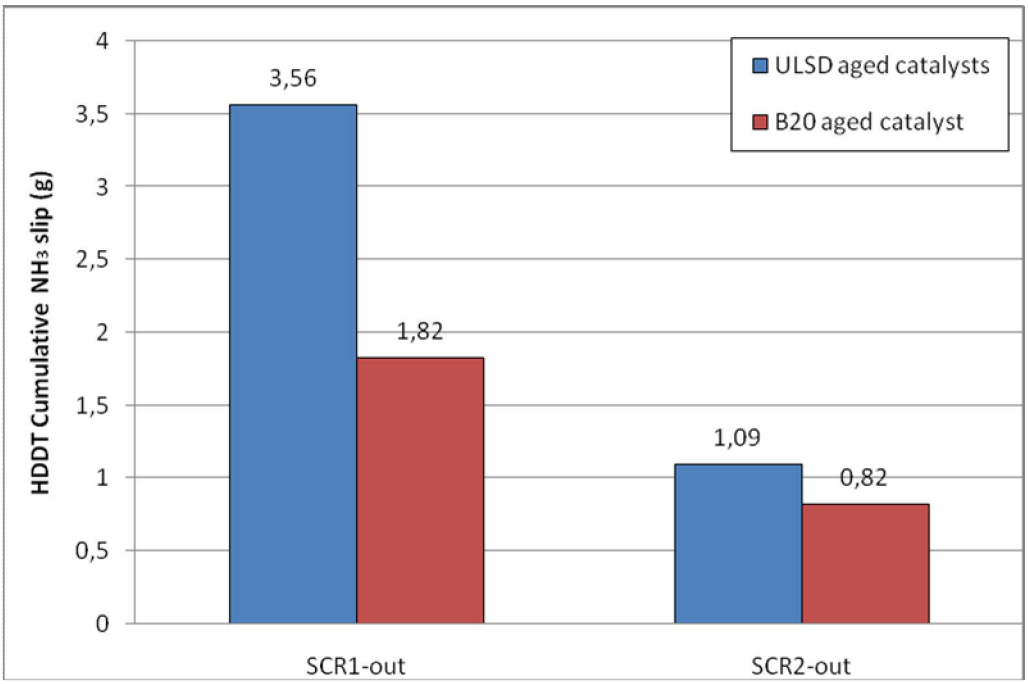

Figure 80. Cumulative ammonia slip for the third HDDT test cycle. (Williams *et al.*, 2011)

The average temperature and the time under specific temperature conditions during the ageing tests are listed in Table 27. The average temperature was slightly higher with ULSD, and the time at temperatures over 550 °C was almost doubled compared to B20. This indicates that thermal deactivation is not likely to be the reason for the results of B20 aged catalysts. In the investigation it was noted that the ash particles were very effectively trapped by the DPFs, so that very little amount would have come to the SCR equipment. Most likely the reason for deactivation was the vaporization of alkali metals during DPF regeneration. The hypothesis introduced in the study claimed that K in the form of hydroxide and sulfate was vaporized in the DPF and transported to the SCR. The investigation group also said that examination of this hypothesis would be the subject of future work.

Table 27. SCR thermal exposure. (Williams *et al*., 2011)

	Units	ULSD	B20
SCR temperature avg	°C	458,2	453,4
<500 °C	hours	74,8	77,1
500 to 525 °C	hours	2,6	16,8
525 to 550 °C	hours	139,7	135,4
550 to 575 °C	hours	16,7	7,4
575 to 600 °C	hours	1,2	0,1

7.7. Conclusions

- Compared to ultra–low sulfur diesel, the B20 blend caused an about 5 % deactivation during 435,000 miles equivalent ageing test, which can be considered a rather small deactivation rate.
- NH_3 slip was smaller with B20 aged catalysts compared to diesel.
- Thermal deactivation was not the reason for the results of B20 aged catalysts, but most probably the vaporization of metals such as K, caused the deactivation in the SCR during the regeneration of the DPF.

8. GENERAL CONCLUSIONS AND SUGGESTIONS

In the light of the findings it is possible to draw some general conclusions. Biofuels and the trace elements they contain seem to have a rather clear effect on the performance of SCR catalysts. It is very important to know the mechanisms of deactivation in order to prevent them. From all trace elements the most basic ones seem to have the greatest effects. K is found to be the single most deactivating trace element no matter in what form it is present. For other trace elements the other bonded molecules in the compound seemed to affect the deactivation power. Especially S was found to be an activating element, but only in small doses, due to its acidity, seen in Chapters 3.6 and 4.1.

The prediction of the possible results with biofuel use is very difficult due to the complexity of the fuels. It is clear that the more K, Ca, Na, Mg and other alkaline or earth alkaline metals the fuel contains, the worse is the prediction. However, this information can mainly be used only when comparing to other fuels, to figure out the possible deactivation risks. More precise predictions could be made if the base-metal compounds in the fuels were known exactly. Unfortunately this is rather impossible and the only way to really find out the effects is to test the biofuel with real equipment. If the fuel could be cleaned or somehow filtrated from the alkali metals, it would help to remain the activity levels. Also some technologies for cleaning the exhaust before the SCR could help to remain the conversion level of the catalyst. For example, the DPF can clean most of the ash if it is installed before the SCR, seen in Chapter 7. Unfortunately this might create a new problem with the aerosols, because the regeneration of the DPF could vaporize the base-metal compounds and they could reach deeper into the SCR catalyst. In an engine power plant the temperatures are often so low that the SCR must be installed before the DPF anyway, to ensure the correct temperature conditions for the catalyst. The order of the catalysts is a compromise, because the DPF regeneration is harder when the temperatures are lower.

The biofuel ash does not seem to be as harmful as the aerosol particles. In Chapter 4 were introduced the results of the ash collected from the biofuel combustion power plant put on an SCR catalyst piece. No deactivation was found, indicating that the particles must go deeper into the catalyst walls and to pores to create an effect. This way the NH_3 adsorption decreases and so does the conversion ability of the catalyst. Ash may have some effect but only at the surface of the inlet, if the holes in the inlet are small enough. Ash still increases backpressure when it accumulates on the surfaces, but this can be managed with frequent soot blowing, that is probably already taken care of in engine power plants. Another way to increase the lifetime of the catalyst would be to build it from identical catalyst blocks. This way their places could be changed, when the first block would be deactivated enough from the ash and possible particles. Increased vanadium content in catalyst seems to increase its ability to resist deactivation by alkali metals, seen in Chapter 5. Also the use of zeolite catalysts should be considered, as they could be more resistant to alkali metals. On the other hand there are poisonous for zeolites as well, and the needed temperature range might be problematic in power plant use.

It is clear that the trace elements in the biofuels and lubrication oils deactivate the SCR catalysts. The deactivation rate depends heavily on the fuel and temperature. The temperature can be controlled in certain limits, and one possibility to decrease the specific amount of the trace elements in the fuel is to blend it with fossil fuels, like in Chapter 7. If this is economically possible it would increase the lifetime of the SCR to some extent. Another possibility in case of deactivation would be to add an oxidation catalyst after the SCR system to control the ammonia slip. This way more ammonia could be delivered to the SCR catalyst and thus better conversion without ammonia slip could be achieved. Downside in this system would be the cost of the oxidation catalyst and increased use of ammonia or urea. In case of severe deactivation this would not probably be economically sustainable, but might give slightly more tolerance if the deactivation is small.

9. SUMMARY

This thesis was a part of the Future Combustion Engine Power plant (FCEP) program, funded by Cleen Ltd. The purpose of this thesis was to gather information about SCR catalyst deactivation by biofuels and the different trace elements they contain. SCR catalysts convert the harmful nitrogen oxides in different exhaust gases back to nitrogen and water. Ammonia in solid or liquid form is also needed as reagent for the conversion. This thesis is an meta-analysis of already published material and no practical measurements were made.

Potassium (K) and other alkali and earth alkali metals have strong deactivating effect on the vanadium based SCR catalysts. The catalyst surface is highly acidic and therefore the basic metals have ability to lower the acidity. This leads to less ammonia being accumulated on the surface and less conversion of nitrogen oxides to happen.

Chemical deactivation by aerosol particles is the primary reason for conversion activity loss. The alkali particles in aerosol form get deeper into the pores of the catalyst surface and decrease the acidity and active pores. Ash accumulation on the surface of the inlet is the secondary deactivation method, as well as masking and fouling the catalyst surface. Ash does not seem to be so harmful chemically, but it has the ability to block the exhaust channels and increase back-pressure. Ash can be handled quite well with soot blowing equipment.

More investigation about the chemical deactivation is needed in order to achieve longer lifetimes for the SCR catalysts. Fuel filtration to reduce alkali metals might be a very powerful way to reject the deactivation. Also the possibility of DPF use before the SCR could decrease the ash and particles travelling into the catalyst, but could on the other hand increase the vaporization of alkali metals in the DPF regeneration phase. If the basic metals could be filtrated from the flue gas or be bound into less deactivating forms the deactivation effects would likely decrease.

BIBLIOGRAPHY

Bergquist, Karl Henrik. *Accelerated phosphorus poisoning of automotive SCR-catalyst*. Lund Institute of Technology, Department of Chemical Engineering, Sweden.

Chen J.P., Buzanowski M.A., Yang R.T., Cichanowicz J.E. (1990). Deactivation of the Vanadia Catalyst in the Selective Catalytic Reduction Process. *Air Waste Manage Association* 40, 1403 - 1409. Available from internet: <http://pubs.awma.org/gsearch/journal/1990/10/40_10_1403.pdf>

G.A.M. Janssen. *Emissions of Diesel Engines Running on Different Biofuels and their Health Related Aspects*. FACT Foundation.

Jensen, Anker Degn; Castellino, Francesco; Rasmussen, Søren Birk; Johnsson, Jan Erik and Fehrmann, Rasmus. (2008). Deactivation of vanadia-based coomercial SCR catalysts by polyphosphoric acids. *Applied Catalysis B: Environmental* 83 110-122. Available from internet: <http://www.sciencedirect.com/science/article/pii/S0926337308000817#>

Jensen, Anker Degn; Castellino, Francesco; Johnsson, Jan Erik and Fehrmann, Rasmus. (2009). Influence of reaction products of K-getter fuel additives on commercial vanadia-based SCR catalysts. Part 1. Potassium phosphate. *Applied Catalysis B: Environmental* 86, 196-205. Available from internet: <http://www.sciencedirect.com/science/article/pii/S0926337308004128>

Jensen, Anker Degn; Castellino, Francesco; Johnsson, Jan Erik and Fehrmann, Rasmus. (2009). Influence of reaction products of K-getter fuel additives on commercial vanadia-based SCR catalysts. Part 2. Part II. Simultaneous addition of KCl, Ca(OH)2, H3PO4 and H2SO4 in a hot flue gas at a SCR pilot-scale setup. *Applied Catalysis B: Environmental* 86, 206-215. Available from internet: <http://www.sciencedirect.com/science/article/pii/S092633730800413X>

Karhu, Toomas, Cappelli, Samuele (2012). *SCR ageing on RSO engine*. Report. Turku University of Applied Sciences.

Kern, P.; Klimczak, M.; Heinzelmann, T.; Lucas, M. and Claus, P. *(2010).* High-throughput study of the effects of inorganic additives and poisons on NH_3-SCR catalysts. Part 2: Fe-zeolite catalysts. *Applied Catalysis B: Environmental 95, issues* 1-2, 48-56. Available from internet: <http://www.sciencedirect.com/science/article/pii/S0926337309004731>

Klimczak, M., Kern, P., Heinzelmann, T., Lucas, M. and Claus, P. (2010). High-throughput study of the effects on inorganic additives and poisons on NH_3-SCR catalysts – Part 1: V_2O_5-WO_3/TiO_2 catalysts. *Applied Catalysis B: Environmental* 95, issues 1-2, 39-47. Available from internet: <http://www.sciencedirect.com/science/article/pii/S092633730900472X>

Kling, Åsa; Andersson, Christer; Myringer, Åse; Eskilsson, David and Järås, Sven G. (2007). Alkali deactivation of high-dust SCR catalysts used for NO_X reduction exposed to flue gas from 100 MW-scale biofuel and peat fired boilers: Influence of flue gas composition. *Applied Catalysis B: Environmental* 69, *issues* 3-4, 240-251. Available from internet: <http://www.sciencedirect.com/science/article/pii/S0926337306001044>

Kröcher, Oliver & Elsener, Martin (2008). Chemical deactivation of V_2O_5/WO_3-TiO_2 SCR catalyst by additives and impurities from fuels, lubrication oils, and urea solution. Part 1: Catalytic studies. *Applied catalysis B: Environmental* 77, issues 3-4 (2008) 215-227. Available from internet: <http://www.sciencedirect.com/science/article/pii/S0926337307001294>

Laine, Marleena (2012). *SCR-katalysaattorikennojen ikäytysparametrit ja alkuikäytys*. Bachelor's Thesis. Turku University of Applied Sciences.

Lisi, L., Lasorella, G., Malloggi, S. and Russo, G. (2004). Single and combined deactivating effects of alkali metals and HCl on commercial SCR catalysts. *Applied Catalysis B: Environmental* 50, issue 4 251-258. Available from internet: <http://www.sciencedirect.com/science/article/pii/S0926337304000402>

Majewski, W. Addy & Khair, Magdi K. (2006). *Diesel emissions and their control*. SAE International. 584 p. ISBN: 978-0-7680-0674-2.

Nicosia, D., Czekaj, I. and Kröcher, O. (2008). Chemical deactivation of V_2O_5/WO_3-TiO_2 SCR catalyst by additives and impurities from fuels, lubrication oils, and urea solution. Part 2: Characterization study of the effect of alkali and alkaline earth metals. *Applied Catalysis B: Environmental* 77, issues 3-4 (2008) 228-23. Available from internet: <http://www.sciencedirect.com/science/article/pii/S0926337307002330>

Nicosia, D., Elsener, M., Kröcher, O. and Jansohn, P. (2007). Basic investigation of the chemical deactivation of V_2O_5/WO_3-TiO_2 SCR catalyst by potassium, calcium, and phosphate. *Topics in Ca-*

talysis Vols. 42-43, numbers 1-4. Available from internet: <http://www.springerlink.com/content/p187q540466212r8/>

Sohrabi, Morteza; Morabi, Farokhbag and Sanati, Mehri. (2007). Deactivation of Pt/Wire-mesh and vanadia/monolith catalysts applied in selective catalytic reduction of NO_X in the flue gas. *Korean Journal of Chemical Engineering*, volume 24, number 4, 583-587. Available from internet: <http://www.springerlink.com/content/f15t201253736624/>

Williams, Aaron; McCormick, Robert; Luecke, Jon; Brezny, Rasto; Geisselmann, Andreas; Voss, Kenneth; Hallstrom, Kevin; Leustek, Matthew; Parsons, Jared and Abi-Akar, Hind (2011). *Impact of biodiesel impurities on the performance and durability of DOC, DPF and SCR technologies*. SAE International.

Zheng, Yuanjing; Jensen, Anker Degn; Johnsson, Jan Erik and Thøgersen, Joakim Reimer (2008). Deactivation of V_2O_5-WO_3-TiO_2 SCR catalyst at biomass fired power plants: Elucidation of mechanisms by lab- and pilot-scale experiments. *Applied Catalysis B: Environmental* 83, issues 3-4, 186 – 194. Available from internet: <http://www.sciencedirectcom/science./article/pii/S0926337308000969>

Zheng Y., Jensen A.D., Johnsson J.E. (2004). Laboratory Investigation of Selective Catalytic Reduction Catalysts: Deactivation by Potassium Compounds and Catalyst Regeneration. *Industrial & Engineering Chemistry Research* 43, 941 - 947. Available from internet: <http://www.mendeley.com/research/laboratory-investigation-selective-catalytic-reduction-catalysts-deactivation-potassium-compounds-ca/>